NASA CR-132597

'7-D

X75-10114

THE GARRETT CORPORATION
AiResearch Manufacturing Division
LOS ANGELES 45, CALIFORNIA

REPORT NO. AP-68-3953

HYPERSONIC RESEARCH ENGINE PROJECT - PHASE IIA
INSTRUMENTATION PROGRAM
TERMINAL SUMMARY REPORT
24 FEBRUARY 1967 THROUGH 3 SEPTEMBER 1968
DATA ITEM NO. 55-8.07
NASA CONTRACT NO. NAS1-666

AP-68-3953 22 October 1968

ISSUED January 1975

NO. OF PAGES 106

DATE 22 October 1968

Drawing Attached
AiResearch Dwg No. 981109

PREPARED BY Engineering Staff

EDITED BY L. F. Jilly

APPROVED BY Henry J. Lopez
Henry J. Lopez
HRE Program Manager

REVISIONS				ADDITIONS			
PAGE	DATE	PAGE	DATE	PAGE	DATE	PAGE	DATE

(NASA-CR-132597) HYPERSONIC RESEARCH ENGINE PROJECT. PHASE 2A: INSTRUMENTATION PROGRAM, DATA ITEM NO. 55-8.07 Terminal Summary Report, 24 Feb. 1967 - 3 Sep. 1968 (AiResearch Mfg. Co., Los Angeles, Calif.) N76-77230

Unclas
00/98 49639

FOREWORD

This Terminal Summary Report on the Instrumentation Program is submitted to the NASA Langley Research Center by the AiResearch Manufacturing Company, Los Angeles, California. The document was prepared in compliance with the guidelines established for the partial termination of NASA Contract No. NAS1-6666.

Part I of this report summarizes the entire Instrumentation Program effort expended under the Hypersonic Research Engine Project, which encompasses the period of 24 February 1967 through 3 September 1968. Part II presents a detailed discussion of the remaining effort not previously covered in an Interim Technical Data Report.

ACKNOWLEDGMENTS

Acknowledgments for assistance in the completion of this document are extended to the following contributors.

PART I

Author	Categories
N. Naves	Double-Sonic Orifice Probe
J. Pratt	Thrust/Drag System
D. Osborn	Engine Metals and Coolant-Temperature Measurements
A. Saur J. Tranter	Pressure Measurements
A. Saur	Hydrogen Mass-Flow Rate Measurements

PART II

J. Pratt

R. W. McIver

CONTENTS

CONTENTS (Continued)

APPENDIXES

ILLUSTRATIONS

TABLES

PART I

SUMMARY OF TASK

1.0 THRUST/DRAG-MEASUREMENT SYSTEM

1.1 PROBLEM STATEMENT

1.1.1 Objective

The objective of the thrust/drag-measurement system is to determine the internal thrust developed by the Hypersonic Research Engine during powered flight. Following the preliminary design conceived during Phase I (Reference 1-1, pp 298-314), development under Phase II was to produce a system capable of determining the value of internal thrust from measurements of the forces acting on a single force block, acting as the front engine support. The forces on this block, designated as indicated thrust, are comprised of effects of internal thrust, drag, inertia, gravity, lift, moments, thermal differentials and vibration. The engine thrust also acts on other members in parallel with the thrust block; namely, the engine rear supports fuel lines and electrical wiring.

The thrust (force) block must be capable of withstanding the stresses imposed, as an active support member in its operational environment, and be designed to measure or take into consideration all forces required to compute the internal thrust within the range accuracy, resolution and frequency response required.

1.1.2 Design Requirements

Incorporation of the re-evaluated aerodynamic, heat transfer and engine performance has led to revision of the initial requirements. Table 1.1-1 shows the comparison of the basic requirements at the beginning of Phase II and at present. Changes are discussed in Appendix A.

1.2 TOPICAL BACKGROUND

The determination of the internal thrust of the engine is the prime purpose of the thrust-measuring system. The use of a single force-measuring block means that account must be made of all significant forces acting on the block in order to derive the internal thrust. Such forces on the block are the inertia forces acting on the engine assembly, aerodynamic drag, and resolved gravitational forces. The inertia forces arise from aircraft acceleration and vibratory forces acting on the mass of the engine assembly, including the fuel lines, electrical cables, etc. The pitch of the engine gives rise to a component of the engine assembly weight acting along the thrust-block-sensitive axis. Aerodynamic drag produces a force on the block opposing the internal thrust.

TABLE I.I-I

DESIGN REQUIREMENTS

Item	Basic Requirements	
	Beginning of Phase II	Present
Internal thrust	0 to 4000 lb	0 to 6000 lb
Indicated thrust	-500 lb (drag) to 4500 lb	-5500 lb to 7000 lb
Force block maximum overload	10,000 lb	15,000 lb
Acceleration (aircraft and engine)	±1 g	±3 g
Frequency response	0 to 100 Hz	0 to 10 Hz
Temperature*	-65°F to +500°F (flight)	-40°F to +250°F (flight) -65°F to +600°F (ground test)
Altitude*	123,000 ft	123,000 ft
Measurement accuracy to within (3σ)	1.75% of full-scale (indicated thrust)	2.70% of full-scale (internal thrust)
Vibration (ground test) input*	20-2000 Hz sine 3 g peak 20-2000 random noise 0.018 g^2/Hz	20-2000 Hz sine 3 g peak 20-2000 random noise 0.018 g^2/Hz
Resolution (indicated thrust)	10 lb	10 lb
Humidity*	---	to 95 RH at 105°F

*For detailed coverage of the environments to be encountered by the engine and subassemblies attention is drawn to Reference I-2.

The engine is supported at the front by the thrust block and at the rear by two supports. The longitudinal stiffness of these supports and of the bridging fuel lines and electrical cables are in parallel with the thrust block, and allowance must be made for the forces they take. Differential thermal expansion between the engine and engine support frame (wishbone) attachment points induces a force shared by the stiffnesses of the block and the parallel restraints. This is reflected as an output from the thrust block and must be either determined or rendered insignificant by suitable design of the parallel members.

Vertical- and side-reaction forces on the thrust block must be considered as affecting the calibration of the block and cross-coupling coefficients established.

Temperature is an important consideration in designing the components of the measuring system. Temperature extremes are experienced ranging from cold-flight conditions to engine-lit conditions. Radiation and conduction from the hot manifolds to the thrust block can give rise to temperature gradients within the block and its transducer, producing significant output due to thermal distortion as well as high stresses. By nature of its design in acting as a support member and having a comparatively high natural frequency, the thrust block is inherently stiff, allowing for a small deflection under maximum thrust conditions. Thus uncorrelated differential micromovement can be significant with reference to the accuracy requirements.

During ground testing, temperatures will be higher due to longer soak periods and higher ambient conditions, and protection may be required for components of the system (Reference I-3, Para 2-2).

1.3 OVERALL APPROACH

Figure 1.3-1 shows the fundamental forces acting on the engine and the relationship for the determination of the internal thrust (T_i). Of the remaining forces acting on the thrust block, only the differential thermal expansion force (F_T) is illustrated. Detail analysis of the total force balance is contained in Reference I-4, Para 2.3.

The approach has been to consider only measurement of the three major components of the force balance and to concentrate on design as providing minimal effects of other forces. Where these forces prove significant, after analysis of basic design, corrective action in terms of design improvement, practical evaluation (e.g., calibration) or, if necessary, additional measurements has been considered. For example, design of the thrust block has included attention to minimization of thermal differential effects, but experimental work is necessary to prove the suitability of design with the backup of the provision of heat radiation shields or active temperature control (or equalization) in mind. As a further example, the stiffness of the so-called parallel restraints (rear supports, fuel lines, electrical cables), while having little contribution to the force-balance in comparison to the stiffness of the thrust

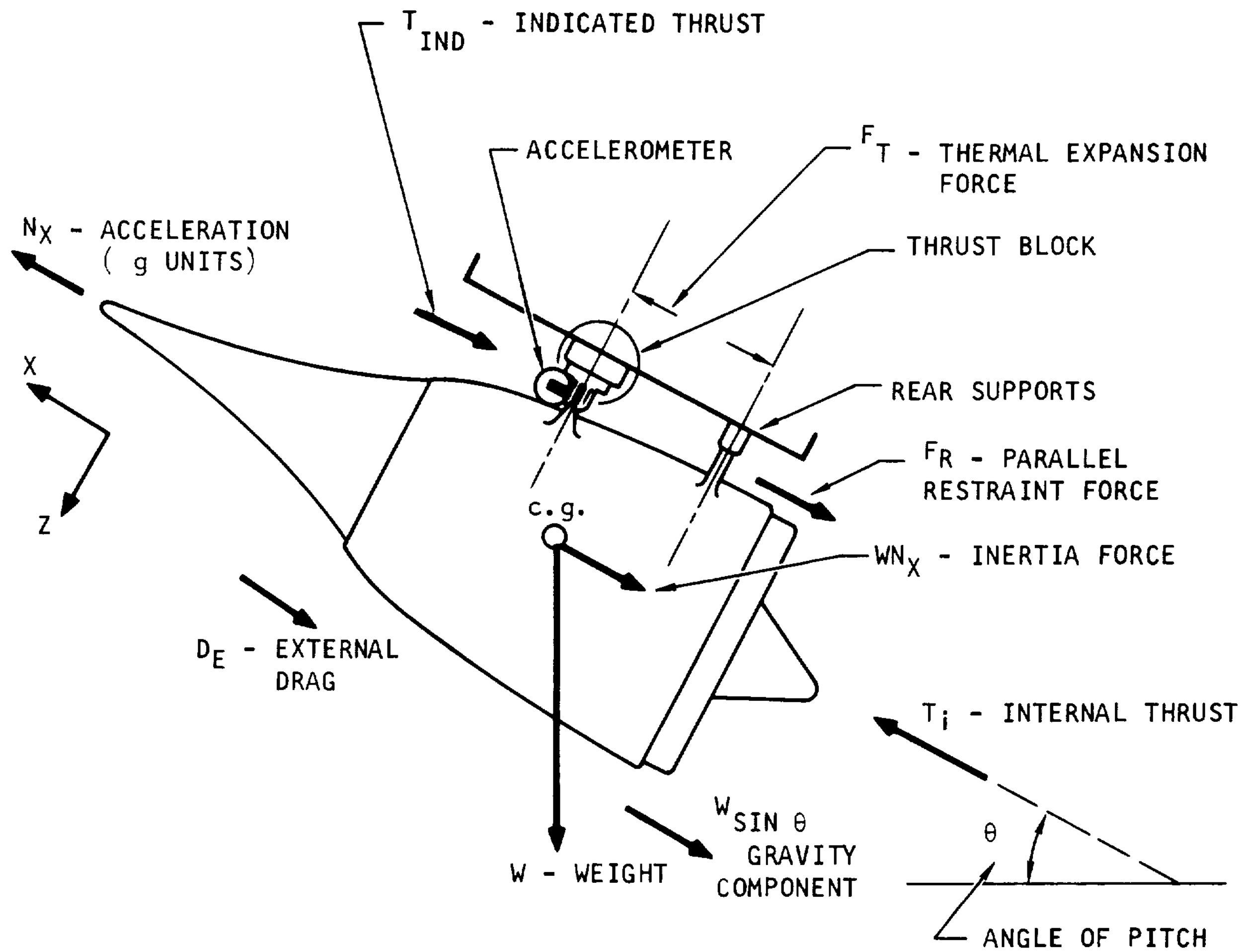

BASIC RELATIONSHIP OF FORCES

$$T_i = (T_{IND} + F_R) + D_E + W(N_X + \sin\theta)$$

Figure I.3-I. Derivation of Internal Thrust block and able to be accounted for in system calibration, does affect to a greater extent the force induced in the block due to differential thermal expansion between the engine attachment points on the engine and engine support frame (wishbone). (See Reference I-4, Para 2.4.2.2.) Minimization of this stiffness is limited by practical design, and experimental data and in-flight determination of temperature may be necessary to provide evaluation of the force contribution within limits consistent with the accuracy requirements for the determination of internal thrust.

With regard to the three fundamental measurements, the approach has been as follows:

1.3.1 Indicated Thrust

The net force in the X-axis is determined using a force-deflection block, firmly attached to the engine suspension frame and pin-mounted to the engine. The measurement of the deflection of the block has been approached in two ways, (1) use of straingages, and (2) use of a differential capacitor displacement transducer.

The straingage approach uses state-of-the-art techniques to determine the bending strain of the beams of the block.

The differential capacitor approach was recommended during the Phase I effort. This approach has certain advantages, particularly with consideration of the effect of temperature and fabrication methods. With this type of transducer, relative movement between a center plate (attached to the engine side of the block) and two outerplates (attached to the top side of the block) produces decreasing and increasing changes of capacitance which can produce a good analog output. The signal produced will have high sensitivity and resolution with good linearity and large over-range. By careful design and choice of materials, thermal effects can be minimized and structural integrity ensured.

1.3.2 Inertial Forces

An accelerometer provides a convenient means of measuring all the inertial forces acting on the engine. The approach has been to consider commercially available instruments capable of meeting the accuracy, resolution, range, and environmental requirements.

1.3.3 Drag

It is proposed to calculate the aerodynamic drag during flight, using a static pressure correlation measurement and data obtained during wind tunnel testing. The methods of measurement and calculation are not requirements of the thrust-system program and are not discussed in this report. Magnitudes of the drag forces and measurement errors have been considered to evaluate the force-balance and error analyses.

1.4 HISTORICAL SUMMARY

1.4.1 Thrust Deflection Block

Consideration of the initial problem statement led to the design of a block having two spring flexures, with a material selection of Ni-Span-C and Ti-6Al-4V as being most suitable to meet the strength and low-coefficient-of thermal-expansion requirements (Reference 1-5, Para 2.4.1.1, 2.4.1.2, and drawing LSK 31194). Revised aerodynamic loadings and thrust measurement range requirements (Reference 1-6, Appendix A, Table A-1) necessitated redesign. With consideration being given to the combined effects of thermal expansion and change of elastic modulus due to temperature changes and differentials, stress analysis led to a design using 17-4PH material for a configuration having four parallel spring flexures (Reference 1-7, Para 2.4-1). Such a block was fabricated and sujected to a structural loading test to 10,000 lb along the X-axis (see Part II of this report). As part of the requirement to study the straingage technique of force determination, the block was instrumented to measure strains along the X-axis and Z-axis (for vertical reaction force evaluation). A photograph of the instrumented block is shown in Figure 1.4-1. Testing performed to assess the straingage method is covered in Part II of this report.

The differential capacitor transducer system was to be tested to determine structural and electrical performance in conjunction with the engine model vibration test utilizing the second deflection block. At the time of termination, the second deflection block was partially completed, hence further work was terminated.

The structural model will be subjected to tests utilizing the initial deflection block.

1.4.2 Differential Capacitor Transducer

The material of the support body for this transducer is Alsimag 447 (American Lava Corporation). Alsimag was selected for its electrical insulation and very low thermal expansion properties. In the original design, the capacitor outer plates were of 0.010-in. thickness made of Invar 36 stock, bonded to the ceramic faces. In order to minimize stray effects of variable capacitance in parallel with the differential capacitor, the bridge diodes are housed within the ceramic block in direct contact with the outer plates. Originally the contact was to have been made using spring contact pressure (Reference 1-5, Para 2.4.2); however, revision to the maximum temperatures requirements in flight (see Para 1.2.2) was reduced to 250°F and the fact that the diodes had been specially chosen to withstand the original temperature requirement of 500°F, permitted a design change to incorporate a direct soldering technique to be used (Reference 1-8, Para 2.4.1.2), in order to give more positive contact and to minimize vibration and shock effects. Although metal coating of the outer plates had been rejected (Reference 1-5, Para 2.5.2) the case for its use was reopened after consideration of the difficulties in

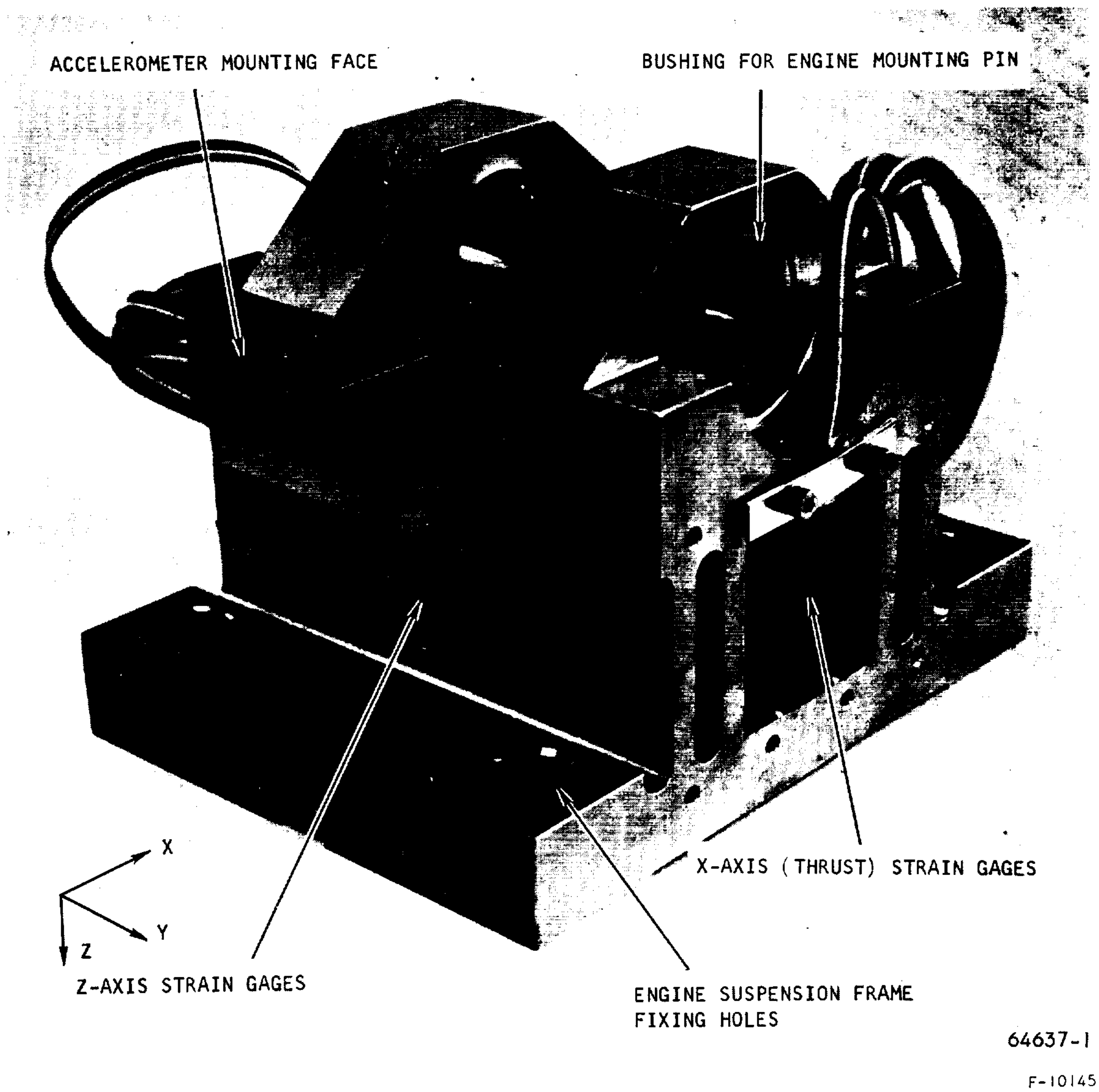

Figure I.4-I. Thrust Deflection Block-Development Model ensuring flat, parallel surfaces and good adhesion using the bonded-plate method. A brush-on silver preparation (DuPont No. 6320) was applied to samples and proven suitable under humidity conditions (Reference I-8, Para 2.5.3). This method was incorporated in the design and, further, gave the advantage of improving the linearity of the transducer as a whole by increasing the gap between the centerplate and outerplates (see Reference I-3, Para 2.4.3 for linearity analysis).

Further consideration was given to the effect of differential thermal expansion between the transducer and the thrust block. Analysis indicated that excessive stress could be present in the ceramic outerplate support. Accordingly the end fixing inserts of the support were redesigned to give comparatively low resistance to longitudinal forces and yet maintain high rigidity in the transverse direction (Reference I-3, Para 2.4.2).

A similar design was incorporated in the centerplate and to minimize differential expansion between the centerplate and the deflection block, the material was changed from Invar 36 to 17-4PH. For the development model, the centerplate is fixed directly to the deflection block, which acts as the common circuit return. In the flight version, however, provision would have to be made to isolate the plate electrically from the block to avoid possible capacitance effects and ground loops, since the block would be grounded to the engine and suspension frame.

At the time of termination, all hardware for the transducer was in fabrication to meet the forthcoming development program, but most of the fabrication had not been completed. Figures I.4-2 and I.4-3 show the original design of capacitor outerplate, the bridge diodes, and the bridging strip to be directly soldered to the common sides of the bridge pairs (see Reference I-8, Figure 2.4-5 for circuit diagram of transducer and electronics).

I.4.3 Differential Capacitor Transducer Signal-Conditioning Equipment

The original circuit of the transducer electronics (Reference I-5, Drawing LSK 31195) was adopted as forming the basis of the signal-conditioning equipment. A unit was constructed to this design together with a special differential capacitor transducer to instrument the force block used during the HRE combustor test program (Reference I-3, Para 2.5.3, 2.5.5). In order to allow for sensitivity adjustment and signal zero-set it was necessary to include an operational amplifier to prevent direct loading on the circuit. A low-pass filter, of 0 to 10 Hz bandwidth, was designed as a requirement to remove unwanted signals outside the frequency band of interest and was incorporated into the overall circuitry, which is shown in Figure I.4-4. A laboratory-model was constructed and tested to determine stability and response (Reference I-8, Para 2.5.2, 2.4.1.4) and was shown suitable for use during ground development testing. However, the stability was only just within the requirement of 0.2 percent variation of full-scale and warm up time of approximately 2 hr was required to reach this condition. Circuit improvements were recommended, including a crystal controlled oscillator for a flight version (Reference I-8, Para 2.4.1.4.2). No action was taken in this respect as a result on the NASA stop order calling for the provision of a laboratory model conditioner only.

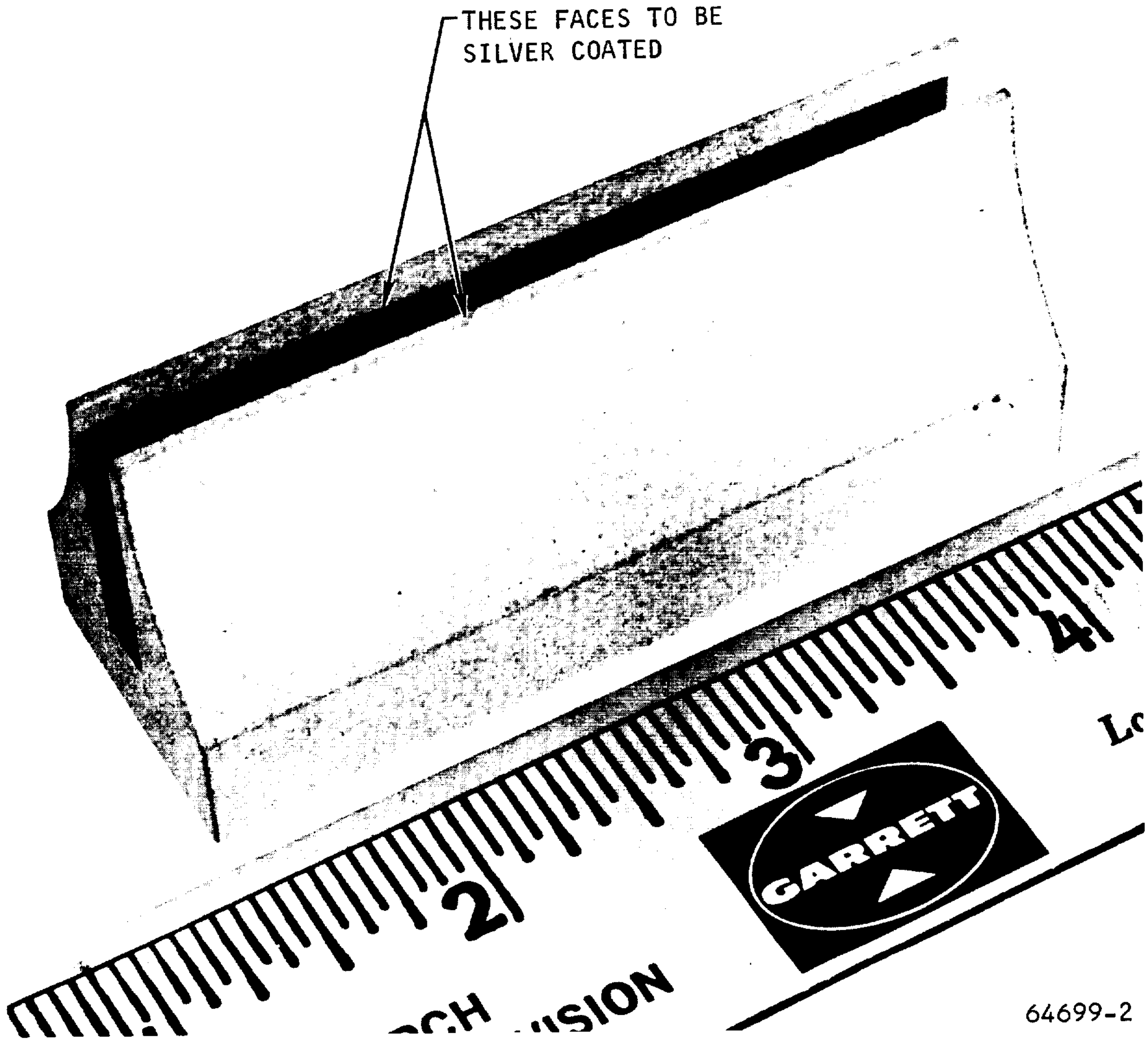

Figure I.4-2. Capacitor Outer Plate Support

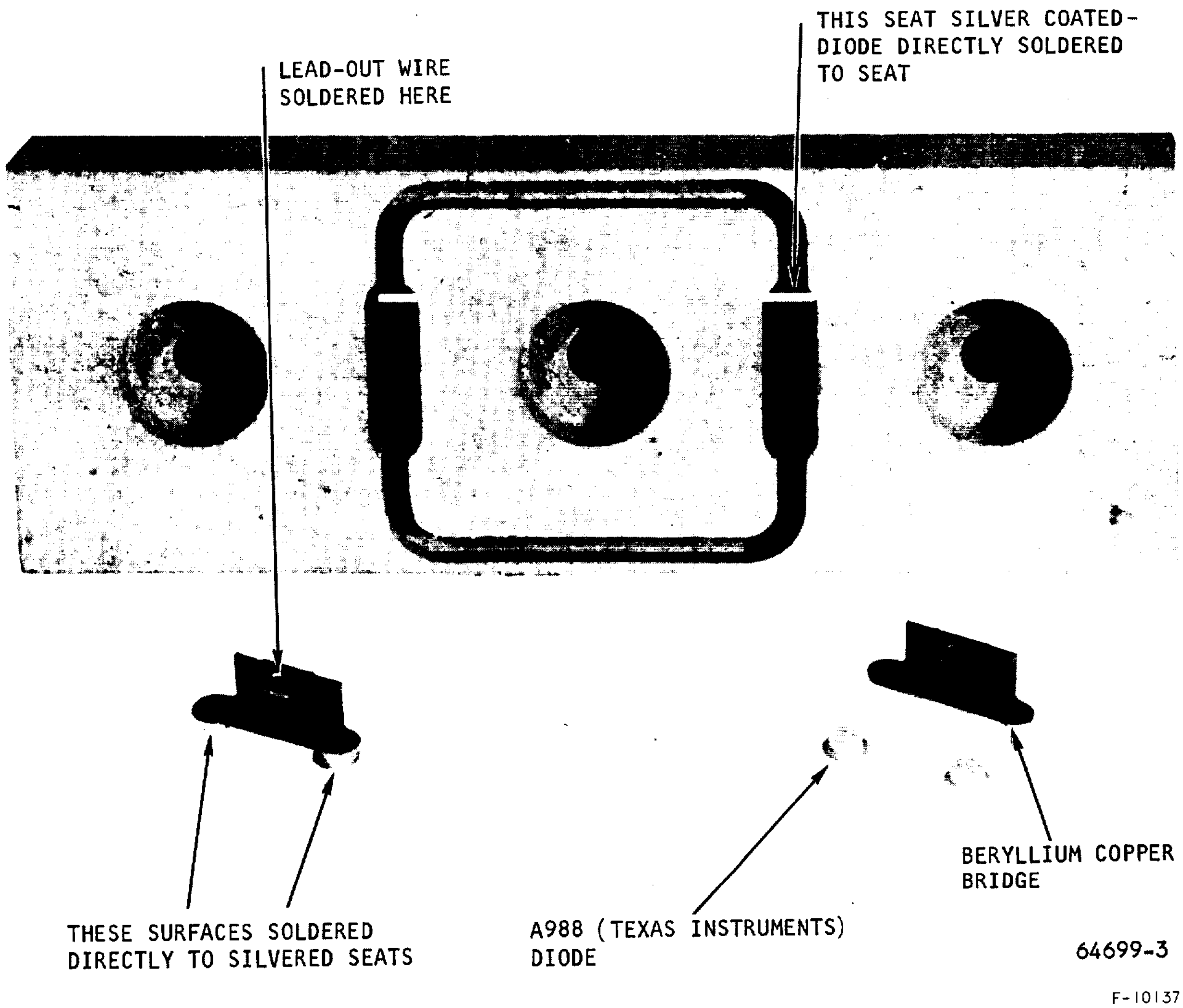

Figure I.4-3. Capacitor Outer Plate Support and Details

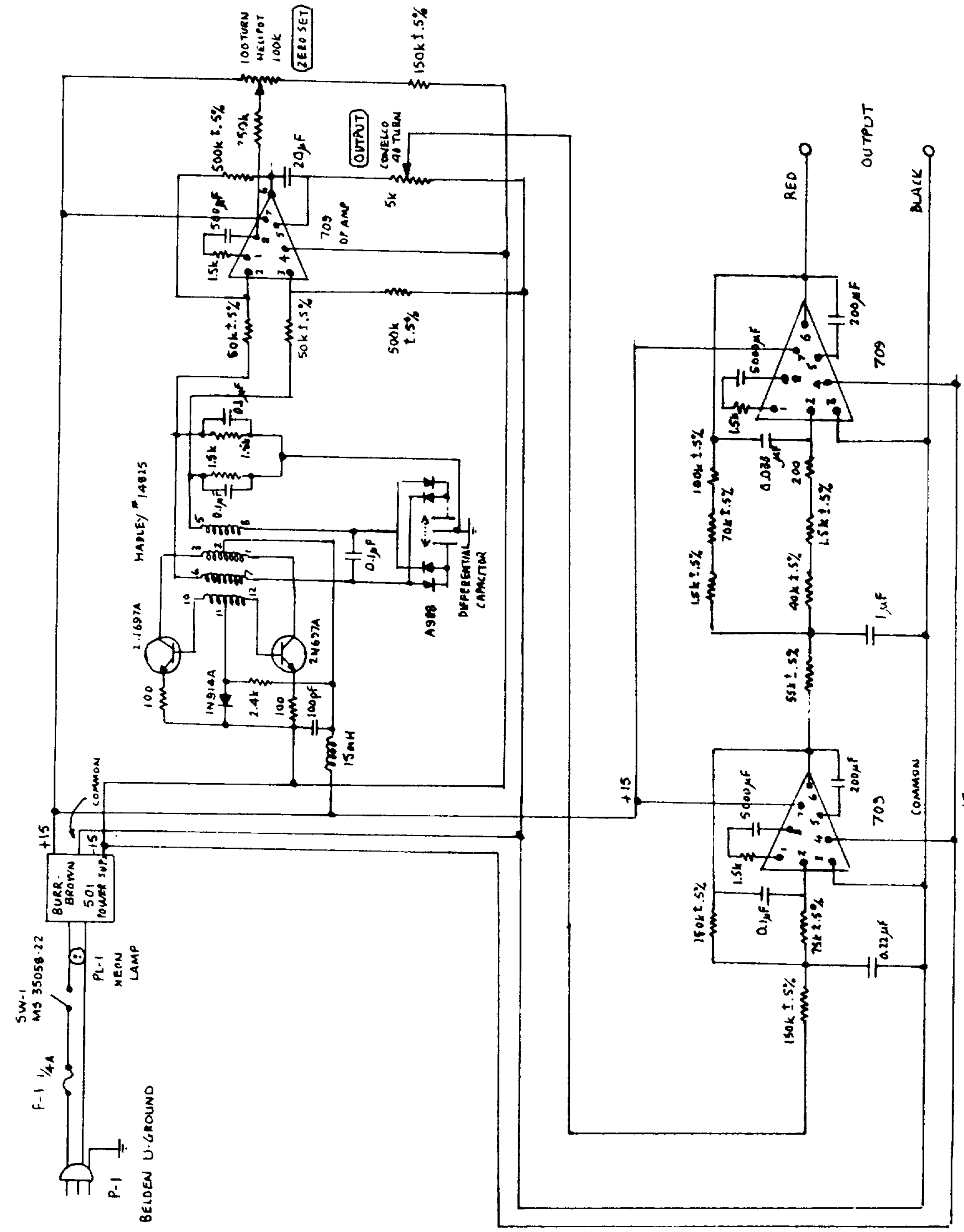

Figure 1.4-4 Thrust Block Signal Conditioner - Laboratory Model

The constructed laboratory model is housed in a rack-mounted panel and incorporates the basic circuit, sensitivity, and zero-set controls, low-pass Butterworth filter, and power supply.

1.4.4 Accelerometer

The original requirement of an upper temperature limit of 500°F imposed restriction on the selection of an accelerometer. No off-the-shelf transducer was available but a manufacturer was selected as providing a commercial item meeting the main specification requirements and capable of modification to meet the temperature requirement. However, with the change of the problem statement (Reference Para 1.2.2) to increase the measuring range from ±1 to ±3 g and with more detailed analysis of the overload range requirement to meet the anticipated vibration conditions (Reference 1-6, Para 2.4.2.6), together with the relaxation of the temperature maximum from 500°F to 250°F, attention was drawn to a standard servo accelerometer manufactured by Kistler. Reference 1-7, Para 2.4.4, covers the selection of the accelerometer and the error analysis associated with it. The accelerometer finally chosen was the Kistler model 303B servo accelerometer.

No action had been taken to procure this model in view of the stop-order confining the activity to specific development testing. Design of the adapter for thrust-block mounting was achieved and a photograph of a prototype version is shown in Figure 1.4-5. It incorporates an insulated spacer bonded to an aluminum body, to minimize conductive heat transfer from the deflection block. Radiant heat transfer is minimized by shielding around the accelerometer.

1.4.5 Heat Shields

To minimize thermal radiation from the manifolds and turbine, heat shields were designed to encompass the deflection block assembly. On the basis of this design, a heat transfer analysis was performed, reflecting mission parameters and deflection block thermal properties (Reference 1-3, Para 2.4.4). The results indicated that thermal differentials would be within the 25°F limit, analyzed as the maximum acceptable to produce a 1-percent error, if the differential were unknown. (Reference 1-7, Para 2.4.2.3.) However, it was realized that experimental data would be required to back up these analyses, and an initial test was proposed using a heat sink and heat sources to effect temperature differentials within the block for assessing the validity of the analysis in Reference 1-7, Para 2.4.2.3. In view of the background experience of other thrust block users (NASA Langley) and the assumptions made in the differential analysis, it is felt that the simple passive control of the block assembly using radiation shields may not prove sufficient to meet the accuracy requirements of the force measurement. No experimental work has been performed on the deflection block assembly to influence this consideration.

1.4.6 Parallel Restraints

This subject has been covered in analysis and design features only. The requirement for minimum forces in parallel with the deflection block has been reflected in the design of the fuel lines and rear supports. The fuel lines

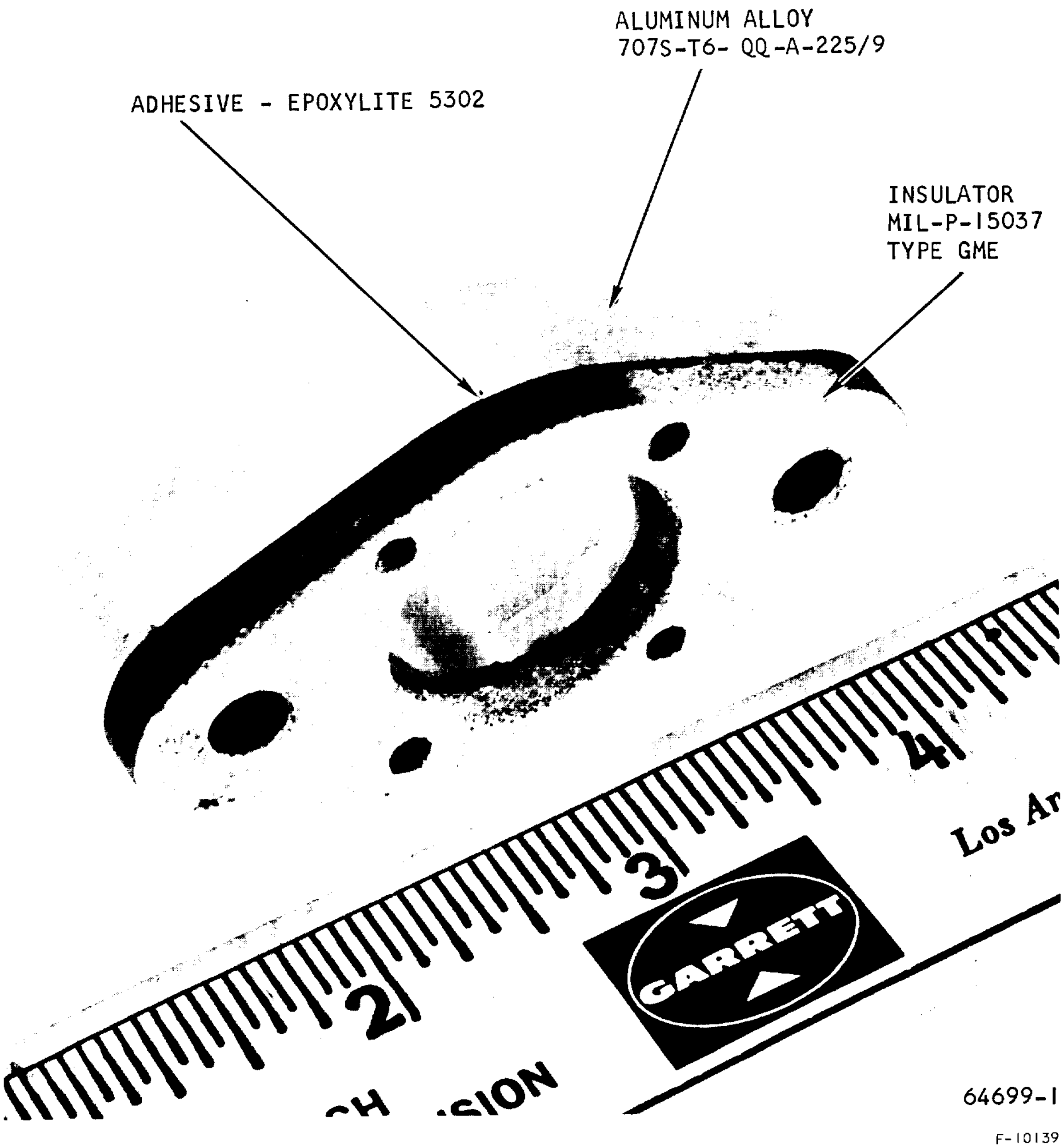

Figure 1.4-5. Accelerometer Adapter

contribute to the force-balance, not only with respect to stiffness, but also as a result of dynamic forces generated by flow around bends. Gimballed bellows have been incorporated in these lines. The rear supports have been designed to offer stiffness in the support direction (Z-axis) with flexibility in the thrust direction (X-axis). A large factor in the force-balance is the force generated under differential thermal expansion between the engine and engine-support frame. In treating the force on the deflection block due to this effect as an error contribution, maximum stiffness of the parallel restraints can be specified (Reference I-4, Para 2.4.2.2). The effect of the stiffness to reduce the apparent spring constant of the deflection block, in taking a share of the thrust loading, can be determined by calibration of the whole system.

No experimental work has been performed in this connection, although an analytical review of the problem was scheduled as part of the flight-development phase. A mock-up engine would be used to provide some experimental data.

1.4.7 Thrust Pin and Deflection Block Fixings

The deflection block is bolted to the engine suspension frame using four 1/2-in. high-strength CRES alloy bolts, with the shear load taken by four shear pins of 0.406 in. diameter.

These fixings have been modified, as a result of revised loading figures and revised stress analysis, from 7/16 in. and 3/8 in., respectively.

The thrust pin material has been selected as 17-4PH, condition H925, to give optimum anti-galling properties, with the deflection-block bushing of 17-4PH, condition H1125, with minimum differential thermal expansion.

1.4.8 Test Equipment

Originally it was intended to perform a frequency response test of the deflection block assembly to cover the range 0 to 100 Hz (Reference I-5, Para 2.3.2). To this purpose, a test fixture was fabricated to utilize a shaker to provide a frequency-forcing function. However, with the change of requirement to the 0 to 10 Hz range, and the block designed with a natural frequency of approximately 170 Hz, it was decided that this test would not be required during development.

The effect of the vertical reaction force on the characteristics of the block when deflected under the axial thrust load (Reference I-7, Para 2.4.5.4) necessitated evaluation of the cross-coupling coefficients. Side loadings and moments were also considered and a test fixture designed and fabricated to meet the test program loading requirements. A photograph of this fixture is shown in Figure 1.4-6. Using a dummy thrust block, tests were conducted to evaluate the fixture, and it was demonstrated that it would be suitable for performing calibration of the thrust block assembly (Reference I-8, Para 2.5.1).

The fixture was used to test the first deflection block for structural integrity and to assess the suitability of the straingage method of force measurement (see Part II of this report).

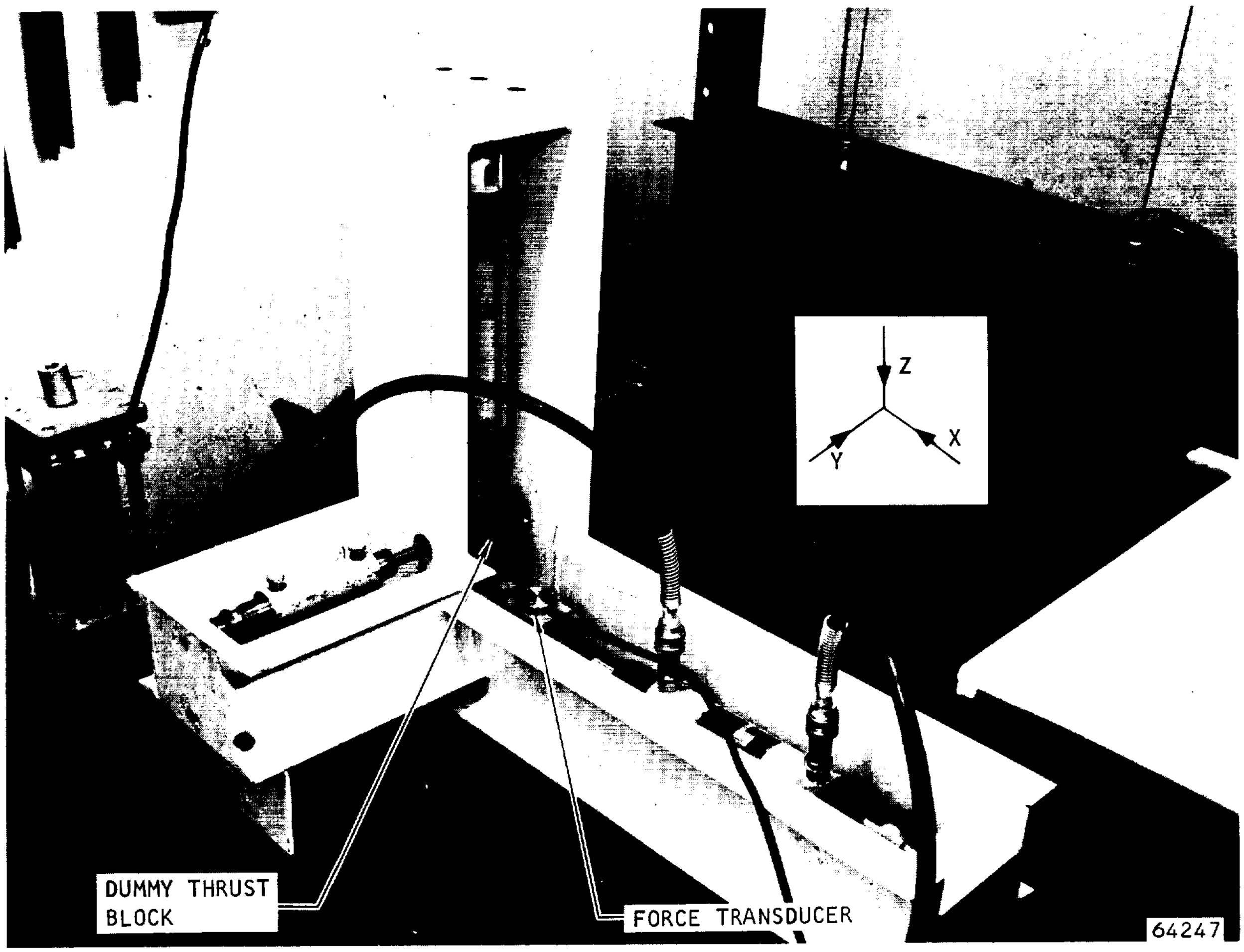

F-10072

Figure 1.4-6. Thrust Block Static-Load Test Fixture 94-7B-3419

1.4.9 Testing

The following testing has been performed.

(a)	Assessment of deflection-block loading test rig	(Reference 1-8, Para 2.5.1)
(b)	Impregnation of capacitor outer support to prevent ingress of water	(Reference 1-8, Para 2.5.3)
(c)	Suitability of direct-soldering of diodes in capacitor outer-plate-support assembly	(No reference)
(d)	Structural integrity of deflection block	(Reference Part II of this report)
(e)	Suitability of straingage method of force-measurement	(Reference Part II of this report)
(f)	Evaluation of laboratory-model signal-conditioner for differential-capacitor-displacement transducer	(Reference 1-8, Para 2.5.2)
(g)	Testing of special differential-displacement transducer for HRE combustor testing	(Reference 1-3, Para 2.5.5)

2.0 DOUBLE-SONIC ORIFICE TOTAL-TEMPERATURE/PRESSURE PROBE

2.1 PROBLEM STATEMENT

Devices are needed to measure the total temperature and total pressure in the internal supersonic flow field of a hypersonic ramjet engine. These devices must be capable of operation to temperatures of approximately 5800°R, a stream velocity of about Mach 3, an oxygen-rich atmosphere, and the effluent gases of an oxygen and hydrogen burner. These devices must be suitable for installation and use in a variety of test configurations for a supersonic ramjet engine test program.

2.2 TOPICAL BACKGROUND

To determine combustor performance and how it is influenced by injector geometry, jet penetration, spreading, and mixing, total temperature and total pressure at several points in the combustor must be measured while the engine is operating. The probe concept and size are affected by the necessity of keeping the combustor duct unblocked so it will not become choked. Also, the probe must be cooled to attain sufficient life to make the tests.

Obtaining temperature and pressure measurements from a supersonic oxygen and hydrogen burner involves many factors. In addition to the probes, the supporting systems must be cooled. The coolant selected must be compatible with the test facility, installation, and test objectives. In the cases discussed here, the test objectives have necessitated circulation of the coolant through the probe.

2.3 OVERALL APPROACH

One gas aspirating cooled-probe design was fabricated. The probe is internally-cooled to a temperature compatible with structural requirements, and the aspirated gas is cooled to about 2300°R or less.

The probe detects the total temperature by two independent methods; (1) the two-sonic orifice method, and (2) the calorimetric method. Both methods of temperature-measurement are incorporated in the same physical probe. Evaluation of the total temperature from the two-sonic-orifice method requires measurements of the total pressure in the inlet nozzle and total pressure and temperature in the second nozzle. The calorimetric method requires the total pressure and total temperature in the second nozzle, a mass-flow rate of the coolant, the inlet and outlet temperature of the coolant, and a check valve for stopping the gas aspiration when taking tare measurements.

Since the flow of gas through the probe must be deadheaded for a brief period to make a tare measurement of heat flux, a total-pressure measurement can be made during this interim. The freestream total pressure may be subsequently computed by using the Rayleigh equation as solved for a real gas. It is possible therefore, to make three determinations with the probe; total temperature by the double-sonic-orifice method, total temperature by the calorimetric method, and total pressure.

2.4 HISTORICAL SUMMARY

Analysis and design of the double-sonic-orifice probe was started in March, 1967. Fabrication of one probe was completed in December of 1967. The overall probe configuration is shown on AiResearch Drawing No. 981109, attached at the end of this report.

The sonic orifices were calibrated on 24 January, 1968. The results of the calibration tests were previously reported in Reference 1-3. The probe coolant circuit was successfully proof-pressured, and leak- and flow-tested on January 10, 1968. These tests completed the preparation of the probe for inclusion and evaluation in the combustor test rig test program. An error analysis of the double-sonic orifice and calorimetric temperature-measuring techniques was completed in March of 1968. Results and discussion of the analysis were included in Reference 1-7.

Several forming and joining techniques developed for the gas-sampling probe were successfully applied to the fabrication of the double-sonic-orifice probe. Since both the double-sonic orifice and gas-sampling probes were intended for use in the segmented combustor test rig, commonality of parts was maintained wherever possible, and many of the parts are interchangeable.

A preliminary test plan for the probe was proposed for the combustor test series utilizing combustor inlet Mach numbers of 1.6 and 2.3. These tests were scheduled to begin several weeks after the termination date of 3 September 1968. No modifications to the original design have been made or proposed.

3.0 FLIGHTWEIGHT ENGINE MEASUREMENTS

3.1 PRESSURE-MEASUREMENTS SUBSYSTEM

3.1.1 Problem Statement

Pressure measurements are required at many points in the HRE flight engine for two purposes. These are (1) to achieve combustion control, and (2) to demonstrate engine performance. The general problem is to design and develop the best system for measuring the pressures, within such specified constraints as accuracy, frequency response, compatibility with control or data telemetry equipment, environmental conditions, system weight, cost, and producibility.

3.1.2 Topical Background

Measured values of pressure are required in the HRE control and data analysis operations because either a given pressure is itself a variable of interest or the pressure is one of the quantities used in the computation of a variable, such as Mach number or hydrogen mass-flow rate, which is not measured directly. Hence, different pressure measurements may have different requirements relating to accuracy, precision, and response time. The objective of the task of designing the pressure-measurement subsystem has been to try to meet these requirements within the constraints imposed by the characteristics of commercially available pressure transducers, the geometrical configuration of the engine, and limitations of weight, available space, and component system reliability.

The pressure measurements can be grouped into four major categories; (1) aerodynamic measurements, (2) combustion control and monitoring, (3) hydrogen flow control and monitoring, and (4) monitoring the performance of auxiliary systems. Most of the aerodynamic measurement points are located on the surfaces of the engine ahead of the combustion region. Included are a pitot-tube measurement at the nose of the spike, several points on the surface of the spike and leading edge of the outer body, and a base-pressure measurement at the tip of the nozzle cap. Combustion pressures are measured at various points on the engine surfaces next to the combustion zone and on surfaces of the nozzle after the combustion zone. Hydrogen pressures are required not only for flow determinations at various points in the system but also to monitor pressures in various hydrogen manifolds. Auxiliary systems which require pressure-monitoring include the spike-extension-and-retraction system, the helium-purge system, and the combustion-igniter system.

The variety and large number of pressure measurements are a consequence of the experimental nature of the engine. Most of the aerodynamic pressure measurements, for example, would not be required in a production-type engine. Since the HRE is an experimental device, it is essential to measure the aerodynamic properties in as much detail and as accurately as possible. In addition, since the aerodynamic properties are not yet known experimentally, it is difficult at present to make a wise choice of the locations for the aerodynamic measurements that would be required on a production engine. Similar arguments apply to combustion pressure measurements.

3.1.3 Approach

The design and development of the pressure-measurement subsystem are based on the use of commercial straingage-type pressure transducers. Because of temperature limitations, the transducers cannot in many cases be placed next to the pressure-measurement points. Consequently, the pressures must be conducted to the transducers through pipes. The transducers must also be mounted in thermally-controlled enclosures in order to avoid errors due to rapid temperature changes at the transducer. These two constraints impose the most significant design problems to be dealt with. The long pipes imply poor high frequency response in the indicated pressures. The rapid temperature changes which the transducers would experience during a flight test if they were not suitably thermally isolated would produce unacceptably large errors in indicated pressures.

Other less serious problems include (1) selecting the transducer types and ranges to withstand the maximum anticipated excess pressures without degrading the accuracy of the indicated pressures, (2) assuring that the transducers are electrically compatible with the electronic systems for control and for data telemetry, (3) designing a system of minimum weight, and (4) achieving a finished pressure-measurement system within the available time schedule and budget.

The frequency-response problem has been considered in a combined analytical and experimental approach. The analytical approach is to apply acoustic transmission theory to the transmission of a pressure change through a pipe to the transducer face. The experimental approach is to test various pipe configurations with a pneumatic function generator and associated instrumentation. This approach is discussed in detail in References I-3, I-7, and I-8. Experimental and analytical results obtained during the program are discussed in Reference I-8.

The approach to temperature control of the immediate environment of the transducers has been to employ thermal isolation by means of radiation shields and a substantial heat capacity of the transducer enclosure. Active control of the temperature would introduce additional complexity in the instrumentation system, therefore, we have proceeded on the expectation that passive control would be adequate, although active control has not been ruled out of consideration. Another aspect of the problem is to determine a realistic limit for the rate of temperature change that can be allowed for a given transducer without incurring too great an error in indicated pressure. This information is not available from the transducer manufacturers because their products are generally used in constant temperature environments. Accordingly, it has been planned to conduct some tests on transducers of the type which might be used in the HRE to determine the relationship between rate of change of temperature and error in indicated temperature. Rates of change between 0^0 and approximately $\pm 10^0$F/min would be studied. These rates of change correspond roughly to the expected rates of temperature change in a rather poorly thermally-isolated transducer in the HRE.

The excess pressure problem can be solved in several ways; one approach is to procure pressure transducers with stops to protect their diaphragms from excessive deformation. Another approach is to provide pressure relief valves to protect the transducers against overpressure. A third is to select transducer ranges to cover the maximum expected pressure excursion. The approach followed in this program is a combination of the first and third ones listed above. The use of special relief valves and other pneumatic or mechanical methods of limiting the pressure at the transducer has been ruled out on grounds of undesirable complexity and poor reliability of such methods.

The control and data recording systems have different electrical input characteristics. As a consequence, transducers used to generate control input signals must have electrical characteristics which differ from those used for recorded data. This problem is discussed in detail in Reference I-8.

3.1.4 Summary of Progress

Progress has been reported in References I-3, I-7, I-8, and 3-I. A brief summary of previously reported work is included herein.

A vacuum-deposited straingage-type of transducer was selected as the pressure sensor in the instrumentation system. Compared with the older wire straingage type, the vacuum-deposited straingage transducer can withstand greater shock and vibration levels without malfunction, and is inherently a more reliable and rugged instrument. Compared with a potentiometric device, the vacuum-deposited straingage transducer exhibits infinite resolution and is not subject to failure due to wear of moving contacts. The specific type of transducer selected was the Statham model PA 856 absolute-pressure transducer. Characteristics of this device are given in Reference I-7.

A procurement specification was written for the pressure transducers. The size, weight, operational characteristics, and requirements as to environmental conditions were compatible with HRE operational and environmental conditions and with the PA 856 transducer. The specification differed from the description of the standard PA 856 in that the HRE application required a higher bridge resistance and a different bridge-balance point than the PA 856. The standard PA 856 has a bridge resistance of about 350 ohms and a balance point at "zero" absolute pressure. The HRE transducer used for data recording requires a bridge resistance of 1000 ohms and a balance point at half-scale pressure. These requirements are embodied in the procurement specification.

The acoustic attenuation in long pneumatic lines was studied both analytically and experimentally. The analytical approach led to an equation for the transfer function of a pneumatic system comprising a small diameter pressure tap, a pipe of large diameter, and an instrument volume. The experimental approach yielded transfer functions of several lengths of 0.070- and 0.097-in.-diameter pipe with restrictions to simulate the pressure tap. Not enough time was available to carry out a thorough comparison of the theoretical equation with experimental data. The data, and such theoretical curves as were calculated, show similarity. It is concluded that after the theory is properly normalized, it can be used to approximate the behavior of a pneumatic system. A more detailed discussion is given in Reference I-8.

A preliminary thermal analysis of a transducer housing having a large heat capacity was made. It was concluded that shielding the enclosure against thermal radiation from hot interior surfaces of the engine was more important than providing a large heat capacity as a means of reducing the rate-of-change of transducer temperature. It is likely that multiple layers of aluminized Mylar will provide adequate thermal shielding. The transducer-mounting boxes were redesigned to be made of thin stainless steel sheet instead of thick aluminum.

The problem of how to connect the transducers to the cables has not been resolved. Two methods have been considered, each with advantages and drawbacks. One method is to weld the cable leads directly to the electrical contact pins of the transducer. This method results in reduced weight and less probability of a bad electrical connection. However, it does not permit easy replacement of an individual transducer in case of failure. The other method is to use cable connectors. Each transducer would be equipped with a short length (about six inches) of cable, terminating in a miniature connector. The cable to the control module or data recording system would terminate in a mating connector. This method assures ease of connecting or disconnecting an individual transucer, with a small decrease in system reliability.

The locations of the transducer-mounting enclosures were determined. Four locations in the engine were assigned for these enclosures, one each in the spike, inner body, nozzle, and outer body. Approximately 117 pressure transducers were required in the flightweight engine.

3.2 TEMPERATURE-MEASUREMENT SUBSYSTEM

3.2.1 Problem Statement

A temperature-measurement subsystem is required to determine metal and engine cooling temperatures during flight and ground tests. These temperature measurements are to be consistent with the desired accuracies for engine performance and structure behavior analyses, with the subsystem compatible with the anticipated environments within the engine structure. Also required under the metal and coolant temperature subsystem, is the sensor design and installation for real-time output compatible with the engine metal coolant control system.

The system is to be used with pulse-coded modulation (PCM) equipment during ground and flight testing, must be compatible with the engine jettisoning procedures and qualify under the Phase IIA qualification test conditions.

3.2.2 Topical Background

Temperature measurement of the metal and coolant temperatures for engine and structural performance analyses are to be provided. This instrumentation must be compatible and contained within the engine confines. Severe environmental conditions within the engine require special instrumentation procedures and approaches which may deviate from generally accepted conventional methods. Thermocouples were selected as the sensing devices for most of the temperature measurements. Where the range and extreme accuracy is above that possible by use of a thermocouple, platinum resistance sensors may be utilized. The number of sensors required to satisfy the recorded information for engine analyses will approach 100. Another 30 hydrogen coolant temperature sensors for the coolant control will be required.

The indicated temperatures from the sensors should be near the true measurand value with minimum corrections required for the true temperature evaluation.

The structural integrity of the control sensors to withstand engine environment is important. Since no redundancy of temperature sensors was provided, due to the limitation of space.

Conditioning the thermocouple output to satisfy the recording system's range capabilities will require the use of more than one thermoelectric sensor combination.

Relative movements between areas of the engine structure require that the thermocouple system be capable of withstanding this movement while still retaining the thermoelectric integrity of the circuit.

3.2.3 Overall Approach

The thermocouple is the basic sensor for the temperature subsystem installation. The constraints placed on the system by temperature, environment and structure rule out most other approaches when considering the total system requirements. Measurements not within the limits of a thermocouple due to accuracy and range limitations can be satisfied by platinum resistance sensors.

Simplification of the system is a requirement dictated by available space and environment compatibility. Using thermocouples of ungrounded configuration, the reference system for the thermocouples can be simplified by using a single power supply and reference-junction module for each thermocouple material and range. Present considerations show that two types of thermocouple materials and two ranges will be required to be compatible with the on-board PCM data acquisition system requirement.

The compensating-type reference junction is to be located in the pylon area, with appropriate thermocouple material leads routed from the sensor to the reference-junction location. Copper leads from the reference junction to the on-board PCM system, through a disconnect plug interface between pylon and aircraft is planned. The use of hard line (Swaged Inconel Sheath and MgO insulation) leads are planned for connecting the sensor to the reference junction. Power supplies for the compensating-type reference system will be located in the instrument bay of the test aircraft.

Several of the sensor installations must be compatible with the structures brazing-cycle procedures, but where possible, the sensors will be installed after the engine braze-cycle is completed.

3.2.4 Historical Summary

Initial efforts for the temperature subsystem involved the definition of the measurand requirements which existed for the intended ground and flight test range of the engine. Much of this information was not immediately available at the start of the subsystem task.

The constraints placed upon the subsystem by engine structures, environment, and the PCM recording system limited the available approaches to the task.

Due to these constraints, the thermocouple appeared to be the most satisfactory type of sensor for the task. The resistance sensor may have application in certain specialized areas especially at cryogenic temperatures with limited range.

The constraint imposed by the PCM system due to its fixed input range, indicated that full-scale ranging of certain sensor outputs could not be achieved with a single thermocouple material. Material selection based on an optimized range and reference level, resulted in the use of Chromel/Constantan and Geminol P and N, each with its own reference level, to satisfy the range and accuracy requirement.

Early analysis of the subsystem thermocouple circuit indicated the system with grounded sensors and individual compensated-type reference junctions for each circuit (a requirement for such a system) with copper output leads from reference modules within the engine, would result in the best overall accuracy from the thermocouple circuit.

The sensor installation was constrained by the fabrication schedule of the engine buildup. Procedures and approaches to make the installation of the sensor follow the engine buildup were made wherever practical.

The specialized nature of the installation and the constraints imposed by the engine environment on each section of the subsystem, made each component a case of special application. In view of the above very little actual hardware was acquired before the terminal date for the temperature subsystem task.

As the engine environment and space became better defined, the original plan of grounded-thermocouple with individual reference circuits appeared less suitable to the task installation requirements. The use of ungrounded sensors could simplify the overall system, and is achievable using proven techniques except for the hot-skin sensor. The coaxial ungrounded sensor was developed to satisfy the hot-skin sensor requirement.

By ungrounding of all the sensors, a common-lead system was possible. The reference junction could be moved to the pylon area and use of a common power supply installed in the test aircraft instrumentation bay was proposed.

The reference junction was modular in concept with 45 channels combined in each module section. Three modules would be required to satisfy the subsystem recording task.

Defining sensor requirements for the control system was considered part of the temperature subsystem task. Analysis had shown that a bare-bead configuration would be necessary to meet the response requirement of the control system. Referencing of the control sensors was not part of the subsystem task.

Several cryogenic measurements near the liquid hydrogen point in the fuel system would require the use of resistive sensing devices to satisfy the accuracy requirement.

Routing of the sensor leads was not defined, but will be determined on the engine mockup model. Several designs are being considered where thermocouple leads will be subject to traversing movement of the spike in relation to the engine inner body.

3.2.5 Subsystem Task Efforts

3.2.5.1 System Constraints

Ambient environment for the temperature-measurement subsystem components was subject to a wide range of temperature extremes and difficult installation, and generally incompatible with routine instrumentation. Minimal environmental conditioning of the subsystem components was planned.

The constraints placed upon the temperature sensor selection by the engine fabrication procedures generally limits the basic selection to the thermocouple-type sensor. Experience has shown that resistive devices cannot be subjected to brazing cycles of 2000°F without extreme calibration shifts. In light of the fabrication constraints imposed on the measuring system, the efforts have been concentrated in adapting the thermocouple, where possible, to satisfy the subsystem measuring requirement.

The PCM system aboard the test aircraft restricts signal level of the subsystem components to ±15 millivolts full-scale. Ranging for maximum resolution must be conditioned to meet these requirements. These limitations, coupled with the installation constraints, have led to the selection of the thermocouple as the basic sensor.

Development of a coaxial thermocouple for hot-skin sensing allowed incorporation of an ungrounded temperature sensing system.

Early consideration was given to sharing some of the same sensors for control and recording applications. This approach was abandoned, due to the fact that requirements (response, range, sensitivity, etc.) were incompatible.

3.2.5.2 Sensor Location and Configuration

The measurand locations were tabulated in Reference I-7, giving pertinent data relative to the measurement location, material, range, number, etc. Technical data reports have defined the sensor configurations adaptable to the measurement, but the description of the specific location and proposed installation have not been described in these reports. There are numerous measurements to be made within the manifold sections of the engine. Consistent with the overall simplification of the subsystem, an analysis was made to standardize on an immersion length for all sensors used in these manifold sections. For a $10^{\circ}F$ conduction error, the required thermocouple L/D ratio ranges from 2.8 to 6.9 as shown in Table 3.2-1. The calculated hydrogen mass fluxes for the manifolds under consideration are tabulated in Table 3.2-2. The thermocouple configuration to be used in the manifold sensing is shown in Figure 3.2-1b. The recommended immersion length should be at least 0.28 in. from the thermocouple tip to the inner manifold surface (L/D = 7.0).

Figures 3.2-2 through 3.2-11 show the thermocouple installations for the structures, controls, and fuel system within the engine body. Radial orientation of the sensor locations, where applicable, is referenced in Figure 3.2-12. Figure 3.2-13 shows the four basic sensors relative to the subsystem. Not shown in the sensor breakdown are the following temperature sensors:

Fuel System

(a) Shut-off and Purge Valve Inlet

(b) Fuel Plenum

(c) Turbine Inlet

(d) Turbine Discharge

(e) Dump Valve Inlet

(f) Dump Valve Outlet

Instrumentation

(a) Reference Junction Monitor

(b) Thrust Block

(c) Instrumentation Package

(d) Pressure Transducer Monitor

Resistance Probes

(a) Flowmeter

(b) Purge Valve Inlet

TABLE 3.2-1

THERMOCOUPLE INSTALLATION REQUIREMENT (L/D_o) FOR 10^oF CONDUCTION ERROR

Section	Item	X-Station, in.	Hydrogen Temp Range T_f, ^oR	Maximum Differences (T_f-T_w), ^oF	H.T. Coefficient h_c, $Btu/hr-ft^2-^oF$	D_o = 0.040 in. (L/D_o)
Nozzle	Cross-over manifold	66.4	300-800	500	465	4.0
	Nozzle plenum	77.33	40-200	500	762	3.0
Inner shell	Outer manifold	51.0	800-1700	900	353	6.9
	Cross-over manifold	65.0	300-800	500	465	4.0
Spike	Coolant outlet manifold	46.0	800-1500	700	397	4.7
	Spike tip plenum	5.2	40-200	500	726	3.1
Leading edge	Inlet manifold	41.445	40-200	500	337	5.0
	Outlet manifold	43.0	250-700	450	343	4.5
Outer shell	Cross-over manifold	44.0	250-700	450	309	4.8
	Outlet manifold	51.0	500-1700	900	309	6.9
	Real-supply manifold	64.9	250-700	450	251	5.3
	Coolant-in manifold	67.6	40-200	500	804	2.8

Notes:
1. Columns 1 through 4 from notes dated 5-28-68 by D. R. Osborn.
2. Columns 6 and 7 at local Mach 6.5, 88,000 ft, per page 5-25 of Report AP-68-3754.
3. Column 7 applies to thermocouple Installation Drawing 980122.
4. T_f = fluid temperature, T_w = wall temperature.

TABLE 3.2-2

CALCULATED HYDROGEN MASS FLUXES

Section	Item	Mass Flux, (ρV), lb/sec-ft^2		
		Inlet	Outlet	Duct
Nozzle	Cross-over manifold	41	7	6
	Nozzle plenum			163
Inner shell	Outer manifold	17	53	15
	Cross-over manifold	41	7	6
Spike	Coolant outlet manifold	47	81	42
	Spike tip plenum			142
Leading edge	Inlet manifold	196	19	30
	Outlet manifold	20	151	31
Outer shell	Cross-over manifold	151	25	26
	Outlet manifold	85	52	3
	Rear supply manifold	22	149	14
	Coolant-in manifold			171

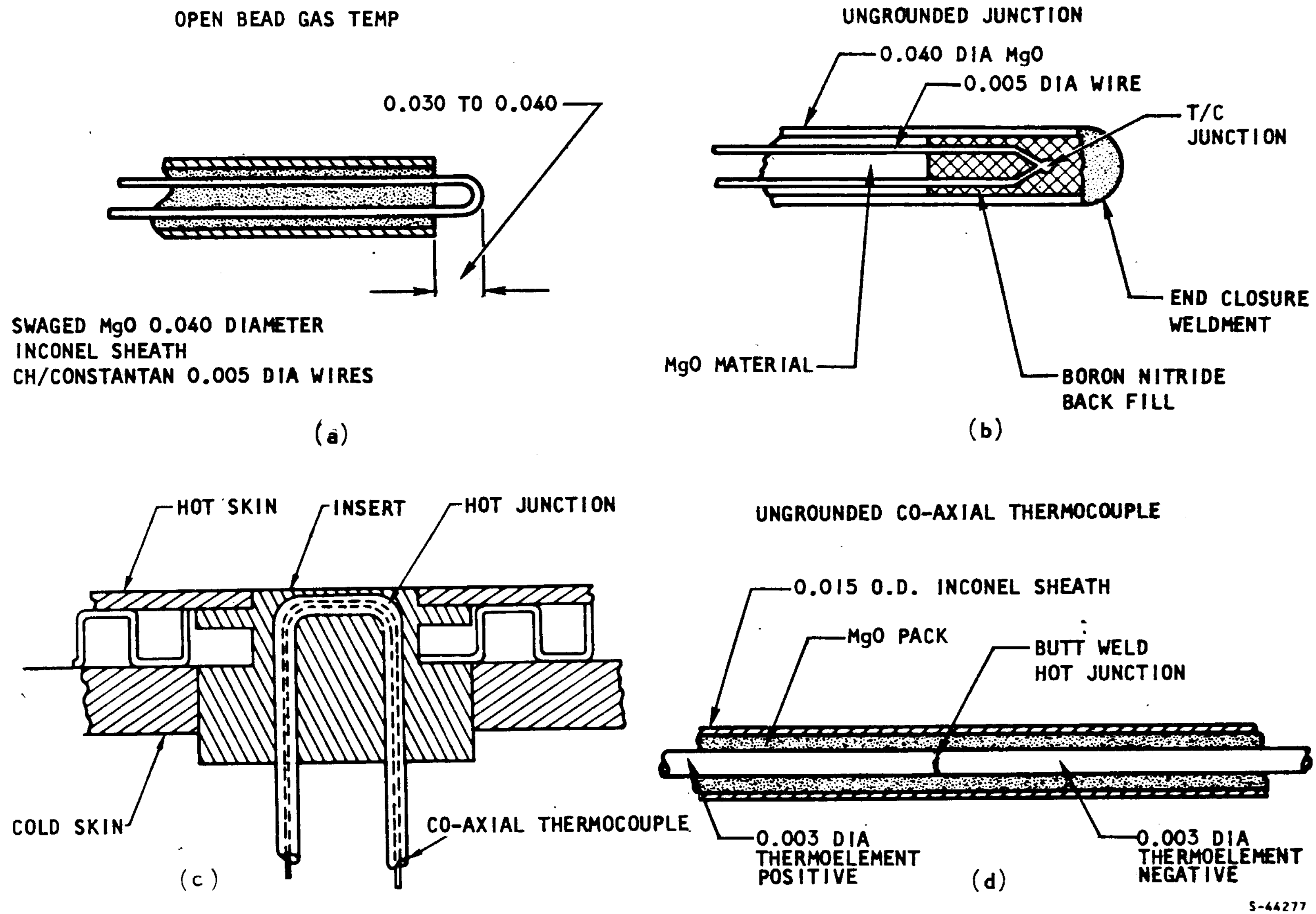

Figure 3.2-1. Thermocouple Configuration for Manifold Sensing

·m 2427

AiRESEARCH MFG. CO.

DATE 5-28-68
PREPARED BY D. R. OSBORN
CHECKED BY

CALC. NO.
MODEL
PART NO.

NOZZLE SECTION

THERMOCOUPLE INSTALLATIONS

STAT. - #66.4
CROSS OVER MANI
H_2 (300 - 800°R)
1 REQ.
CH/CON

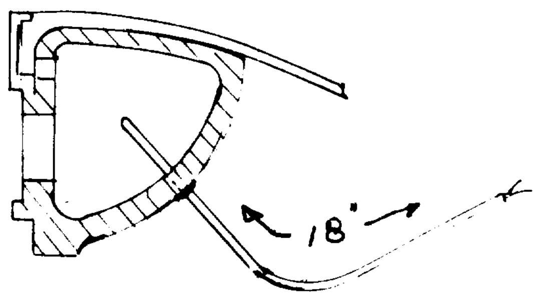

RADIAL LOC. = 0°

STAT - #77.35
NOZZLE PLENUM
H_2 (40 - 200°R)
1 REQ.
CH/CON

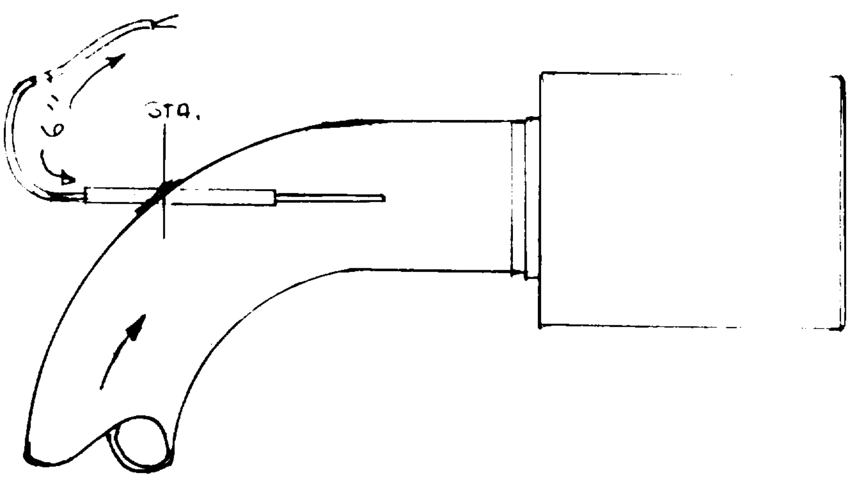

STATION
0° 68.6 - (200-700°R)
0° 75.6 (40-500°R)
1 EA REQ
COLD SKIN TEMP.
CH/CON

STATION
65.6 (350 - 600°R) (0°)
ACCUMULATOR TANK
1 REQ
COLD SKIN TEMP
CH/CON

STATION
5° 68.6 (500-1400°R) GEN P & N
5° 75.6 (300 - 900°R) CH/CON
1 EA. REQ
HOT SKIN TEMP

TOTAL REQ - 7

Figure 3.2-2. Thermocouple Installations

m 2427

AIRESEARCH MFG. CO.

DATE 5-28-68 CALC. NO.

PREPARED BY D.R. Osborn MODEL

CHECKED BY PART NO.

INNER SHELL

STATION #51 (355° - 175°) LOCATION

OUTER MANIFOLD

2 REQUIRED

H_2 (800 - 1700°R)

GEMINOL P/N

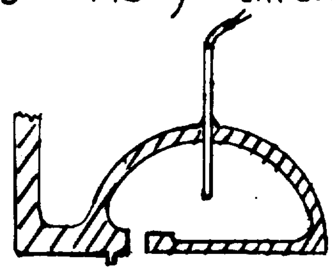

STATION #65 (0°)

CROSS OVER MANIFOLD

1 REQUIRED

H_2 (300 - 800°R)

CH/CON

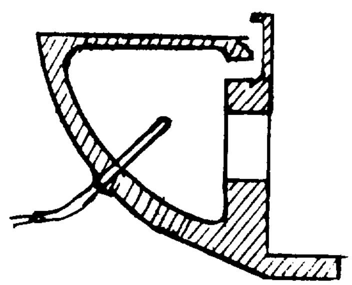

STATION #59.5 (0°)

ACTUATOR FRAME

1 Req (300 - 800°R)

CH/CON

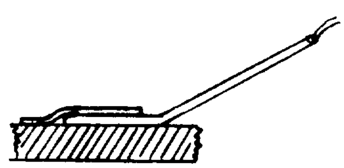

STATION #62.5 (0°)

ACTUATOR TUBE

1 Req (350-600°R)

CH/CON

STATION #57 (0°)

STRUT SOCKET

1 Req. (500-1600°R)

GEMINOL P/N

STATION #64.0 (0°)

ACTUATOR MTG. PAD

1 Req (200 - 800°R)

CH/CON

STATION #53 (1 Req) (800 - 1700°R) (5°)
#54 (1 Req) (800 - 1700°R) (0°)
#57.25 (1 Req) (600 - 2200°R) (0°)
#58.25 (1 Req) (600 - 1600°R) (5°)

COLD SKIN

GEMINOL P/N

Figure 3.2-3. Thermocouple Installations

AIRESEARCH MFG. CO.

DATE 5-28-68
PREPARED BY DR. OSBORN
CHECKED BY

CALC. NO.
MODEL
PART NO.

INNER SHELL

STATION #52 0°, 60°, 120°, 180°, 240°, 300°

CONTROLS

H_2 6 REQ
(800 - 1700°R)
CH/CON

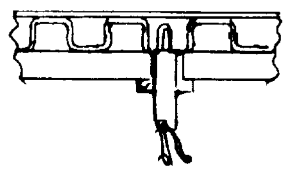

STATION #53 (2 REQ) (500 - 2200°R) (0° - 180°)
#54 (1 REQ) (1200 - 2200°R) (0°)
57.25 (1 REQ) (800 - 2200°R) (0°)
58.25 (1 REQ) (800 - 2200°R) (0°)

HOT SKIN

GEMINOL P & N

STATION #58

CONTROLS

H_2 6 REQUIRED
(800 - 1800°R)
CH/CON

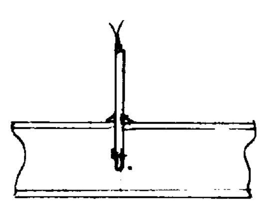

BARE BEAD

TOTAL REQ
16 - STRUCTURES
12 - CONTROLS

Figure 3.2-4. Thermocouple Installations

rm 2427

AiResearch Mfg. Co.

DATE 5-28-68
PREPARED BY D.R. OSBORN
CHECKED BY

CALC. NO.
MODEL
PART NO.

SPIKE
THERMOCOUPLE INSTALLATION

STATION # 46
COOLANT OUTLET MANIFOLD
2 REQUIRED
H_2 (800-1500°R)
GEMINOL P & N

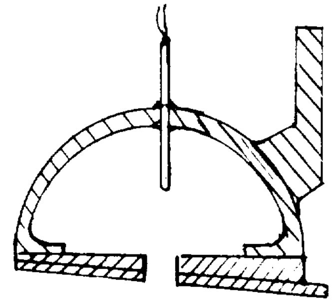

5° & 355°

STATION # 49
CONTROLS
6 REQUIRED
H_2 (600-1500°R)
CH/CON

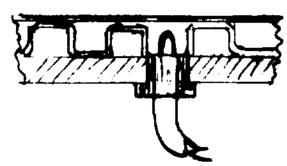

MUST BE SEALED IN BELLOWS AREA, THESE LIE UNDER BELLOWS,
0°, 60°, 120°, 180°, 240°, 300°

STATION # 5.2
SPIKE TIP PLENUM
1 REQUIRED
H_2 (40-200°R)
CH/CON

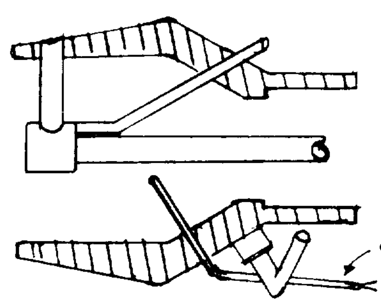

5°

STATION # 47.5
BELLOWS
1 REQUIRED
COLD SKIN (500-1600°R)
GEMINOL P & N

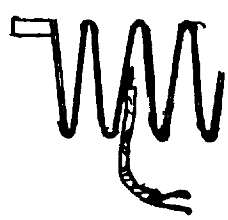

0°

STAT. # 24 (1 REQ) 355°
35.7 (1 REQ) 355°
44.3 (1 REQ) 5°
COLD SKIN
CH/CON

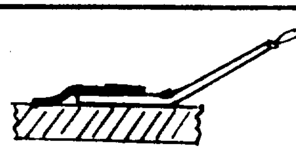

STAT. # 24 CH/CON 5°
35.7 CH/CON 5°
HOT SKIN 44.3 GEM. P & N 355°

TOTAL REQ
10 - STRUCTURES
6 - CONTROLS

Figure 3.2-5. Thermocouple Installations

12427

AiResearch Mfg. Co.

DATE 5-28-68
PREPARED BY D.R. OSBORN
CHECKED BY

CALC. NO.
MODEL
PART NO.

LEADING EDGE
THERMOCOUPLE INSTALLATION

STAT # 41.445
INLET MANIFOLD
2 Req. 180° APART
H_2 (40-200°R)
CH/CON

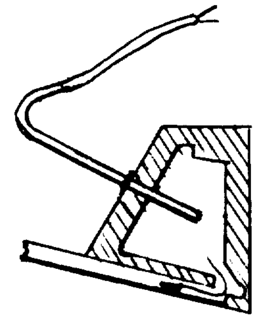

355° & 175°

STATION # 43.0
OUTLET MANIFOLD
2 REQ 180° APART
H_2 (250-700°R)
CH/CON

STATION # 43.4
OUTLET MANIFOLD FLANGE
" (200-1000°R)
COLD SKIN
CH/CON 1 REQ

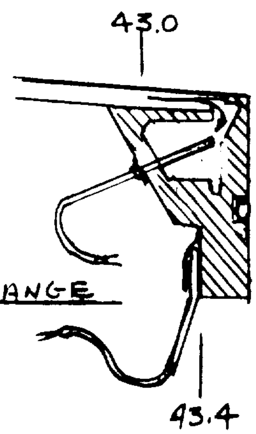

0° & 180°

0°

STATION # 41.9
CONTROLS H_2
6 REQ. CH/CON

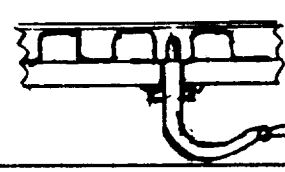

0°, 60°, 120°, 180°, 240°, 300°

STAT. # 37.6 1 REQ (I.J.)
38.4 1 REQ (O.J.)
40.4 2 REQ (O.J.)
COLD SKIN CH/CON

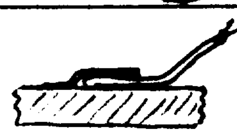

0°
0°
5° & 185°

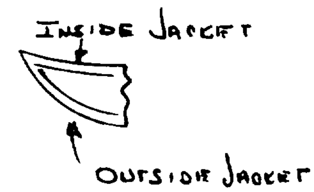

STAT # 38.4 1 Req O.J. 0°
40.4 2 Req O.J. 0°-180°
HOT SKIN CH/CON

TOTAL REQ -
12 STRUCTURES
6 CONTROL

Figure 3.2-6. Thermocouple Installations

OUTER SHELL

STATION #44
CROSS OVER MANIFOLD
1 REQUIRED
H_2 (250 - 700 °R)
CH/CON

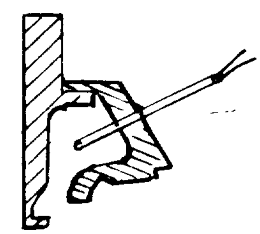

0°

STATION #51.0
OUTLET MANIFOLD
2 REQUIRED
H_2 (800 - 1700°R)
GEMINOL P!N

STATION #51.0
OUTLET MANIFOLD
1 REQ
COLD SKIN (500 - 1700°R)
GEMINOL P!N

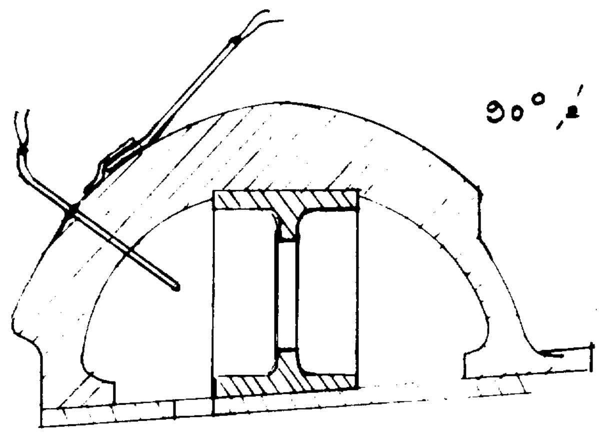

90° & 270°

45°

STATION #64.9
REAR SUPPLY MANIFOLD
1 REQUIRED
H_2 (250 - 700°R)
CH/CON

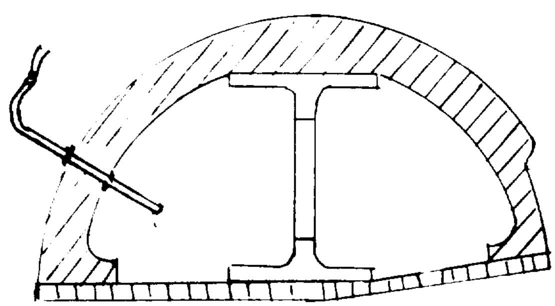

0°

STATION #67.6
COOLANT IN MANIFOLD
2 REQUIRED
H_2 (40 - 200°R)
CH/CON

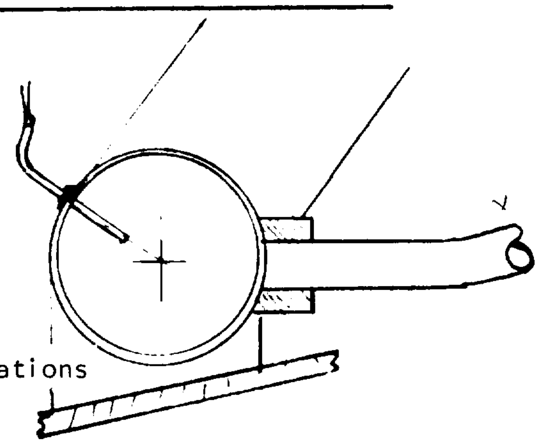

0° - 180°

Figure 3.2-7. Thermocouple Installations

AIRESEARCH MFG. CO.

DATE 5-28-68
PREPARED BY D.R. OSBORN
CHECKED BY

CALC. NO.
MODEL
PART NO.

OUTER SHELL

STATION # 50.50
CONTROLS
H_2 (600-1700°R
6 REQ
CH/CON

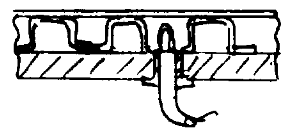

30°, 90°, 150°, 210°
270°, 330°,

STATION # 50.25
COLD SKIN JACKET
90° APART
2 REQ. (700-1600°R)
CH/CON

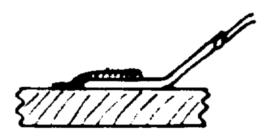

5° & 180°

STATION # 50.25
HOT SKIN
1 REQ INLINE WITH STRUT ℄
(1200 - 2200°R)

0°

STATION # 54.16
CONTROLS
H_2 (800-1700°R)
6 REQ
CH/CON

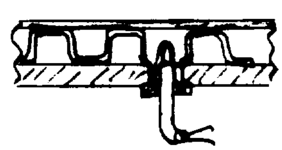

35°, 90°

STATION # 54.16
COLD SKIN JACKET

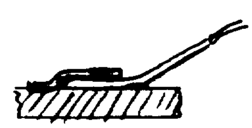

175° & 185°

2 REQ (700-1600°R)
CH/CON

STATION # 53.8
HOT SKIN
1 REQ (800-2000°R) IN LINE STRUT ℄
GEMINOL P & N

Figure 3.2-8. Thermocouple Installations

2427

AIRESEARCH MFG. CO.

DATE 5-28-68
PREPARED BY D. R. OSBORN
CHECKED BY

CALC. NO.
MODEL
PART NO.

OUTER SHELL

STATION #62.3 (0°)
HOT SKIN
1 REQ (800-1800°R)
GEMINOL P & N

STATION #62.5
COLD SKIN
1 REQ (300-1000°R)
CH/CON

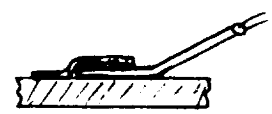

(5°)

TOTAL REQUIREMENTS

15 - STRUCTURES
12 - CONTROLS

Figure 3.2-9. Thermocouple Installations

rm 2427

AIRESEARCH MFG. CO.

DATE 6-6-68
PREPARED BY R.Q. OSBORN
CHECKED BY

CALC. NO.
MODEL
PART NO.

FUEL SYSTEM

STATION # 43.0
H_2 (800 - 1700°R)
REQUIREMENTS
CONTROLS - 1 REQ
CH/CON
MONITOR - 2 REQ
GEM P&N
INJECTOR #1
(INNER BODY)

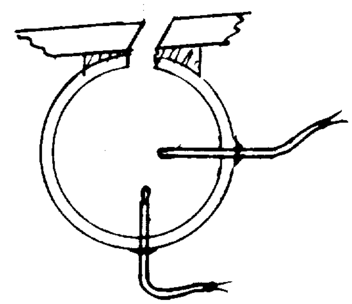

STATION # 48.5
H_2 (500 - 1600°R)
GEM. P&N 2 REQ.
(OUTER BODY)
INJECTOR # 1

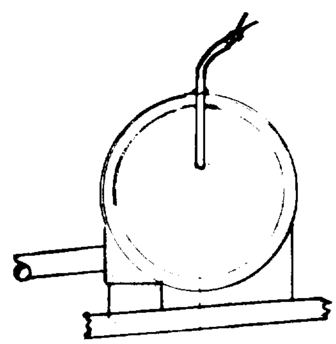

STATION # 54.6
H_2 (800 - 1700°R)
GEM P&N 2 REQ.
INJECTOR # 2
OUTER BODY

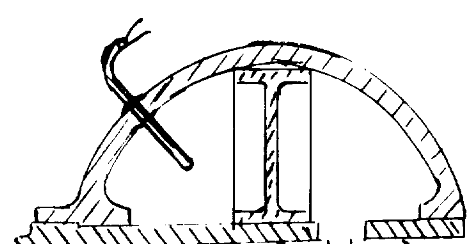

STATION # 59.4
H_2 (800 - 1700°R)
GEM. P&N 2 REQ
INJECTOR # 3
OUTER BODY

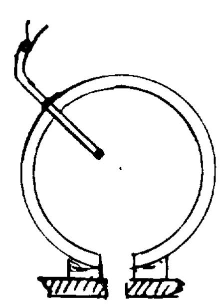

Figure 3.2-10. Thermocouple Installations

AiRESEARCH MFG. CO.

DATE 6-6-68
PREPARED BY D. R. OSBORN
CHECKED BY

CALC. NO.
MODEL
PART NO.

FUEL SYSTEM

STATION # ~~55.67~~ 56.25
H_2 (800 - 1700°R)
INJECTOR #2
INNER BODY
CONTROLS - 2 REQ - 1 USED
CH/CON
MONITOR - 2 REQ
Gem P/N

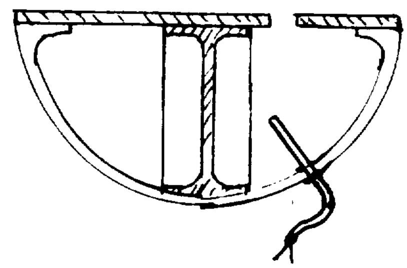

STATION # 59.53
H_2 (800 - 1700°R)
INJECTOR #3
INNER BODY
CONTROLS - 2 REQ - 1 USED
CH/CON
MONITOR - 2 REQ
GEMINOL P/N

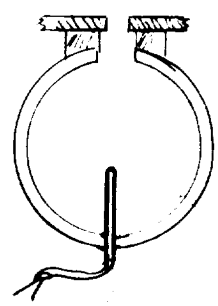

Figure 3.2-11. Thermocouple Installations

AIRESEARCH MFG. CO.

DATE
PREPARED BY
CHECKED BY

CALC. NO.
MODEL
PART NO.

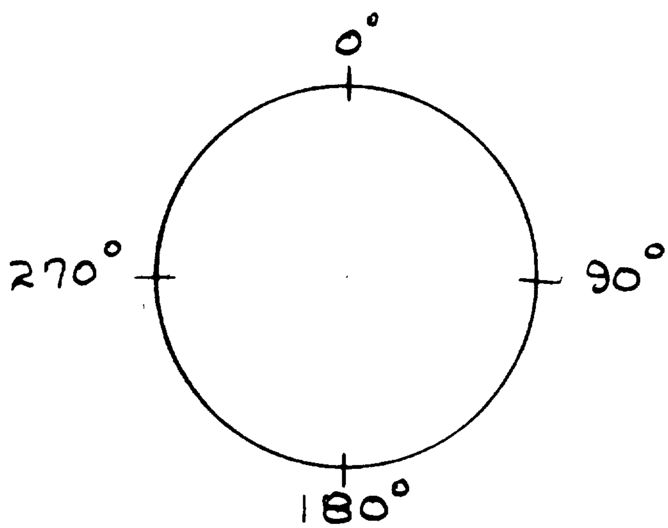

LOOKING AFT, STANDING AT SPIKE TIP

Figure 3.2-12. Temperature Instrumentation Subsystem Radial Orientation

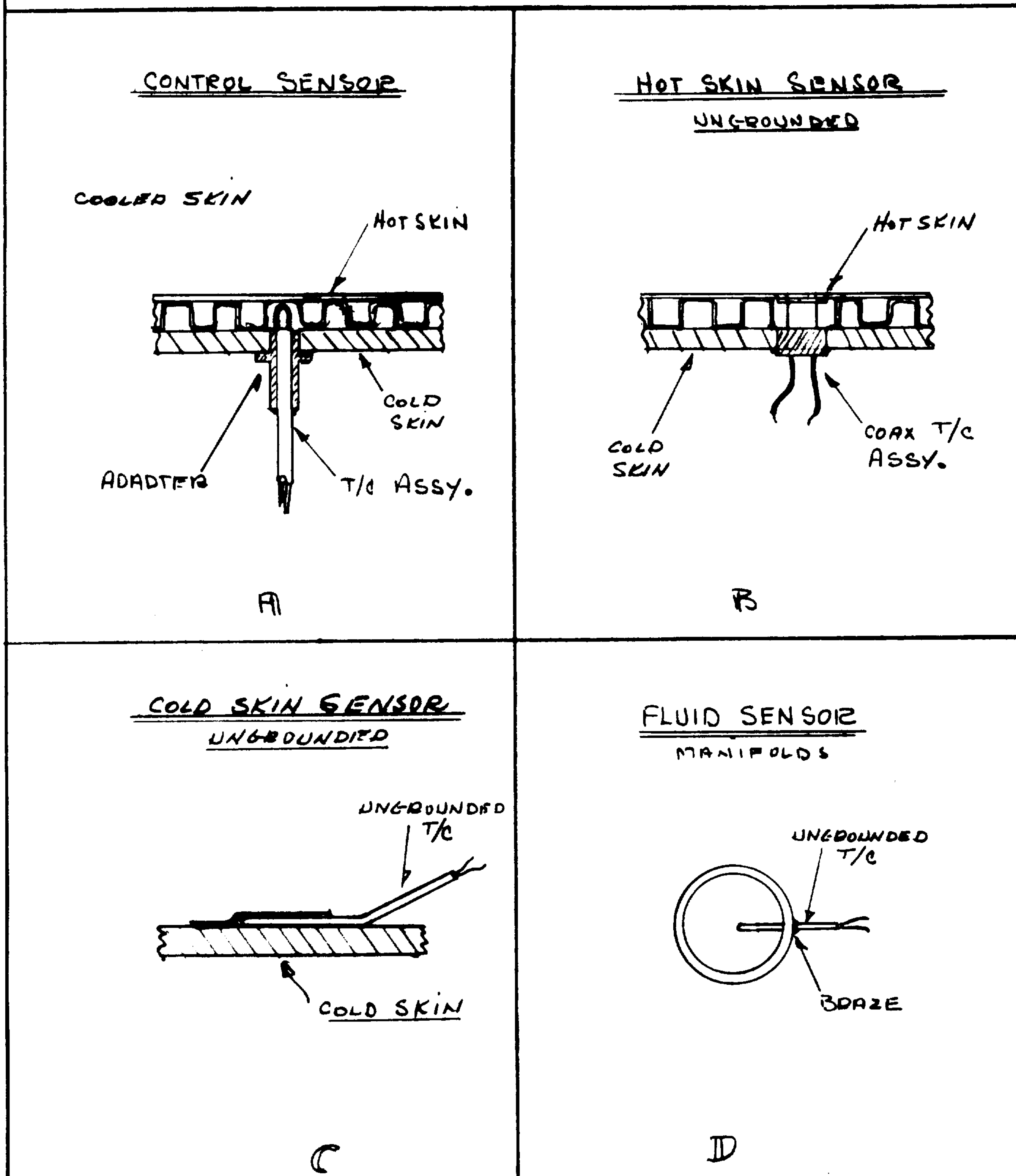

Figure 3.2-13. Basic Installations - Thermocouple

(c) Pump Inlet

(d) Pump Discharge

The subsystem design allows for temperature-sensing contingencies beyond the tabulated measurand locations for the thermocouple sensors.

The station locations as referenced, are based on the spike in full-open position.

3.2.5.3 Thermocouple System

The thermocouple system in relation to the engine is shown in the simplified schematic of Figure 3.2-14. Since the sensing locations were covered in a previous section of this report, reference here will be confined to the remaining portions of the system.

Terminating the wires of a thermoelectric circuit demands that certain precautions be observed. Reference 1-3, Section 6.3.2.1.6 and Figure 6.3-7 describes the termination methods proposed where thermoelectric joining is required. The continued effort to simplify the components resulted in the termination configuration as shown in Figure 3.2-15. This method amounts to a simplification in fabrication time, reduction in weight, and accessibility for installation on contoured surfaces. The Al_2O_3 may be sprayed directly to the engine internal surface and the structure used as the termination base. To protect the termination from possible damage a thin blanket of insulating material is placed over the spliced terminals and then a sheet of thin stainless steel material spot-welded over the insulation to retain and protect the wire from damage. The location of these terminal points were to be determined when the wire routing was installed in the engine mock-up assembly.

During translation of the spike, the thermocouple wires are required to flex a distance of about 5.3 in. The thermocouple wires must be adequately supported throughout the excursion to prevent a vibration-induced failure of the wire leads. The supporting mechanism must also produce a minimum, predictable degree of wire flexing. Figures 3.2-16 and 3.2-17 show a prototype model scissors-type of transverse fabricated to study the feasibility of traversing the distance using hard-line (swaged) materials. The advantages of using hard-line leads of the same material as the sensor has been covered in earlier TDR. The design shown in the photos would satisfy the traverse requirement; however, structure-wise it was felt the mechanism could stand simplification. These simplification efforts are given in Reference 1-8, Para 5.2.5 and in Figure 3.2-18 of this report.

The nozzle section of the engine being removable for access to the components in the aft section of the inner body, requires the sensing circuits between the cooled-skin of the nozzle section and the routing through the inner body to have a disconnect capability. This has been taken care of by making the disconnect accessible for the pressure lines and temperature leads when the nozzle plenum cap is removed.

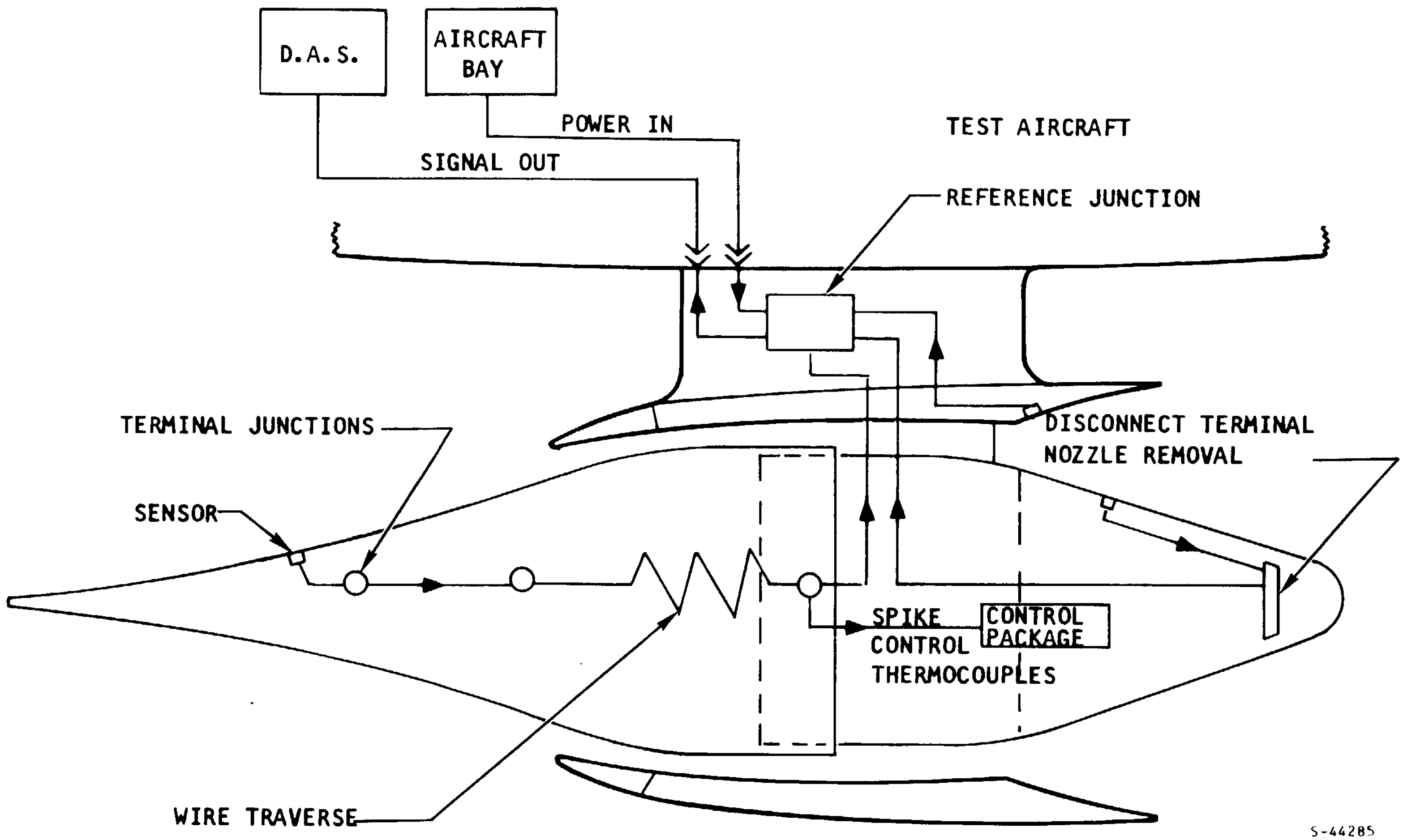

Figure 3.2-14. Engine Metal and Coolant Temperature Subsystem-Thermocouples

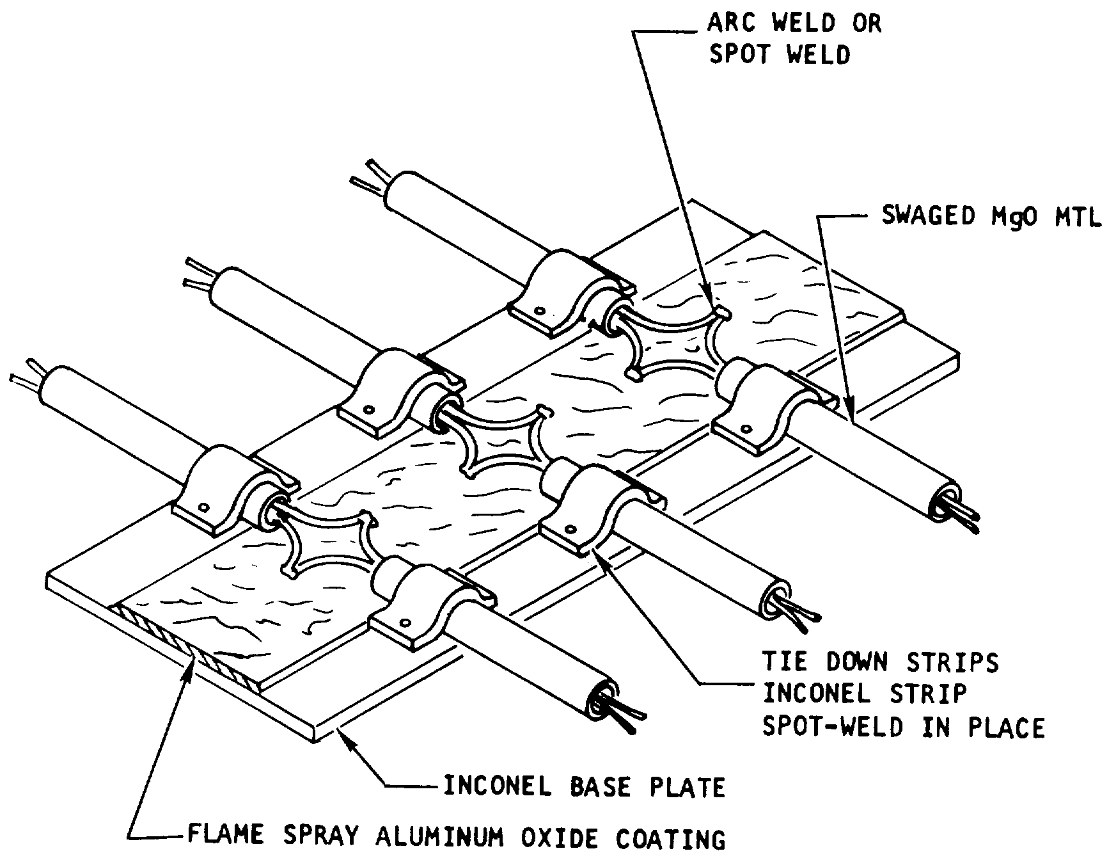

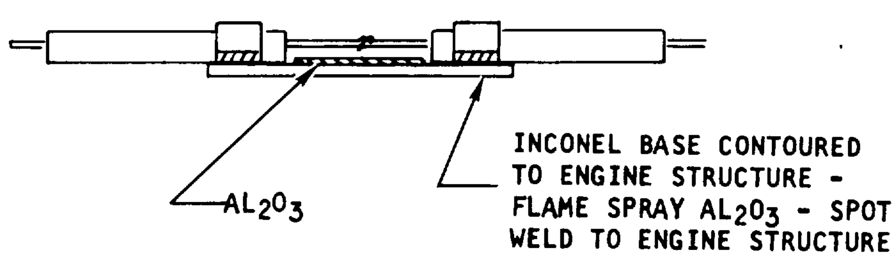

TERMINATION CONFIGURATION

S-44281

Figure 3.2-15. Termination Configuration

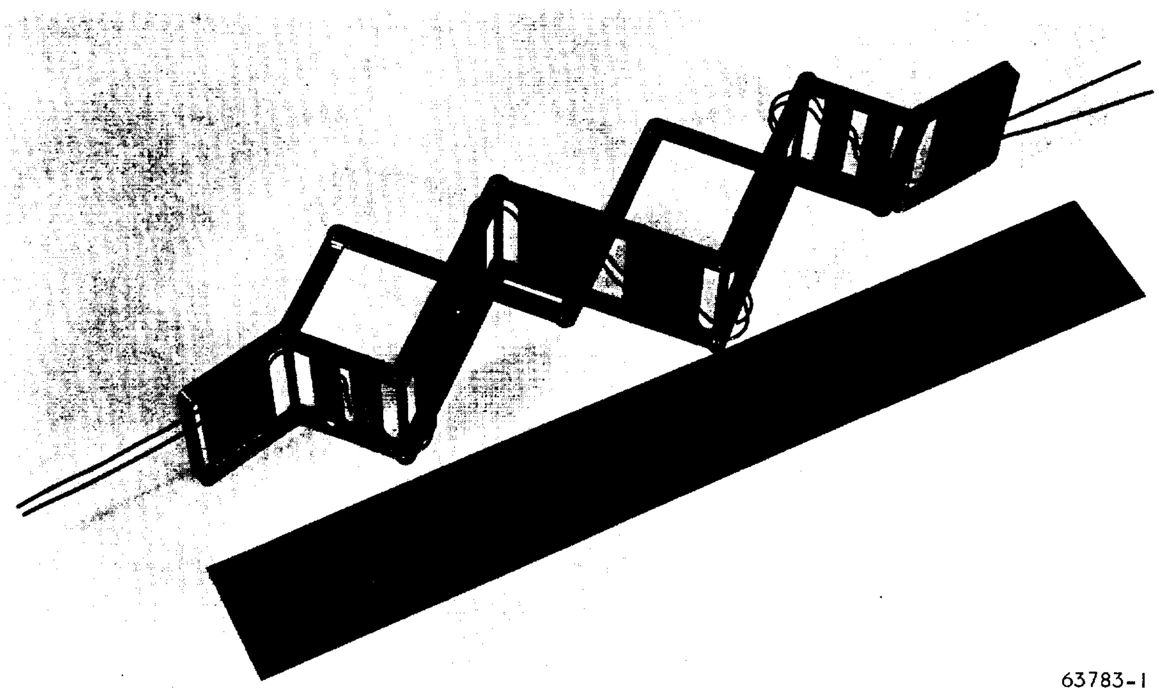

63783-1

Figure 3.2-16. Traverse Mechanism - Open

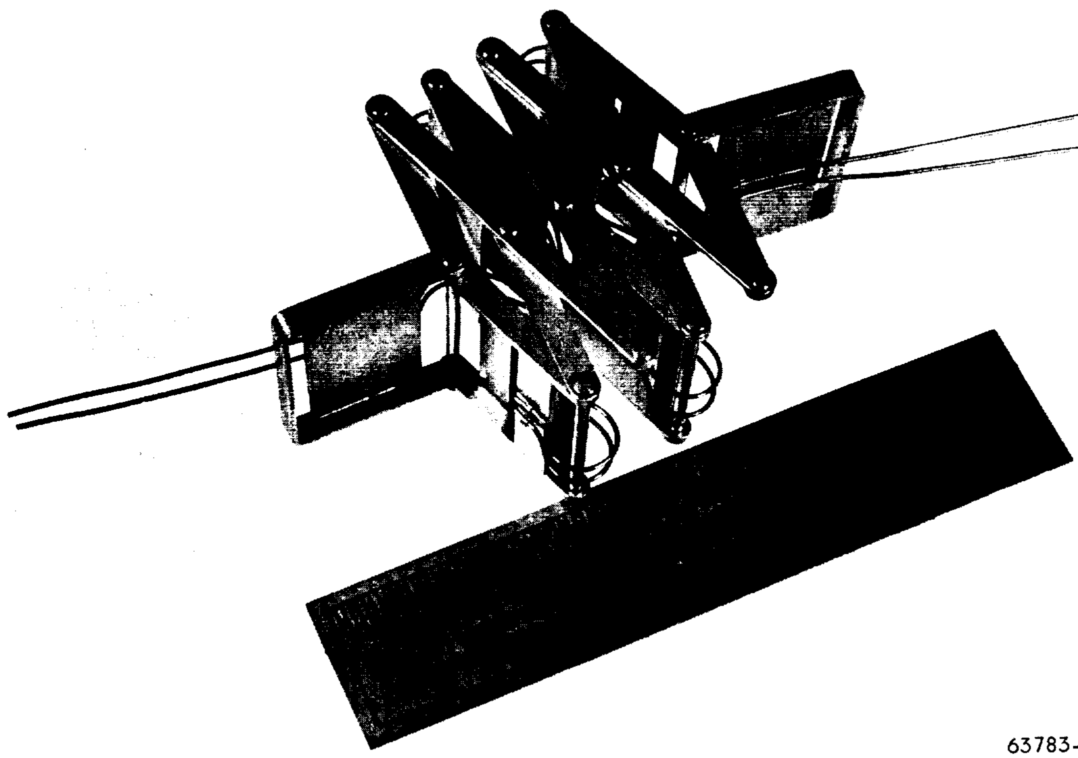

Figure 3.2-17. Traverse Mechanism - Closed

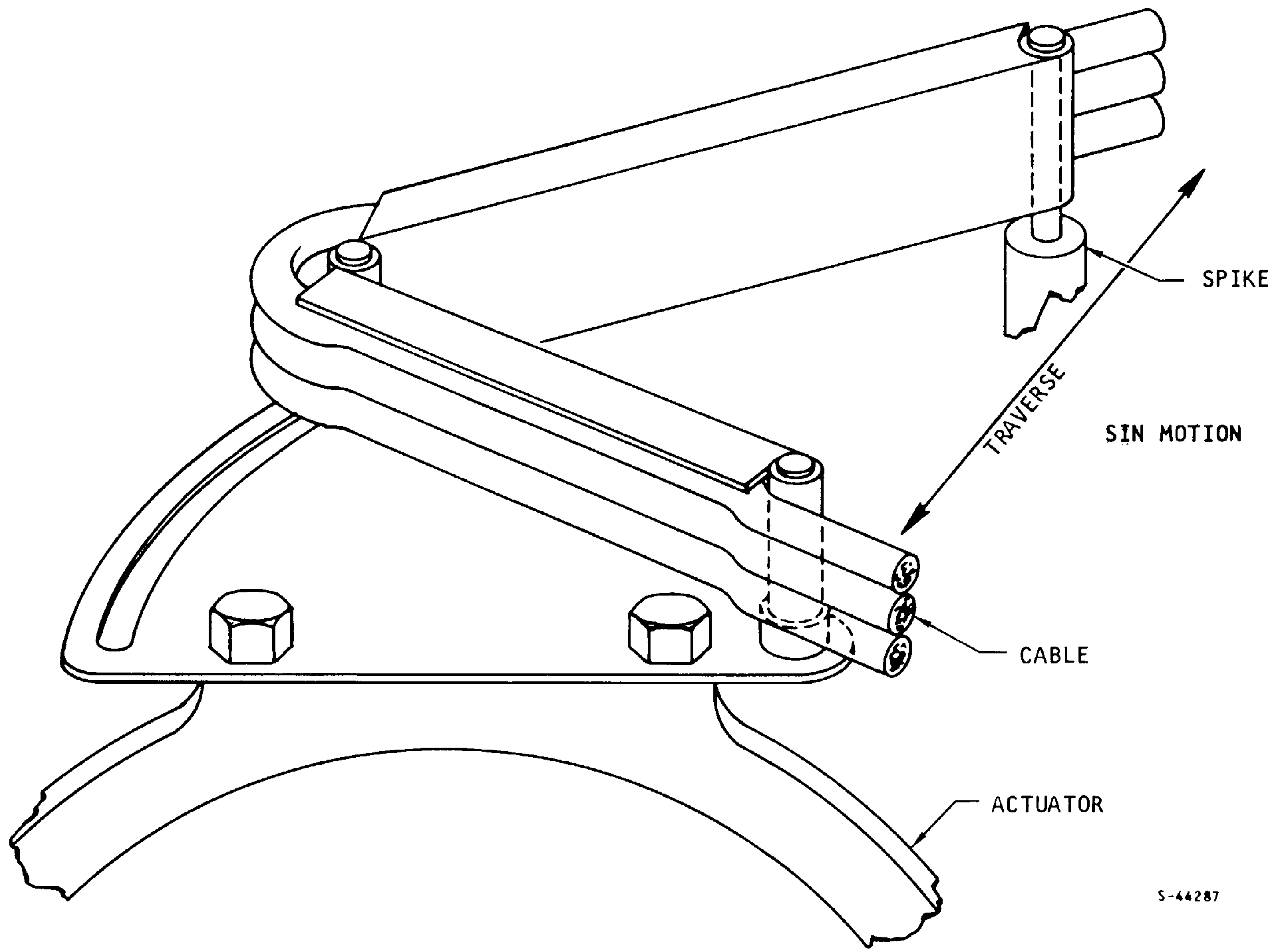

Figure 3.2-18. Single Pivot Scissors - Wire Traverse

The reference junction is located within the pylon area just forward of the thrust block. The present requirements indicate the need of three junction modules; each module capable of handling 45 circuits of a specific thermocouple material at a set reference level. The unequal distribution of the thermocouple types requires that three sections be used even though the total quantity of circuits is less than the capability of two reference modules. Design details for the reference-junction modular concept were presented in Reference I-8, Para 5.2.6.

The compensating-type reference junction requires bridge supply voltages which are well regulated. The power supply for the reference modules are placed in the test aircraft instrument bay. Control-sensing lines from the reference junction to the power supply are necessary to apply bridge-voltage regulation at the compensating network. The required power supply voltage and regulation is 5 volts ±0.05 percent.

3.2.5.4 <u>Static Error Analyses</u> (Refer to Table 3.2-3)

The analysis of the subsystem errors associated with the two thermocouple materials to be used in the system are reviewed in this section. The manufacturing tolerance placed on the limits of error assigned to the respective thermocouple material is quoted by the supplier as being a guaranteed limit of error. The errors associated with the PCM system are 3σ. The following definitions apply to the treatment included.

Guaranteed maximum error	No error will be greater than the guaranteed maximum error
3σ error	The probability is that 99.7 percent of all errors will lie between the limits $\pm 3\sigma$
Standard error	$\pm 1\sigma$
Probable error	$\pm 0.675\sigma$. The probability is that 50 percent of all errors will lie between the limits $\pm 0.675\sigma$

The random errors are summed by the root-sum-square method. Like-errors associated with similar system components are summed by a root-mean-square method.

The temperature errors associated with the system are maximum in the cryogenic areas where the thermal EMF output is at a minimum, and the reflected errors of the reference junction and associated subsystem components are maximum. Characteristics of the Chromel/Constantan at cryogenic temperatures are based on past experience and application.

The errors due to inhomogeneity of the thermocouple material when placed in zones of steep temperature gradients are weighted inputs based on past experience with thermocouple materials and the projected application of the thermoelectric material in the flightweight engine.

TABLE 3.2-3

TEMPERATURE SUBSYSTEM ERROR ANALYSIS

Subsystem	Chromel/ Constantan		Geminol P and N	
	Temp, ^{o}F	μV	Temp, ^{o}F	μV
Reference junction set point	±1/2	17	±1/2	10
Wire routing, 4 terminations	±3	100	±4	56
Inhomogeneity in steep temperature gradient		75		25
Reference junction bridge voltage reg, 0.05 percent		2.4		12
Wire calibration sensor	±3	77.5	±4	56
PCM system		75		75
Systematic uncertainty				
Reference junction temperature monitor, 1-1/2 percent of $50^{o}F$		45		10.2
Reference junction isothermal equib, $3^{o}F$	±1	30	±1	20
Root-sum-square values =		$\sqrt{27361}$ 164		$\sqrt{13229}$ 117
3σ errors	$40^{o}R$ = $\pm 27^{o}R$ $100^{o}R$ = $\pm 15^{o}R$ $300^{o}R$ = $\pm 6.6^{o}R$ $460^{o}R$ = $\pm 5.3^{o}R$		$5.8^{o}R$ (From $500^{o}R$ to $2200^{o}R$)	

EMF Output Chromel/Constantan

$40^{o}R = 6\mu V/^{o}R$
$200^{o}R = 20\mu V/^{o}R$
$400^{o}R = 29\mu V/^{o}R$
$460^{o}R = 31\mu V/^{o}R$

The reference-junction compensation contributes a major error to the total subsystem accuracy due to (1) the compensating error assigned to the compensating network which is related to the ambient excursion of the network and its ability to track the thermocouple curve, and (2) the inability to maintain a completely isothermal condition in the reference-junction body during the rapid thermal transient conditions. The design goal is to keep the gradient within 3°F during this transient period.

Item (1) noted above may be reduced by temperature monitoring of the reference-junction body. The anticipated temperature excursion of the reference junction is -65°F to +300°F and the compensation error is 1-1/2 percent of the ambient excursion. By monitoring the temperature of the body, this systematic error can be reduced to 1-1/2 percent of ±20°F, the uncertainty in measurement of junction block temperature. Thus the compensation error can be reduced to ±0.3°F which is considered to be reasonable.

Both of the errors associated with the reference junction can be treated as time-dependent systematic errors and will require a further investigation as to the dynamic response to the location environment.

3.3 HYDROGEN MASS-FLOW RATE MEASUREMENTS

3.3.1 Problem Statement

Hydrogen is to be used in the flightweight engine as both coolant and fuel. Flow rates of hydrogen must be measured at various points in the piping system for at least three reasons; (1) the amount of hydrogen burned must be measured as carefully as possible and compared with the measured thrust in order to compute internal specific impulse, an important measure of engine performance, (2) the flow rate of hydrogen must be measured in real time with sufficient precision to enable the control system to maintain a given air-to-hydrogen ratio in the combustion regions, and (3) the amount of hydrogen dumped without burning to achieve temperature control should be measured, to assess the overall efficiency of the engine.

3.3.2 Topical Background

The layout of the hydrogen piping system imposes several constraints on the methods which can be used for measuring hydrogen flow rates. The only point at which it is feasible to measure total hydrogen flow is in the inlet line to the turbopump, where the hydrogen is at a temperature of about 50°R. Feasible methods of measuring the hydrogen flow to the burners are limited by the rather high temperature of the gas as it leaves the fuel plenum (up to 1600°R), by the multiplicity of parallel pipes between the fuel control valves and the injector manifolds, and by the requirement of avoiding any additional unnecessary pressure drops in these pipes. Similar problems exist for other flow measurement in the piping system. In essence, the usual piping requirements for making accurate flow measurements, such as providing flow straightening sections for the meters, were not included in the design criteria for the hydrogen flow system.

The thermodynamic properties of the hydrogen are not perfectly defined. Normal gaseous hydrogen at elevated temperatures is a mixture of ortho- and para-hydrogen in the ratio 3:1. The stable form of liquid hydrogen is almost pure para-hydrogen. It is not known how rapidly para-hydrogen gas, which results from heating and expanding liquid hydrogen, reverts to the normal ortho-para mixture. It is also not known how the reaction of para to normal hydrogen, if it were occurring at an appreciable rate, would affect the reading of a flowmeter.

5.3.3 Overall Approach

Flow rates are to be measured at the inlet to the turbopump, at the outlets of the three fuel control valves, at the outlet of the dump valve, and through the turbine. The mass-flow rate of hydrogen to the burners can then be determined both by direct measurement and by a difference method. The mass-flow rate of hydrogen used for cooling only is measured directly by summing the dump and turbine flow rates.

Total hydrogen volumetric flow through the pump is to be measured by a turbine flowmeter. Volumetric flow is converted to mass flow by using the density of hydrogen, determined from the measured temperature and pressure of hydrogen at the pump inlet.

The hydrogen dump flow is to be measured by using either a choked-orifice or a velocity-head meter in series with the dump valve. The temperature of the gas precludes the use of most other types.

The flow rate through the turbine is to be measured by calibrating the turbine as a choked-orifice.

A small fraction of the total hydrogen flow into the turbopump leaks through the bearing and does not go through the engine. This bypass flow is very small--less than the usual errors of measurement--and is not measured.

The signals corresponding to the total flow Q_T, the dump flow Q_{D_1}, and the turbine flow Q_{D_2} are applied to the data telemetry and recording system. The flow rates are computed after the test run, as functions of time. From these data, the flow rate to the burners, Q_f, is computed. At steady-state conditions, the following equation holds:

$$Q_f = Q_T - Q_{D_1} - Q_{D_2}$$

In the data analysis following the test, the fuel-flow rate to the burners is computed according to the preceding equation.

The mass-flow rate to the burners can also be determined by direct measurements of flow in each of the three sets of lines connecting the fuel control valves with the injector manifolds. Three techniques have been considered for this measurement during the course of the program. They are as follows:

(a) Measure pressure and temperature of the gas in the injector manifolds; assume that the injectors behave as simple choked-orifices with constant-discharge coefficients, and compute mass flow from the choked-orifice equation.

(b) Infer flow rate from the positions of the valve-poppet stems, the temperature and pressure of gas in the fuel plenum, and the pressure drop across each valve.

(c) Place flowmeters immediately downstream from fuel control valves, with such flow straightening devices as can be accommodated in the available space.

It has been decided that the direct measurement of fuel flow to the burners would be used to generate control signals and not data-monitoring signals. Hence, precision or repeatability in this measurement is more important than absolute accuracy. That is, it is more important to be able to establish, maintain, and repeat a given flow rate than to have accurate knowledge of what the flow rate is. The absolute flow rate can be determined after the test during the data analysis from the recorded information about Q_T, Q_{D_1}, and Q_{D_2}.

3.3.4 Summary of Progress

Although no hardware was built or tested during the program, several design problems were analyzed and resolved, and a description of the flow measuring system was realized. This work has been reported in detail in several AiResearch reports (see References 1-3, 1-4, 1-5, 1-7, and 1-8) and is merely summarized here.

Early in the program it was determined that enough flow measurements would have to be made to account for all the hydrogen used. Hydrogen is used as fuel, as coolant, and as a power source to drive the turbine. There are four different hydrogen mass-flow rates to be measured; namely Q_f, Q_T, Q_{D_1}, and Q_{D_2} (see Section 3.3.3, above, for definitions of these symbols). It was determined that these four flow rates would be measured by the techniques summarized below.

Q_f, the mass-flow rate of hydrogen to the burners, was to be determined by measuring the pressures and temperatures of the hydrogen in the injector manifolds. We assumed that the burners would behave as choked-orifices. Mass-flow rate of hydrogen to a given set of burners would be calculated from the equation for the choked-orifice, which has the following form:

$$Q_{fi} = \left(A_i P_i T_i\right)^{-1/2}$$

In the equation, the subscript i refers to the i^{th} set of burners, A is an empirically determined constant (it is proportional to the effective total-area of the burners), and P and T respectively, are the absolute pressure and absolute temperature of the hydrogen in the injector manifold. This technique is discussed and analyzed in Reference I-3.

Q_T, the total mass-flow rate of hydrogen to the engine, was to be measured by means of a turbine flowmeter in the inlet line. At this point, the hydrogen is a cryogenic liquid. A turbine flowmeter was selected because it is the most accurate method of measuring volumetric flow rate and because the environment permits its use (see Reference 3-1). A turbine flowmeter cannot be used for measuring the flow rate of the hydrogen gas after it has been heated by passing through the heat exchangers for cooling the engine, for example, because the temperature is too high.

Q_{D_1}, the dump flow, and Q_{D_2}, the flow through the turbine, cannot be measured by turbine flowmeters, because of the reason just mentioned. It was decided that these two flow rates would be measured by choked-orifice-type meters. In the case of the dump flow Q_{D_1}, a sonic nozzle would be installed in the discharge line from the dump valve. In the case of the turbine flow, it was decided that the turbine itself would serve as a choked orifice.

This system of measuring Q_f, Q_T, Q_{D_1}, and Q_{D_2} has the advantage that one of the measurements is redundant; hence, Q_f can be determined in two independent ways. First, Q_f is measured directly. Second, Q_f is determined by difference by means of the following equation:

$$Q_f = Q_T - Q_{D_1} - Q_{D_2}$$

This method of difference is discussed and analyzed in References I-7 and 3-1.

Recently, the problem of measuring Q_f was reviewed critically. It has decided that the discharge coefficients of the burner orifices would not be constant or even predictable because of the supersonic cross-flow of air past the orifices. This problem is mentioned in Reference I-3 and discussed in Reference I-8. As a consequence, another method was chosen for measuring Q_f, namely, to place flowmeters in series with the through fuel flow control valves. Several types of flowmeters were considered and a short Venturi meter was selected for this application. An analysis of the problem is presented in Reference I-8.

There has been no previous published documentation of the reasons for selecting the sonic nozzle for measuring Q_{D_1}. Therefore, it is worthwhile to review the alternatives that have been considered and show why the sonic nozzle is believed to be the best compromise.

The various types of flowmeter that might be used for measuring the dump flow are as follows:

(1) Turbine flowmeter

(2) Hot-wire anemometer

(3) Heat flow type of flowmeter

(4) Venturi meter

(5) Drag-body flowmeter

(6) Other velocity head types, such as the elbow

(7) True-mass flowmeter

(8) Choked-orifice

The objections to some of the various types fell into the following categories:

(a) The meter has a bearing, rotating seal, or other component affected by temperature, and will not operate at the high temperature of the exhaust hydrogen (1600°R).

(b) The meter contains delicate parts and has not been developed as a piece of commercially available, reliable flight hardware.

(c) The meter has a long time constant.

These objections rule out types (1), (2), (3), (5), and (7).

The Venturi and elbow-type meter operate with a very small line-pressure drop. In some applications this is an advantage. In the present application, the gas is exhausted at a high pressure to near-vacuum conditions. A Venturi or other velocity-head meter would have to be placed upstream from the dump valve in order to operate properly. A velocity-head meter has the disadvantage that three measurements are required to determine mass-flow rate of a gas: inlet pressure, inlet temperature, and a pressure difference (or throat pressure). In addition, the inlet pressure and temperature in the proposed application are relatively constant, and most of the effect of a change in flow rate would appear as a change in the pressure difference. This pressure difference is approximately proportional to the square of the flow rate, a circumstance that limits the measurement range of a velocity-head meter.

The sonic nozzle flowmeter, by contrast, requires only two measured quantities, namely, a pressure and a temperature. In addition, if the temperature is constant, the measured pressure is a linear function of mass-flow rate.

For these reasons, the sonic (choked) nozzle was selected as the best method of measuring the dump flow, Q_{D_I}.

A minor disadvantage of the sonic nozzle is that it imposes a substantial back pressure on the dump valve. The effect of the sonic nozzle on the valve has not yet been assessed. This is not a serious objection to the sonic nozzle, since the valve can be designed to operate in conjunction with the nozzle.

REFERENCES

1-1. Hypersonic Ramjet Experiment Project - Phase I, Preliminary Design Report (U), Volume II, Appendix A, AiResearch Report Number AP-66-0168-2.

1-2. Hypersonic Research Engine Project - Phase IIA, Environmental Specification, Data Item No. 4.02, AiResearch Report No. AP-68-4130, 14 August 1968.

1-3. Hypersonic Research Engine Project - Phase IIA, Instrumentation Program, Fifth Interim Technical Data Report, Data Item No. 55-8.05, AiResearch Report No. AP-68-3847, 12 June 1968.

1-4. Hypersonic Research Engine Project - Phase IIA, Instrumentation Program, Third Interim Technical Data Report, Data Item No. 55-8.03, AiResearch Report No. AP-67-3020, 21 December 1967.

1-5. Hypersonic Research Engine Project - Phase IIA, Instrumentation Program, First Interim Technical Data Report, Data Item No. 55-8.01, AiResearch Report No. AP-67-2203, 7 June 1967.

1-6. Hypersonic Research Engine Project - Phase IIA, X-15A-2 Integration Program, Third Interim Technical Data Report, Data Item No. 55-9.03, AiResearch Report No. AP-68-3426, March 11, 1968.

1-7. Hypersonic Research Engine Project - Phase IIA, Instrumentation Program, Fourth Interim Technical Data Report, Data Item No. 55-8.04, AiResearch Report No. AP-68-3429, April 10, 1968.

1-8. Hypersonic Research Engine Project - Phase IIA, Instrumentation Program, Sixth Interim Technical Data Report, Data Item No. 55-8.06, AiResearch Report No. AP-68-4273, 27 September 1968.

3-1. AiResearch Report L-9544, Conceptual and Preliminary Design of the Instrumentation for Ground and Flight Test, (no date).

APPENDIX A

CHANGE OF DESIGN REQUIREMENTS-- THRUST/DRAG SYSTEM

APPENDIX A

CHANGE OF DESIGN REQUIREMENTS--THRUST/DRAG SYSTEM

INDICATED THRUST (AND DRAG)

Initial

The initial requirements were based on Reference I-1

Maximum internal thrust at Mach 4 and 59,000 ft	4053 lb
Maximum external drag at Mach 4 and 59,000 ft	318 lb
Maximum longitudinal acceleration	-1 g
Angle of pitch	-2 deg
Estimated weight of engine	630 lb

Balance of forces yields T_{ind} (indicated thrust)

Design requirements were

Thrust	4500 lb
Drag	500 lb

Present

The present requirements are based on Reference I-6, Appendix A

Maximum internal thrust at Mach 5	5950 lb
Maximum external drag at Mach 5	699 lb
Maximum longitudinal acceleration	-2 g
Angle of pitch (angle-of-attack)	8.8 deg
Estimated weight of engine	780 lb
Balance of forces yields T_{ind}	6690 lb
Design requirement taken as	7000 lb

Maximum negative thrust (drag direction) is computed from Reference I-6, Appendix A

External drag (Mach 8.0)	1807 lb
Longitudinal acceleration	4.5 g
Angle of pitch (angle-of-attack)	10.4 deg
Internal thrust	0
Balance of forces yields T_{ind}	-5458 lb
Design requirement taken as	5500 lb

FORCE BLOCK MAXIMUM OVERLOAD

Initial

From Reference I-I

Maximum airplane angle-of-attack	30 deg (taken as angle of pitch)
*Maximum longitudinal inertia force loading	+4.5 g
*Maximum normal inertia force loading	+6.8 g
Maximum internal thrust	4053 lb
Taking the worst case, and a factor of safety of 1.5, loading is	10,340 lb
Design requirement was taken as	10,000 lb

Present

It was considered that the maximum fatigue stress condition imposed on the block during the ground vibration test would be a sound criterion for design. Assuming a magnification at resonance of approximately 7 with an input sinusoid of 3 g peak load is approximately 15,000 lb. Using the computation in the preceeding paragraph with the revised thrust maximum, and combining this with anticipated flight vibration, the design figure of 15,000 lb would cover with a factor of safety included.

Thus, design requirement was taken at 15,000 lb.

---

*Do not occur simultaneously

Acceleration

More detailed information on mission parameters, as given in Reference I-6, Appendix A, has led to revision of the acceleration figure.

Frequency Response

Initially, the frequency response characteristic of 0 to 100 Hz was based on the need to establish the performance well above the 15 to 17 Hz band to be avoided by mechanical resonance (Reference NASA Statement of Work L-4947-B, Para 4.6.2.1). Reconsideration in the light of the quasi-steady state nature of the measurements to be made during the engine-lit condition and the comparatively high natural frequency implied by the block design (approx. 150 Hz) has led to revision of the frequency response requirement for the measurement system to become 0 to 10 Hz.

Temperature

Heat transfer analyses of typical mission conditions using the proposed flight-type hardware configuration indicate that thrust block temperatures will be well below the initial temperature upper limit of 500^{0}F. Analyses of proposed ground tests show that, in certain conditions, the block would attain temperatures to 600^{0}F.

Measurement Accuracy

Based on the initial design figures and assuming a maximum permissible error in the derivation of internal thrust of 2.5 percent, individual measurement errors were accounted for on a weighted summation approach to give an allowance of ±1.75 percent full scale error allowable in the indicated thrust measurement (Reference I-I, page 302).

Updated design figures and adoption of the root-mean-square method of error analysis have led to a revised internal thrust allowable error of ±2.70 percent full-scale with a requirement of a maximum of ±1.1 percent full scale error in the indicated thrust (Reference I-7, Para 2.4.2.2).

PART II

TECHNICAL DATA REPORT ON REMAINING EFFORT NOT PREVIOUSLY COVERED

1.0 THRUST/DRAG MEASUREMENT SYSTEM

1.1 INTRODUCTION

The development test program was scheduled to commence with a structural test on a first deflection block, to prove design and to determine stress concentrations using Stress-coat techniques. This was to be followed by the installation and evaluation of straingages as a method of force-determination in the thrust axis and in the vertical reaction force axis. A second model was to be assembled which would include a differential capacitor transducer for evaluation under combined loading.

This report covers the testing performed on the first deflection block to the time of termination of the thrust system effort.

1.2 TEST PLAN

The overall test plan is shown in Appendix A. Deviations from the test plan, governed by available time and equipment, are noted at the end of Appendix A.

1.3 TEST EQUIPMENT AND METHOD

1.3.1 Stress-coat Tests

These tests were performed using Stress-coat ST-75, Magnaflux Corporation (for use at a nominal temperature of 75°F), with loading to 10,000 lb in the thrust axis direction, with the deflection block installed in the test fixture 94-7B-3419 (see Figure 1.4-6, Part I). Calibration-Stress-coated bars were used during the tests, referenced against temperature. Testing was at nominal room temperature. Photographs were taken of the stress patterns at the conclusion of testing. (Reference Figures 1.3-1 through 1.3-4.)

1.3.2 Straingage Tests

The block was instrumented with a full-bending bridge with two active gages in each leg as shown in Figures 1.3-5 and 1.3-6 and for calibration against P_X loading. A Poisson's bridge was installed on the outer faces of the outer flexures as shown in Figures 1.3-7 and 1.3-8

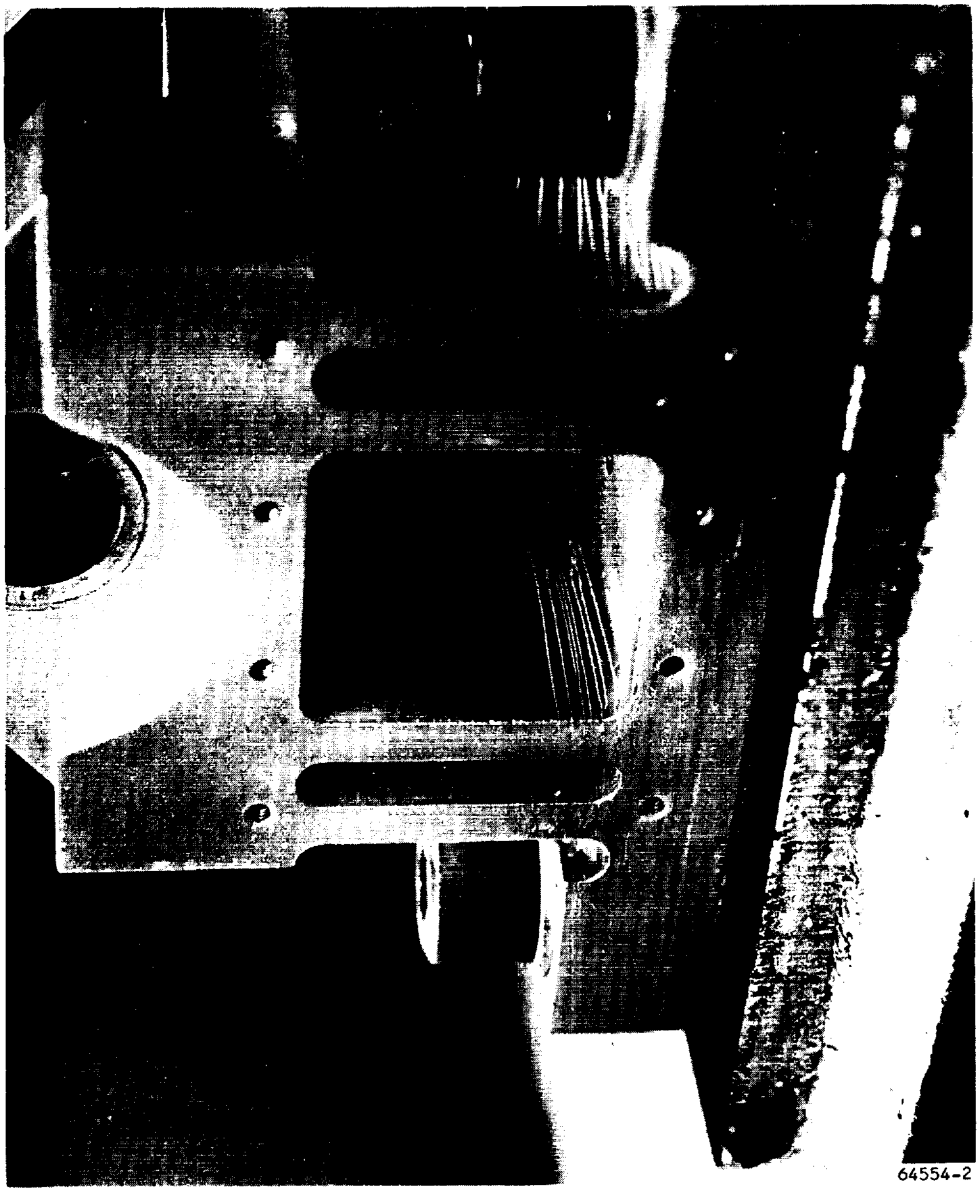

64554-2

Figure 1.3-1. Stress-coat Pattern

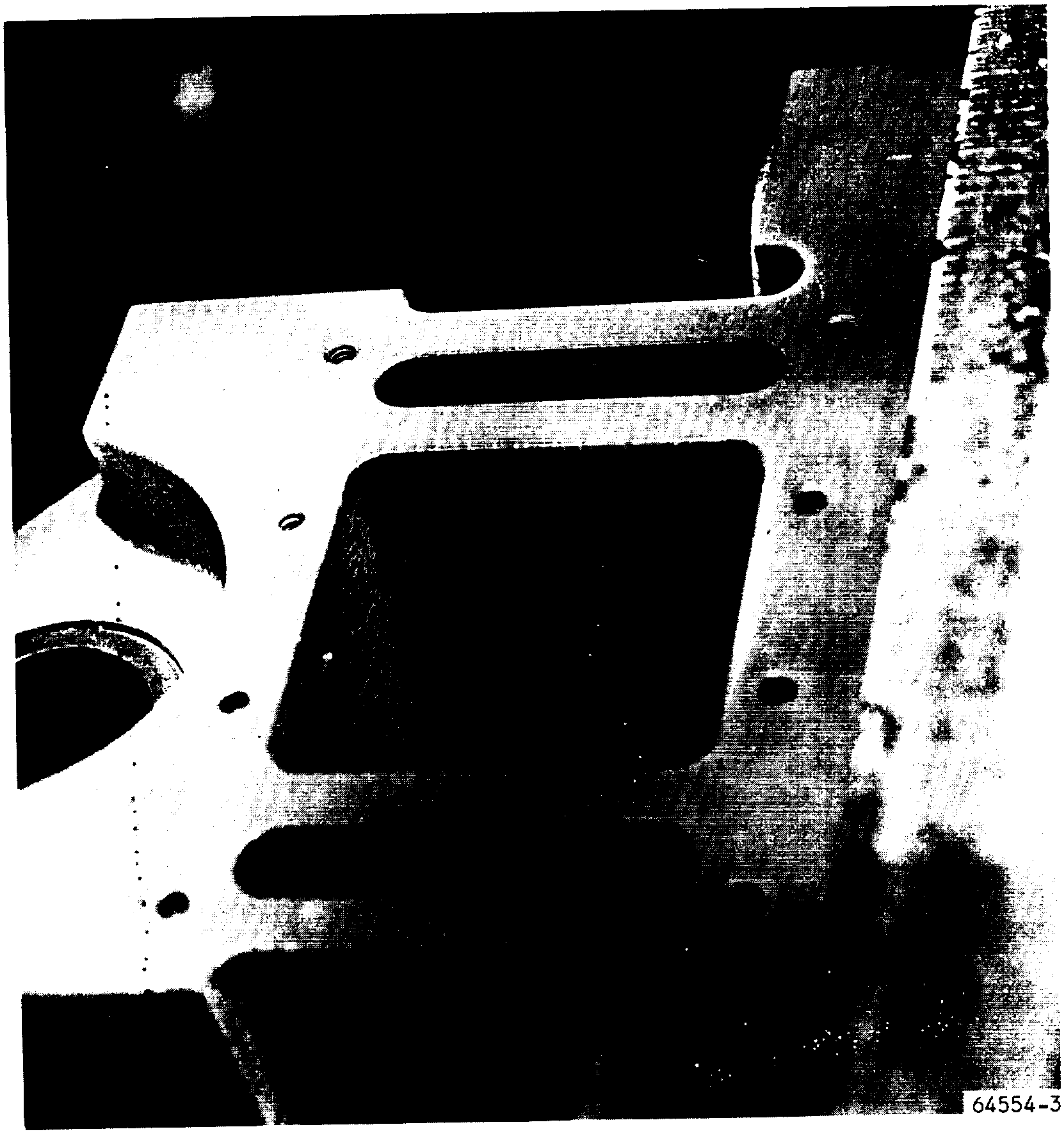

Figure I.3-2. Stress-coat Pattern

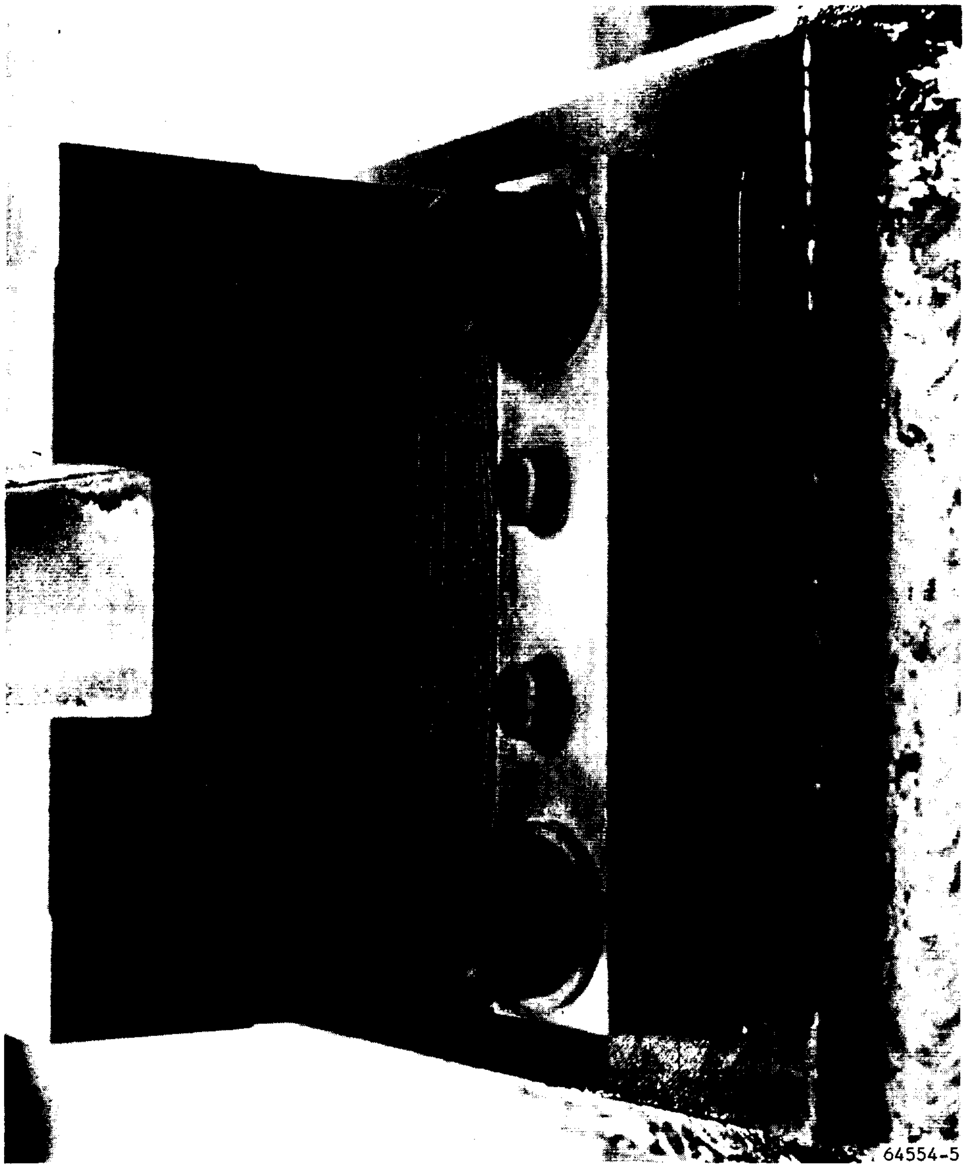

Figure I.3-3. Stress-coat Pattern

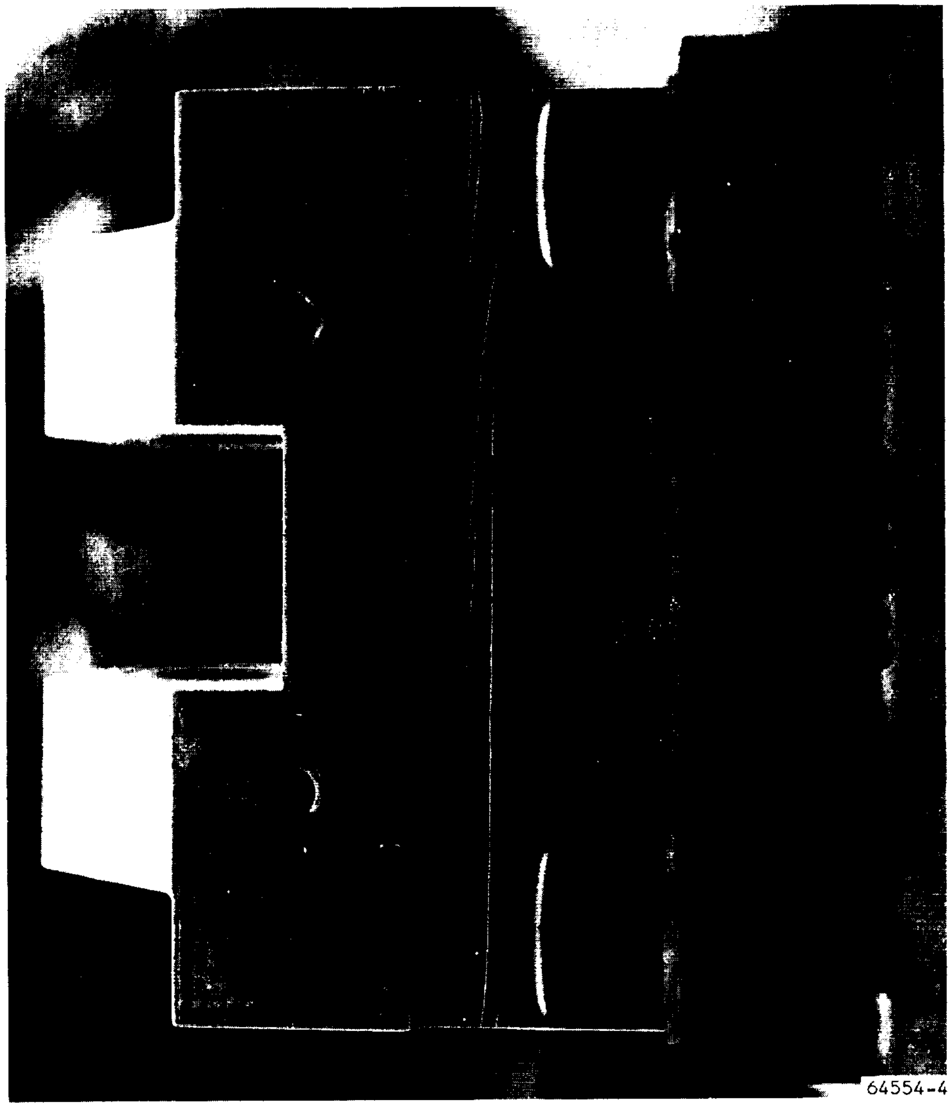

64554-4

Figure I.3-4. Stress-coat Pattern

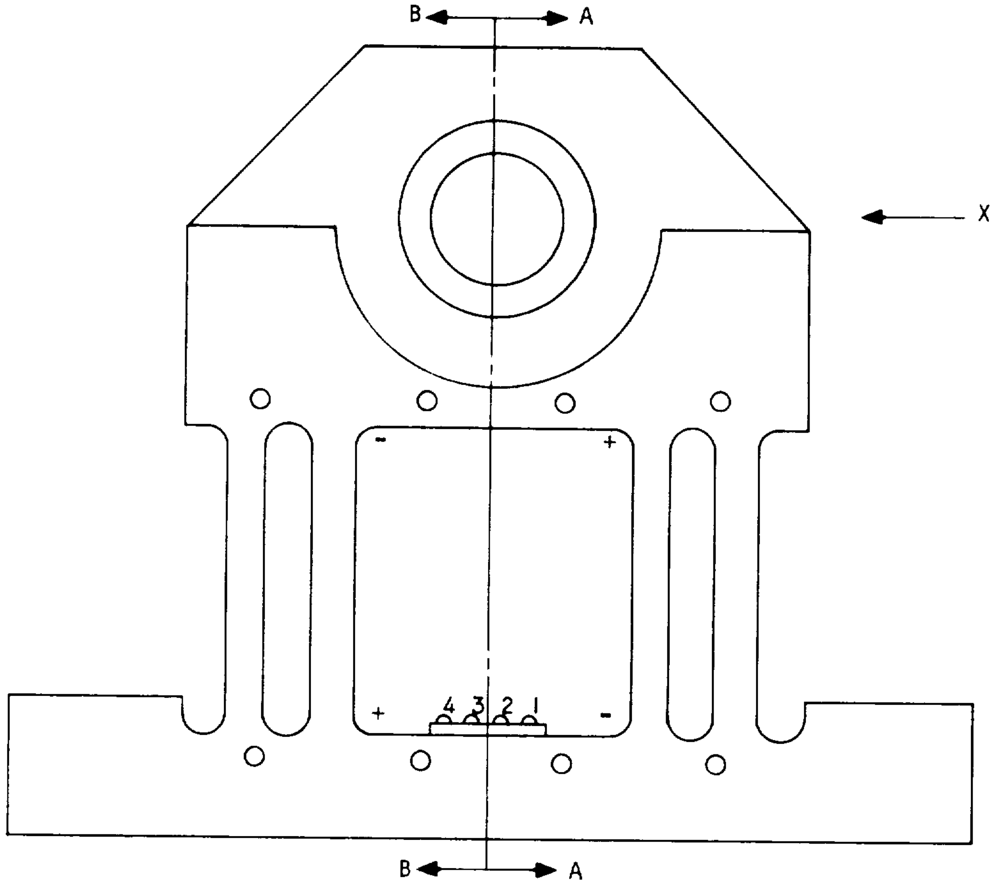

DEFLECTION BLOCK THRUST BRIDGE

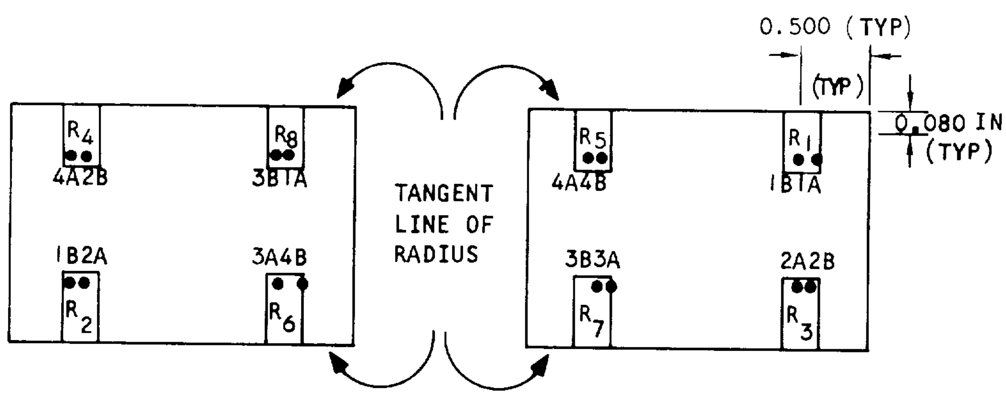

VIEW B-B

VIEW A-A

NOTE: CONNECT TABS MARKED THUS (●●) TO MAIN TT-50 TERMINAL STRIP

Figure 1.3-5. Thrust Bridge Installation

DEFLECTION BLOCK THRUST BRIDGE

ϵ_I = STRAIN

V = APPLIED VOLTAGE

ΔE_O = OUTPUT VOLTAGE

GF = GAGE FACTOR

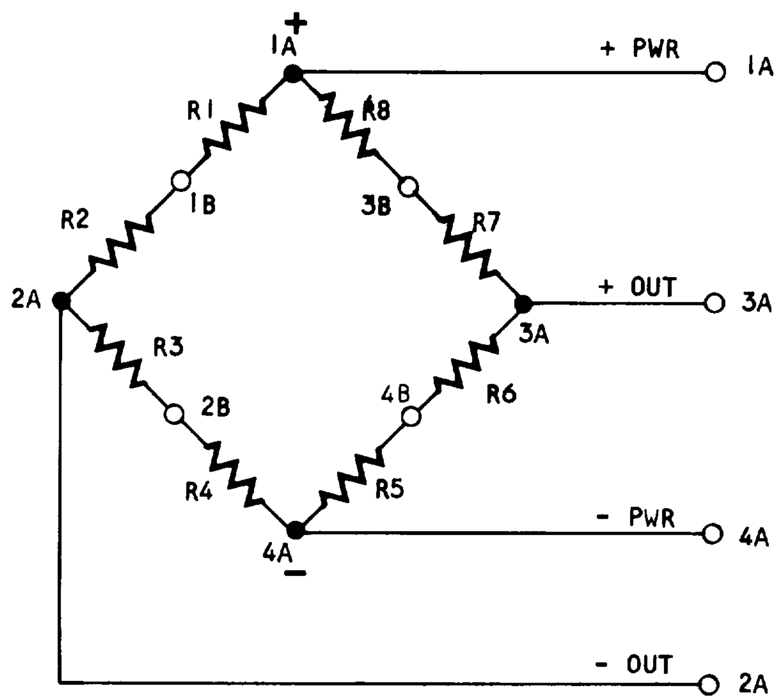

$$\Delta E_O = \frac{V}{4}(4\ \epsilon_I)\ GF$$

$$R_{NET} = 240\ \Omega$$

S-44295

Figure 1.3-6. Thrust Bridge Schematic

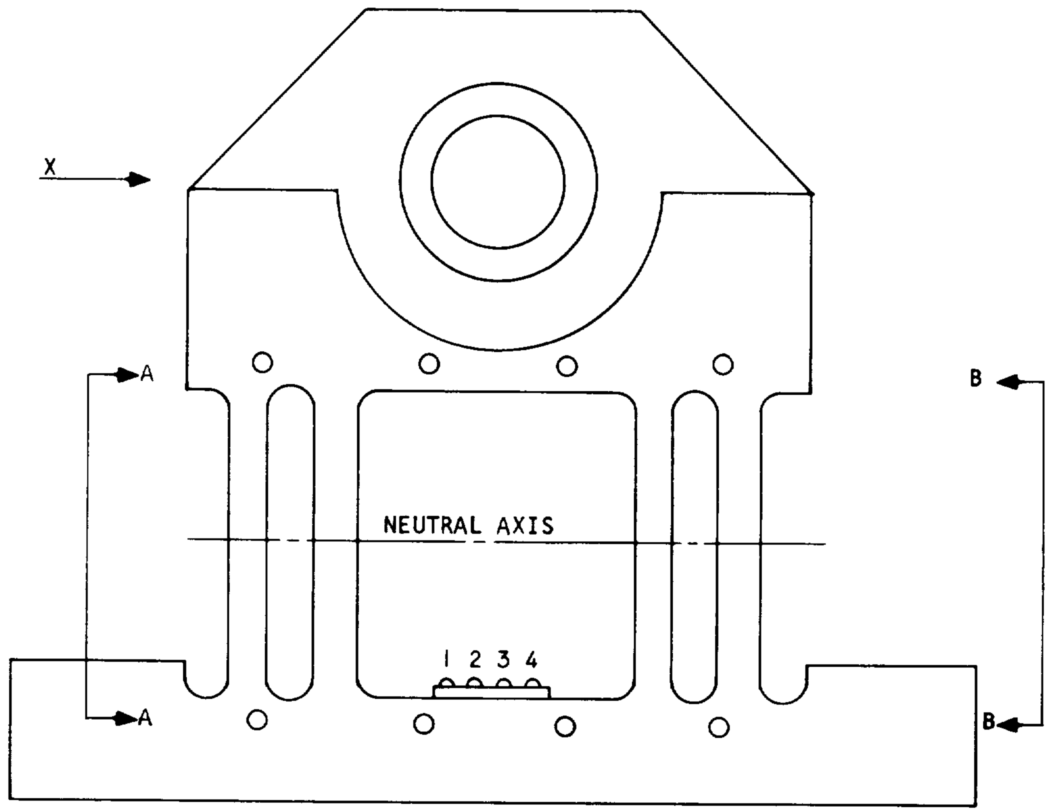

DEFLECTION BLOCK POISSON'S BRIDGE

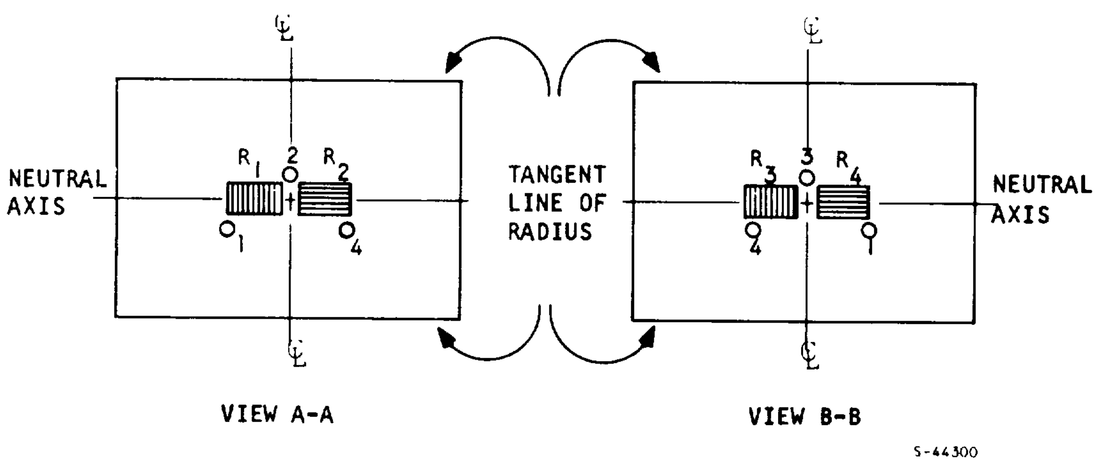

Figure I.3-7. Poisson's Bridge Installation

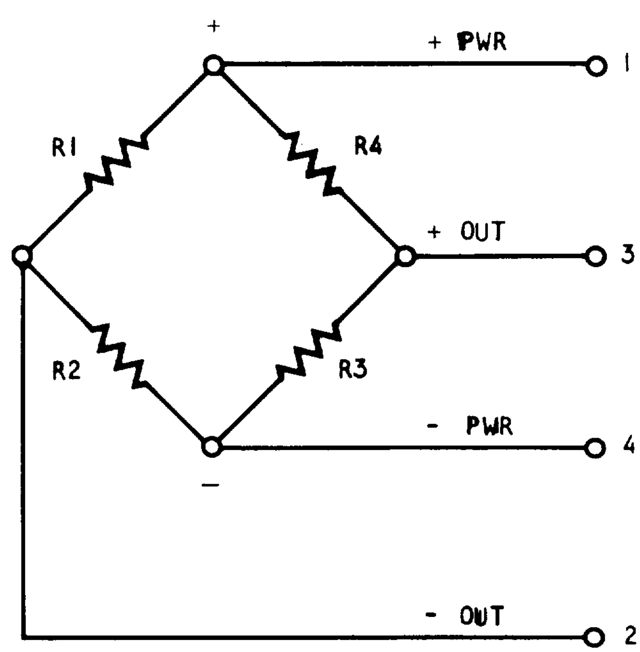

ϵ_1 = STRAIN

GF = GAGE FACTOR

V = APPLIED VOLTAGE

ΔE_o = OUTPUT VOLTAGE

$$\Delta E_o = \frac{V}{4}\left[4\epsilon_1\right] GF$$

$$R_{NET} = 120\ \Omega$$

S-44296

Figure 1.3-8. Poisson's Bridge Schematic

Gage characteristics were as follows:

Bridge	Gage Type	Gage Factor	Gage Resistance
Thrust	MA-13-062AA-120	2.07 ±0.5%	120 Ω ±0.15 %
Poisson's	MA-13-125T6-350	2.11 ±0.5%	350 Ω ±0.5 %

Bonding was BR-600 cured for 1 hr at 250°F

A photograph of the overall instrumented block is shown in Figure 1.4-1, Part I. Part views are shown in Figures 1.3-9 and 1.3-10 of this part of the report (Part II).

Thrust loading was applied using the test fixture 94-7B-3419 with a Schaevitz load cell, type JP-10,000 SN 13595 used as a load reference. This load cell had been calibrated to an accuracy of 0.11 percent full-scale. Bridge voltage was 5.00 vdc. Bridge output was read on an integrating digital voltmeter.

1.4 TEST RESULTS

For full test data refer to Appendix C.

1.4.1 Stress-coat Tests

Photographs of the stress patterns at the conclusion of the application of loads in the thrust direction up to 10,000 lb, are shown in Figures 1.3-1 through 1.3-4.

Stress cracks began to appear between loads of 2000 and 4000 lb with a calibration strain of 369 microinches/in.

Sufficient pattern was established at 10,000-lb loading to indicate the neutral axis and stress distribution.

Upon removing the deflection block from the test fixture, indication that there had been movement of the fixture block retaining plate relative to the frame (see Para 1.4.2 of this section) was noted.

1.4.2 Straingage Tests

Loads were applied in increments of 1000 lb up to 10,000 lb in increasing and decreasing directions. Outputs of both bridges were recorded. During calibration, the deflection block moved in the fixture, the locating pins on the fixture sheared, and the block-base rotated slightly, relative to the applied thrust axis.

Figure I.3-9. Thrust Bridge Installation

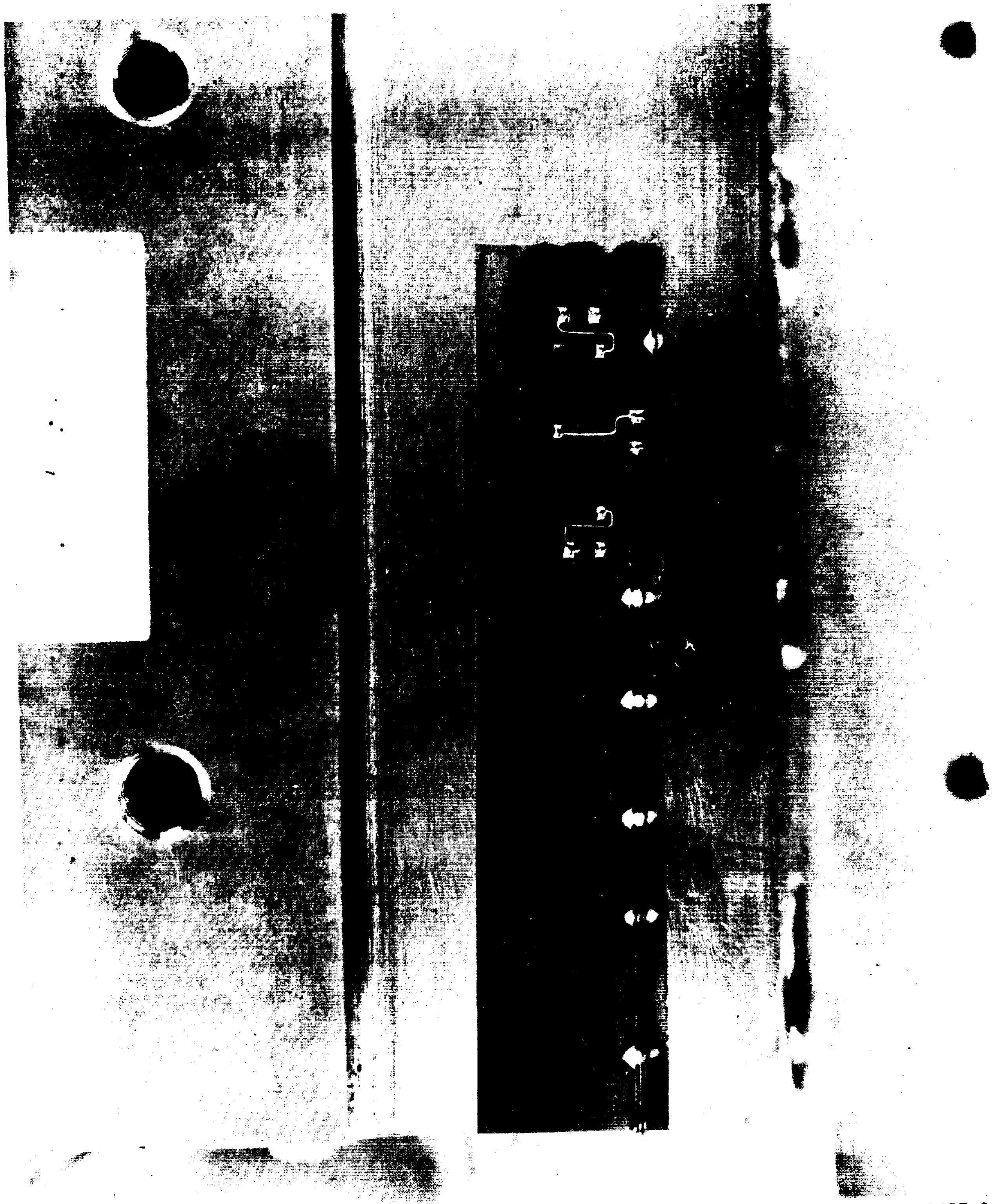

64637-2

Figure 1.3-10. Poisson's Bridge Installation

1.4.2.1 Thrust Bridge

Figure 1.4-1 shows the output-versus-applied-load characteristics giving a nominal output of 15μv/lb. Figure 1.4-2 shows the percentage deviation relative to full-scale at each increment with reference to the nominal output of 15μv/lb. Figure 1.4-3 shows a similar plot with reference to an output sensitivity of 15.044μv/lb, to give equal positive and negative deviation.

1.4.2.2 Poisson's Bridge

No calibration of the Poisson's bridge was made with P_Z (vertical) loading. Output from the bridge with thrust load applied was recorded and the following analysis is presented to show the correlation of this output with the expected full-scale output under P_Z loading.

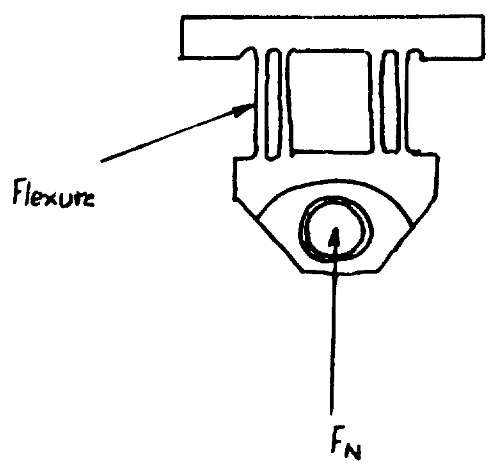

Let cross-sectional area of flexure in thrust direction be A sq in., let modulus of elasticity for the material be E lb/sq in. Then

$$\text{Stress in flexure} = \frac{F_N}{4A}$$

$$\text{Compressive strain} = \frac{F_N}{4AE}$$

From dimensions of deflection block A(nominal) = 4 x 0.217 = 0.868 sq in. Expected maximum value of F_N (Reference 1.7, Part I, Para 2.4.5.1.1) = 5000 lb. and for 17-4PH

$$E = 29 \times 10^6 \text{ lb/sq in.}$$

$$\therefore \text{ expected maximum strain } (\epsilon_m) = \frac{5000}{4 \times 0.868 \times 29} \times 10^{-6}$$

$$\epsilon_m = 50 \text{ microinches per inch}$$

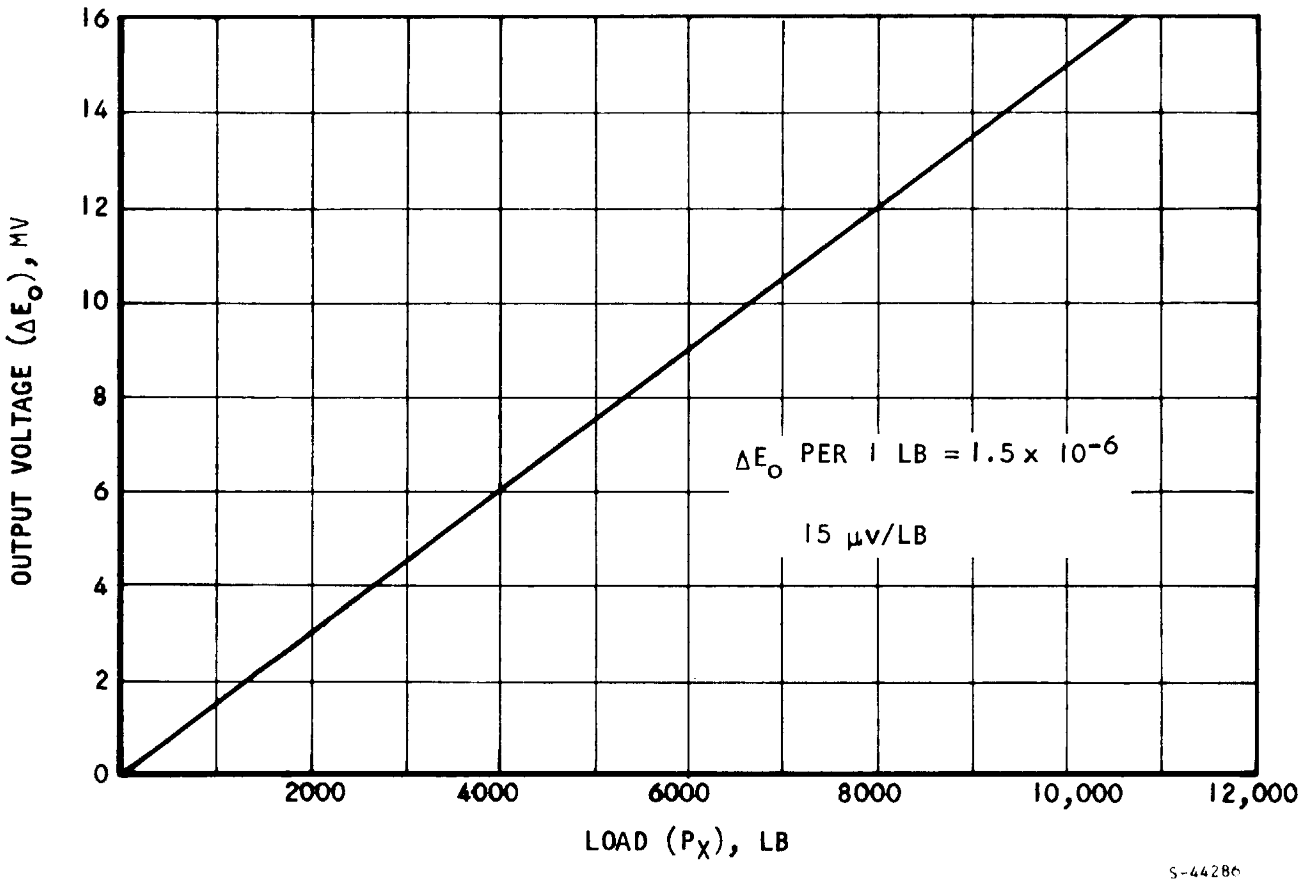

Figure 1.4-1. Calibration of Thrust Block Straingage Bridge

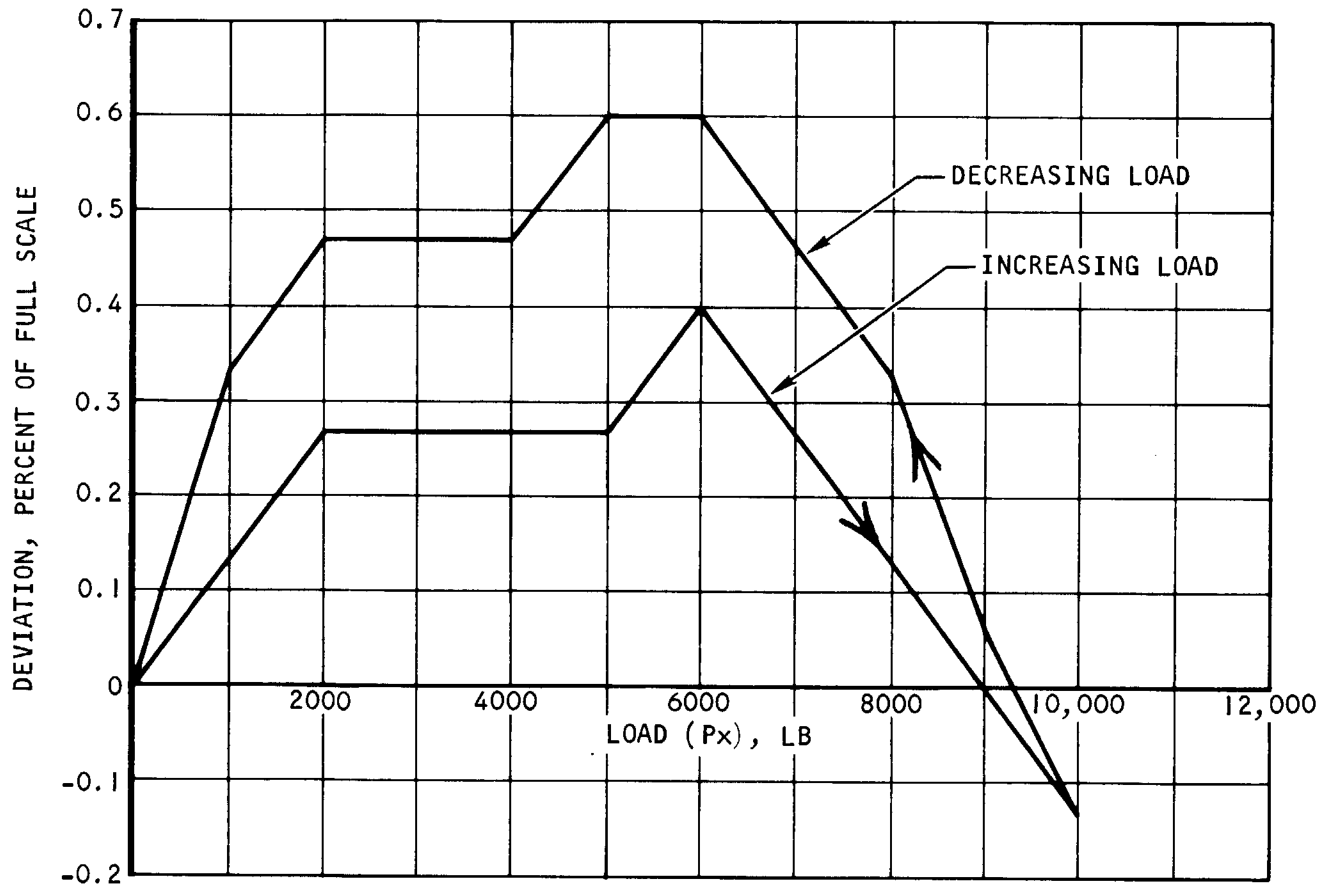

SENSITIVITY TAKEN AS 1.5 μV PER POUND

FULL-SCALE (10,000 LB) = 15 MV

S-44294

Figure 1.4-2. Thrust Deflection Block - Straingage Calibration

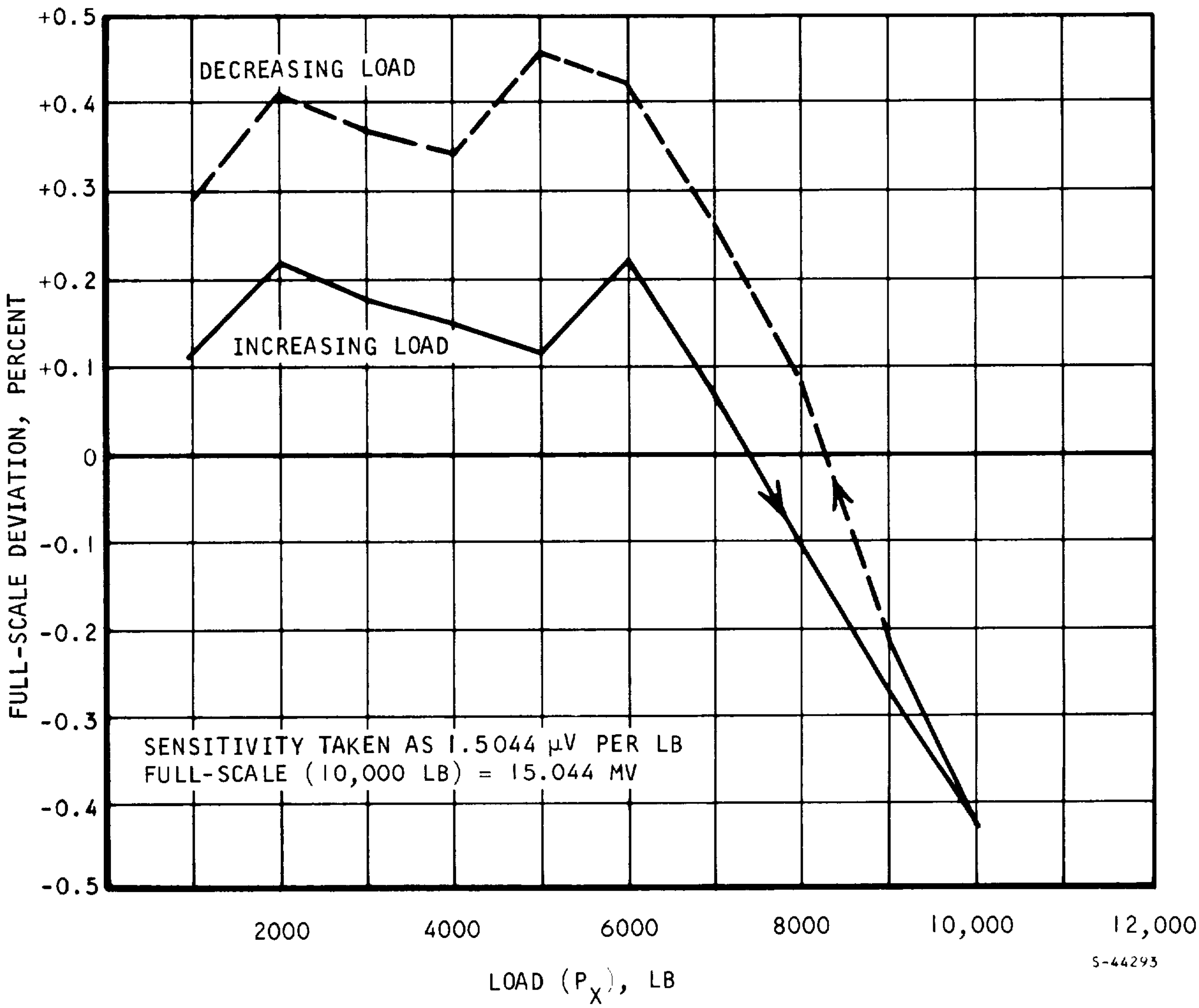

Figure 1.4-3. Thrust Deflection Block - Straingage Calibration Error

With reference to Figure 1.3-8 and Appendix B, the output from the bridge is given by

$$\Delta E_o = V\epsilon_x(GF)$$

where ΔE_o = bridge output

V = bridge applied voltage

ϵ = strain

GF = gage factor

Then

$$\epsilon = \frac{\Delta E_o}{V(GF)}$$

Substituting

$$\left.\begin{aligned} V &= 5.00 \\ GF &= 2.11 \end{aligned}\right\} \quad \text{(Reference Para 1.3.2)}$$

$$\epsilon = \frac{\Delta E_o}{10.55}$$

Let

R = percentage output strain relative to full-scale

Then

$$R = \frac{\epsilon}{\epsilon_m} \cdot 100$$

Hence

$$R = \frac{\Delta E_o}{10.55} \times \frac{100}{50 \times 10^{-6}} \%$$

for ΔE_o in millivolts, this becomes

$$R = 190\ \Delta E_o\ \%$$

Figure 1.4-4 shows R plotted incrementally against the applied load (P_X). For ideal conditions, R should be zero.

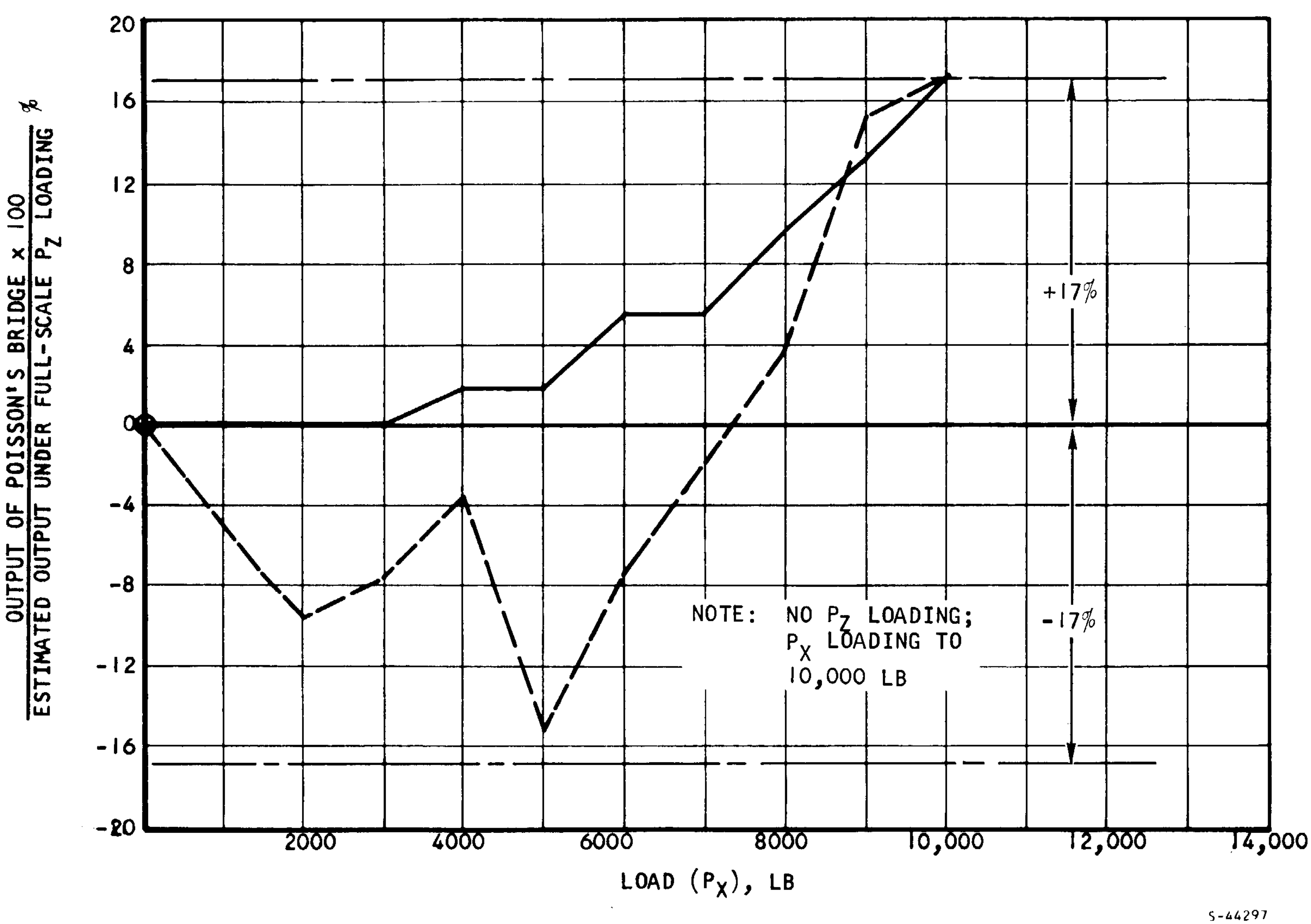

Figure 1.4-4. Output of Poisson's Bridge Under Thrust Load

1.5 COMMENTS AND CONCLUSIONS

1.5.1 Stress-coat Tests

Loading produced the anticipated stress patterns, although some nonlinearity in the stress distribution was apparent across the block (see Figure 1.3-4 which is a view looking at the front end of the block as it would be installed in the engine assembly).

Based on test data obtained, probable stress at the root can be determined as follows.

From Reference 1-7 (Part I) Para 2.4.1.2, design stress under 14,000 lb thrust is 72,500 lb/sq in.

With reference to Paragraph 1.4.1 of this appendix, and taking the load at which the stress cracks first appear as 2500 lb, with a linear relationship to 14,000 lb. Indicated stress at 14,000 lb loading would be

$$fi = \frac{14,000}{2500} \times \epsilon E$$

where ϵ = indicated strain

E = modulus of elasticity for 17-4PH in lb/sq in.

Substituting

$$E = 29 \times 10^6$$

ϵ = 369 microinch/in. (calibration data)

then

$$fi = \frac{14,000}{2500} \times 29 \times 10^6 \times 369 \times 10^{-6}$$

$$fi = 60,000 \text{ lb/sq in.}$$

This value compares favorably with the design value of 72,500 psi in view of variables that must be considered, such as temperature effect of Stress-coat, etc.

1.5.2 Straingage Tests

1.5.2.1 Thrust Bridge

The straingage bridge output indicated a linear output with respect to the applied load to within better than ±1/2 percent in spite of difficulty encountered during testing (see Para 1.4.2). The straingage installation appears satisfactory for room temperature conditions, and further testing will be required for other ambients. Output sensitivity (15 mv full scale) and resolution (1 part in 1500) are satisfactory for the application.

The effect of temperature, and temperature gradients within the block, their effect on the straingage-bridge output and methods of compensation, are not discussed in this report.

1.5.2.2 Poisson's Bridge

The output of the Poisson's bridge under thrust load only (Reference Figure 1.4-1) can be approximately 17 percent of the anticipated full-scale output under vertical load (P_Z). While this appears high, the importance of the measurement of this vertical force is governed by its part in the overall indicated thrust equation. Reference to the Fourth TDR (Reference 1-7) suggests that the forces appearing in the equation derived from the vertical reaction force, namely, resolved vertical force due to block deflection, transferred moment, and misalignment, could total approximately 40 lb. An error of 20 percent in the determination of vertical force would be reflected as an 8-lb error in the indicated thrust. On a direct basis, this represents an error only of $8/7000 \times 100 = 0.114$ percent. On a root-square-error analysis this would be less.

Thus, the Poisson bridge can be used to estimate the vertical reaction force.

APPENDIX A

TEST PROCEDURE

APPENDIX A

TEST PROCEDURE
HRE 4600 STRUCTURAL TESTS FOR DEFLECTION BLOCK
PART NUMBER 981041
(CATEGORY I SERIES TESTS)

1.0 SCOPE

This series of tests is intended to provide information to support the following evaluations.

1.1 Determination of room temperature spring constant of the deflection block.

1.2 Determination of locations of stress concentrations and their relative magnitudes.

1.3 Verification of results of preliminary stress analysis.

1.4 Preliminary determination of performance of deflection block under application of design loads.

1.5 Preliminary evaluation of suitability of straingages as primary sensors of thrust axis loads applied to the deflection block.

2.0 EQUIPMENT TO BE USED

2.1 Stress-coat ST-75, Magnaflux Corporation or equivalent.

2.2 Thrust-block test fixture, AiResearch tool No. 94-7B-3419.

2.3 Dial gage, 0.010 in. unidirectional range, 0.0001-in. resolution or equivalent; and clamping accessories. Installation per Figure A-1.

2.4 Load cell, JP-10X, 0 to 10,000 lb range or equivalent. Schaevitz Engineering Company.

2.5 Integrating digital voltmeter, Dymec PN 2401B or equivalent.

2.6 Universal bridge box, AiResearch PN 41S-136 or equivalent.

2.7 Switch and balance unit SB-1, Budd Company, or equivalent.

2.8 Hydraulic pressure sources.

2.8.1 Enerpac Model PM 241 electric pump. 0 to 10,000 psi or equivalent.

2.8.2 Enerpac Model P80 with 4-way valve, or equivalent.

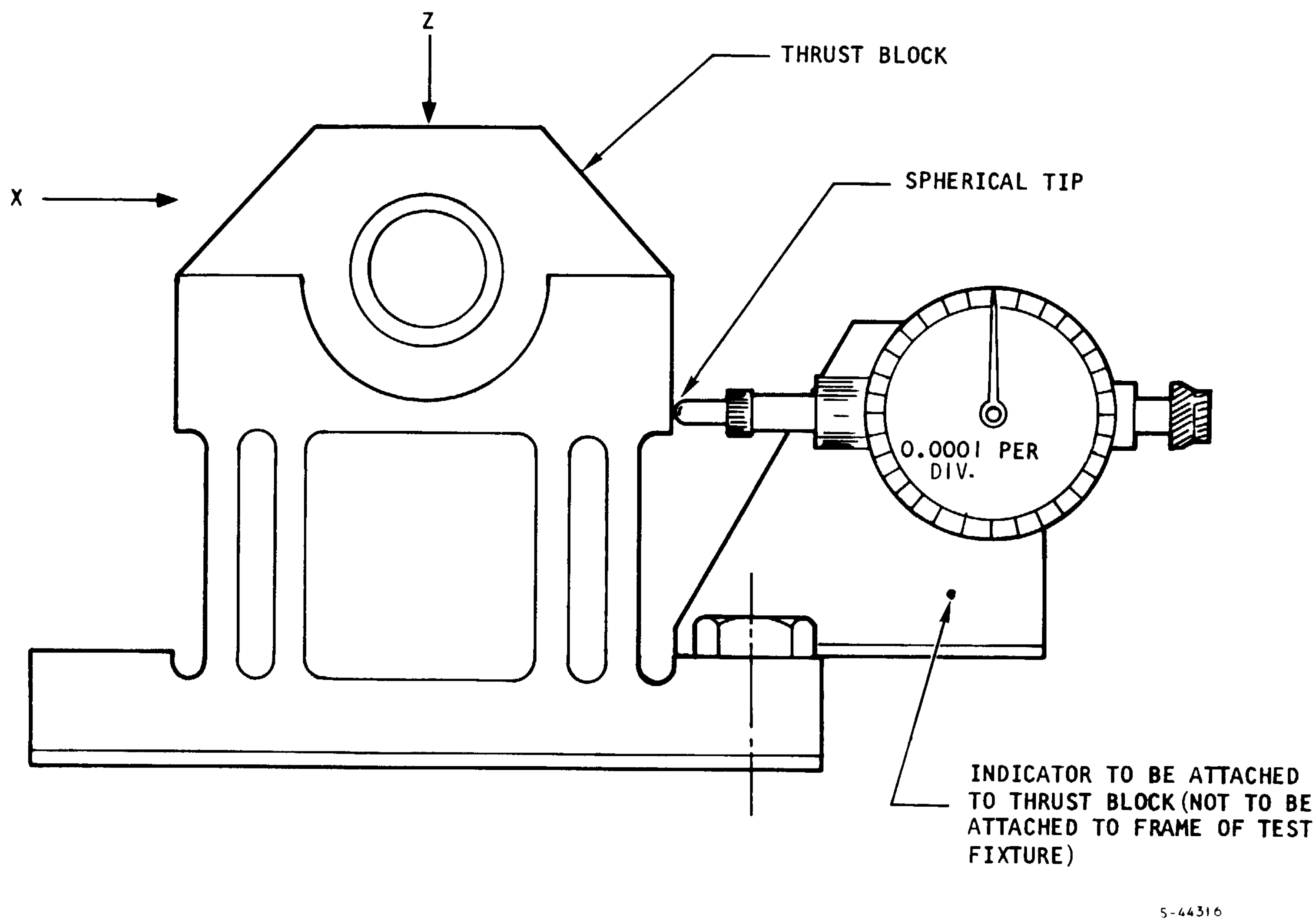

Figure A-1. Measurement of Block Deflection

2.9 Straingages.

2.9.1 MA-09-060CC-350, Micro Measurements Company.

2.9.2 MA-09-062TT-120, Micro Measurements Company

2.9.3 BR-600 adhesive, W.T. Bean, Incorporated.

2.10 Pressure gage 0 to 10,000 psi, ±1/4 percent accuracy, (P_z).

3.0 PROCEDURE

3.1 STRESS-COAT TESTS

Apply Stress-coat to the flexure and fillet areas of the deflection block. Mount the deflection block in the test fixture and apply such loads in the X-axis as are required to determine locations and relative magnitudes of stress concentrations. Record appropriate data on the data sheet. Do not apply X-axis loads in excess of 15,000 lb. This load results in fillet stresses of approximately 78,000 psi.

3.2 STRAINGAGES

The Stress Laboratory will communicate the results of the Stress-coat testing to the instrument project engineer. At that time, the exact location of the straingages will be decided. Apply the gages and record the locations. (See Figure A-2 for simple arrangement.)

3.3 CALIBRATION TESTING

3.3.1 Perform tests in order shown on the schedule of tests. On increasing inputs, approach loads from increasing direction only, and conversely. This requirement is to obtain data to evolve hysteresis characteristics.

3.3.2 Manual application of negative X-axis loading may be necessary to overcome internal friction of the load cylinders to achieve zero-loading from a decreasing direction.

3.3.3 Estimate deflection to 1/2 division or 0.00005 in.

3.3.4 P_Z force to be applied with the load-cylinder rod-end located in the center threaded hole.

3.3.5 Apply loads as shown on the test schedule, at room temperature. Record pressures, deflections, load-cell voltages, and straingage voltages.

3.3.6 At test No. 5, determine the mathematical relation between applied pressure and load-cylinder output. Use this pressure-load relationship for application of the Z-axis loads.

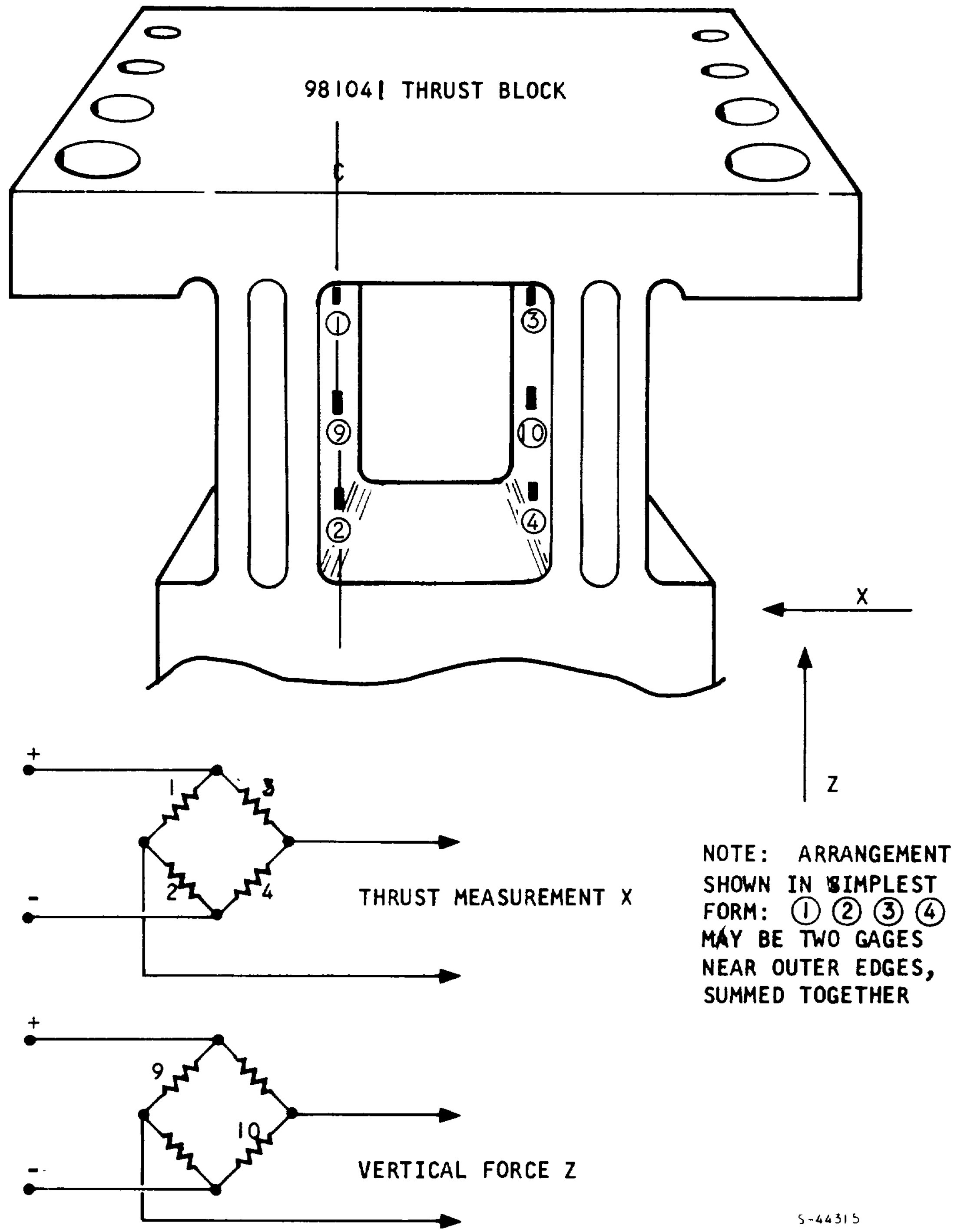

Figure A-2. Suggested Straingage Installation

4.0 SCHEDULE OF TESTS

Test No.	P_x, lb (X-Axis)	P_z, psi (Z-Axis)	E_o, volts (Load Cell)	ΔX, in.	E_x, volts (S/G)	E_z, volts (S/G)
1	0	0				
2	2000					
3	4000					
4	6000					
5	10000					
6	12000					
7	14000					
8	15000					
9	12000					
10	6000					
11	4000					
12	2000					
13	0					
14		6000				
15		12000				
16		15000				
17		18000				
18		12000				
19		6000				
20		0				
21	0	2000				
22	2000					
23	4000					
24	6000					
25	2000					
26	0					
27	0	4000				
28	2000					
29	4000					
30	6000					
31	2000					
32	0					

TABLE A-1

DEVIATION FROM TEST PLAN

Para Ref	Deviation	Reason
1.1	Deferred	Dial gage with sufficient resolution not available (see Para 2.3)
1.4	Deferred	Dial gage with sufficient resolution not available (see Para 2.3)
2.3	Not available at time of testing	On order
2.9	More suitable gages used (see Para 1.3.2, Part II, of this report)	Advice of stress department
3.3.3	Deferred	No dial gage
3.3.4	Deferred	Test not concluded due to termination order
3.3.6	Deferred	Test not concluded due to termination order
4.0	(a) Loading schedule increments changed to 1000 lb up to 10000 total load.	Better definition. 10000 lb limit sufficient to establish stress patterns.
	(b) No P_z loads applied	Test not concluded due to termination order
Fig A-1	Not applicable	No dial gage
Fig A-2	Two active gages used in thrust bridge (see Figure 1.3-6, Part II, of this report.)	Better averaging

APPENDIX B

FULL STRAINGAGE
BENDING-BRIDGE ANALYSIS

APPENDIX B

FULL STRAINGAGE BENDING-BRIDGE ANALYSIS

Consider the deflection block thrust bridge of figure 1.3-2, reproduced below

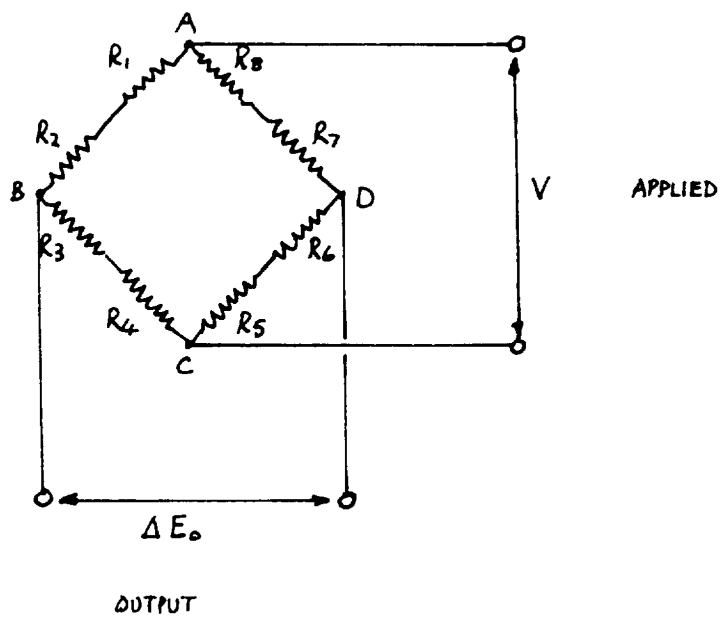

With reference to figure which shows the position of the gages

R_1 and R_2 are on opposite flexures at opposite ends and are in tension (+)
R_5 " R_6 " " " " " " " " " " "
R_3 and R_4 " " " " " " " " " " compression (−)
R_7 and R_8 " " " " " " " " " " "

Let ΔR_1, ΔR_2 etc be the change of resistance of R_1, R_2 etc under the application of a load P to the thrust block to produce a strain ϵ

Let the applied bridge voltage be V

Let the change of output from the null position be ΔE_0

Let $R_1 = R_2 = R_3 = R_4 = R_5 = R_6 = R_7 = R_8 = R$.

Form 2427

AIRESEARCH MFG. CO.

DATE ______ CALC. NO. ______
PREPARED BY ______ MODEL ______
CHECKED BY ______ PART NO. ______

Then the voltage across AB is

$$V_{AB} = \frac{(R+\Delta R_1) + (R+\Delta R_2)}{(R+\Delta R_1) + (R+\Delta R_2) + (R-\Delta R_3) + (R-\Delta R_4)} \cdot V$$

$$V_{AB} = \frac{2R + (\Delta R_1 + \Delta R_2)}{4R + (\Delta R_1 + \Delta R_2) - (\Delta R_3 + \Delta R_4)} \cdot V$$

Similarly $$V_{AD} = \frac{2R - (\Delta R_7 + \Delta R_8)}{4R + (\Delta R_5 + \Delta R_6) - (\Delta R_7 + \Delta R_8)} \cdot V$$

Thus the output voltage ΔE_0, which is given by $V_{AB} - V_{AD}$, is

$$\Delta E_0 = \left(\frac{2R + (\Delta R_1 + \Delta R_2)}{4R + (\Delta R_1 + \Delta R_2) - (\Delta R_3 + \Delta R_4)} - \frac{2R - (\Delta R_7 + \Delta R_8)}{4R + (\Delta R_5 + \Delta R_6) - (\Delta R_7 + \Delta R_8)} \right) V$$

Close approximation can be expressed as :

$$\frac{\Delta E_0}{V} = \frac{\cancel{8R^2} + 2R(\Delta R_5 + \Delta R_6) - 2R(\Delta R_7 + \Delta R_8) + 4R(\Delta R_1 + \Delta R_2) - \cancel{8R^2} - 2R(\Delta R_1 + \Delta R_2) + 2R(\Delta R_3 + \Delta R_4) + 4R(\Delta R_7 + \Delta R_8)}{16R^2 + 4R(\Delta R_5 + \Delta R_6) - 4R(\Delta R_7 + \Delta R_8) + 4R(\Delta R_1 + \Delta R_2) - 4R(\Delta R_3 + \Delta R_4)}$$

$$\frac{\Delta E_0}{V} = \frac{2R\left[\Delta R_1 + \Delta R_2 + \Delta R_3 + \Delta R_4 + \Delta R_5 + \Delta R_6 + \Delta R_7 + \Delta R_8\right]}{16R^2 + 4R\left[(\Delta R_1 + \Delta R_2 + \Delta R_5 + \Delta R_6) - (\Delta R_3 + \Delta R_4 + \Delta R_7 + \Delta R_8)\right]}$$

$$\frac{\Delta E_0}{V} = \frac{\Sigma \Delta R}{8R + 2(\Sigma \Delta R_T - \Sigma \Delta R_c)}$$

where $\Sigma \Delta R$ is the algebraic sum of the resistances changes
$\Sigma \Delta R_T$ is the " " " " tensile resistance changes
$\Sigma \Delta R_c$ " " " " " " comp. "

Form 2427

AiRESEARCH MFG. CO.

DATE

PREPARED BY

CHECKED BY

CALC. NO.

MODEL

PART NO.

Now the term $2(\Sigma \Delta R_T - \Sigma \Delta R_c)$ is very small compared to $8R$ for a balanced installation and may be ignored

Thus $$\frac{\Delta E_o}{V} = \frac{\Sigma \Delta R}{8R}$$

Introducing the gage factor GF where $GF = (\Delta R/R \div \text{strain})$

then the strain ϵ is given by

$$\epsilon = \frac{\Delta E_o}{V} \cdot \frac{1}{GF}$$

where ϵ represents the average strain at the eight locations

Non-linearities in the relationship between the average strain and the bridge output voltage will be introduced by the second order terms and by the term $(\Sigma \Delta R_T - \Sigma \Delta R_c)$

Balanced gages and balanced installation will minimize the non-linearity

APPENDIX C

DETAILED TEST OBSERVATIONS

TABLE C-1

STRESS COAT TESTS

Applied Load P_x (lb)	Length in Calibration Beam to Produce Cracks under Cal. Load (inches)	Calibration Strain ϵ_T microinches/inch (from column 2 and ref. data)	Time (hrs)	Temperature (°F)	Description of Cracks	Remarks
0	2	369	14^{00}	66	-	-
1000			14^{13}	66	No cracks	Return to zero load and inspect
2000			14^{17}	66	" "	" " "
4000	2	369	14^{24} 14^{26}	68 71	At (A) Cracks all along to 1/2 inch from mounting flange At (B) Cracks to 1/4 inch from flange on left. One crack on right	CAL. SECOND BAR Return to zero load and inspect
5000			14^{32}	70	No significant change. But cracks on left denser than on right	Return to zero & inspect
6000	2.1	388	14^{34} 14^{36}	68 68	At (C) Cracks not parallel - more stress on left. At (B) cracks for 1/4 inch	CAL THIRD BAR Return to zero - inspect. Apparently some torsion in block. Cracks in all radii
10000	2.3	424	14^{43} 14^{46}	68 68	Little change, showing that stresses fall off rapidly and are concentrated in radii. Considered sufficient lines to indicate neutral axis	CAL FOURTH BAR Fixture mounting plate moved considerably. Thrust pin not directly removable.

Refer to Figure C-1 for Location Identification

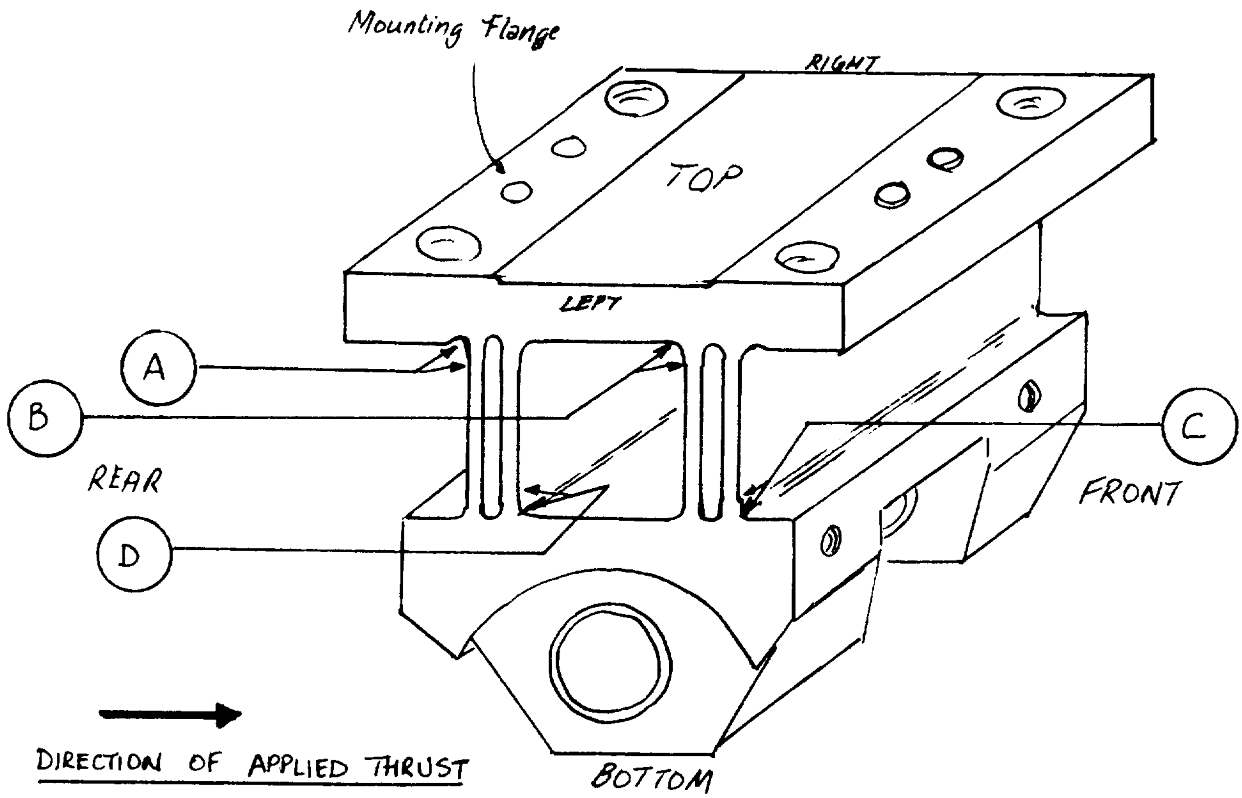

Figure C-1. Thrust Deflection Block - Identification for Stress-coat Tests

Straingage Tests

The attached test sheets cover the straingage calibration performed on the deflection block following the stress coat tests

The Poisson's bridge was not tested under the application of vertical loading (P_z) although the hydraulic ram used to provide the thrust load (P_x) was calibrated against the force transducer. P_z loading would not be applied through a force transducer, by nature of design of the test equipment, and it was intended to obtain an indication of P_z loading by inference from the hydraulic ram pressure. Similar rams would be used for P_x and P_z loading. (See Test procedure para 3.3.6)

The following symbols apply:

Symbol	Explanation
Page II-C5 P_x	Applied thrust (X axis) in lb.
P_x Ref (E_o) [2nd Column]	Output of force transducer in millivolts
Thrust E_o	Absolute Output of thrust straingage bridge in millivolts
Thrust ΔE_o	(Output of thrust straingage bridge at load P_x) − (Output of bridge for $P_x = 0$) in millivolts
P_x Ref (E_o) [5th column page]	Output of pressure transducer in millivolts
p_x [6th column]	Pressure of hydraulic fluid in ram (thrust) in p.s.i.g. (from pressure transducer calibration)
Poisson's E_o	Absolute output of Poisson's Straingage bridge in millivolts
Poisson's ΔE_o	(Output of Poisson's bridge at load P_x) − (Output of bridge for $P_x = 0$) in millivolts
p_x x area	Equivalent ram pressure force = area x pressure (for calibration of ram pressure versus force transducer)

Page II−C6

Symbol	Explanation
E_o	as thrust E_o page
ΔE_o	as thrust ΔE_o page

Calibration of thrust bridge - equivalent load based on output sensitivity of 2.995 mV/V

FORM #1339A
AIRESEARCH MFG. CO.

LAB DATA SHEET

Page ______ of ______

EWO: CYL. EFF. AREA IN ADVANCE MODE = 3.14 in^2 DATE ______ TEST PURPOSE: P_x REF. N JP-10,000, S/N 13595

P/N ______ BAROM ______

S/N ______ TEMP ______ TEST PERS. P_x REF. N STATHAM PA 324TC-5M-350

NO.	P_x (Lb)	Ch. 1 P_x REF E_o (MV)	Ch. 2 THRUST E_o (MV)	THRUST ΔE_o (MV)	Ch. 4 P_x REF E_o (MV)	P_x (PSIG)	Ch. 3 POISSON'S E_o (MV)	POISSON'S ΔE_o (MV)		$P_x \times A$						REMARKS
	1	2	3	4	5	6	7	8	9	10	11	12	13	14	15	NOTE: ALL BRIDGE EXCITATION VOLTAGE = 5.00 VOLTS, DC
1	0	0	+1.77	0	0	0	+.58	0		0						
2	1000	-15.13	+3.29	+1.52	+2.57	358	+.58	0		1124						Pressure Transducer
3	2000	-30.26	+4.81	+3.04	+4.93	687	+.58	0		2157						Sensitivity w/5.00 V.D.C.
4	3000	-45.38	+6.31	+4.54	+7.41	1032	+.58	0		3240						Excitation =
5	4000	-60.51	+7.81	+6.04	+9.73	1355	+.59	+.01		4255						0.00718 MV/psi
6	5000	-75.64	+9.31	+7.54	+12.11	1687	+.59	+.01		5277						
7	6000	-90.76	+10.83	+9.06	+14.36	2000	+.61	+.03		6280						
8	7000	-105.89	+12.31	+10.54	+16.67	2322	+.61	+.03		7241						
9	8000	-121.02	+13.79	+12.02	+18.69	2603	+.63	+.05		8175						
10	9000	-136.15	+15.27	+13.50	+21.15	2946	+.65	+.07		9250						
11	10,000	-151.28	+16.75	+14.98	+23.39	3258	+.67	+.09		10,230						
12	9000	-136.15	+15.29	+13.51	+20.25	2820	+.65	+.08		8855						
13	8000	-121.02	+13.83	+12.05	+17.93	2497	+.59	+.02		7840						
	7000	-105.89	+12.35	+10.57	+16.01	2230	+.56	-.01		7062						
	6000	-90.76	+10.87	+9.09	+13.26	1847	+.53	-.04		5800						
	5000	-75.64	+9.37	+7.59	+11.45	1595	+.49	-.08		5008						
	4000	-60.51	+7.85	+6.07	+9.72	1354	+.55	-.02		4252						
	3000	-45.38	+6.35	+4.57	+6.45	898	+.53	-.04		2820						
	2000	-30.26	+4.85	+3.07	+4.01	558	+.52	-.05		1752						
	1000	-15.13	+3.33	+1.55	+1.76	245	+.53	-.04		767						
	0	0	+1.78	0	-.31	-43	+.57	0		-135						

LOAD TRANSDUCER CALIBRATION DATA SHEET

Model No. *LWS #1280*　Calibration Date *8-30-68*　Data:

Serial No. *THRUST*　Excitation Voltage *5.00* V.D.C.　Output At Rated Capacity

Capacity *10,000 Lb*　Load Step Value *1000* LB/STEP　*+2.995* MV/V

MV/V

JP-10,000; S/N 13595 USED AS REF. STD.

	PUSH IN				+X DIRECTION											
	UPSCALE				DOWNSCALE				UPSCALE				DOWNSCALE			
LOAD STEP (N)	LOAD (lb)	E_o (MV)	ΔE_o (MV)	DEV. (MV)	LOAD (lb)	E_o (MV)	ΔE_o (MV)	DEV. (MV)	LOAD (lb)	E_o (MV)	ΔE_o (MV)	DEV. (MV)	LOAD (lb)	E_o (MV)	ΔE_o (MV)	DEV. (MV)
0	0	+1.77	0	0	0	+1.78	0	0								
1	1000	+3.27	+1.52	+.02	1000	+3.33	+1.55	+.05								
2	2000	+4.81	+3.04	+.04	2000	+4.85	+3.07	+.08								
3	3000	+6.31	+4.54	+.05	3000	+6.35	+4.57	+.08								
4	4000	+7.81	+6.04	+.05	4000	+7.85	+6.07	+.08								
5	5000	+9.31	+7.54	+.05	5000	+9.37	+7.59	+.11								
6	6000	+10.83	+9.06	+.07	6000	+10.87	+9.09	+.11								
7	7000	+12.31	+10.54	+.05	7000	+12.35	+10.57	+.09								
8	8000	+13.79	+12.02	+.04	8000	+13.83	+12.05	+.07								
9	9000	+15.27	+13.50	+.02	9000	+15.29	+13.51	+.04								
10	10,000	+16.75	+14.98	0	10,000	+16.75	+14.97	0								

68-3953
Page II-C6

	+X		COMPRESSION	
	UP	DOWN	UP	DOWN
Avg. ΔE_o, mv	+1.498	+1.497		
Max. Error, ±%	+0.47%	+0.73%		
Sens., mv/v/lb				
Avg. Sensitivity		mv/v/lb		mv/v/lb

OUTPUT AT RATED CAPACITY (10,000 Lb) $= + \frac{14.975}{5.00} = +2.995 \frac{MV}{V}$

	R_c ±½%	+ CALIBRATION X E_o (MV)	ΔE_o (MV)	EQUIV. LOAD (lb)	− CALIBRATION E_o (MV)	ΔE_o (MV)	EQUIV. LOAD (lb)
	.0	+1.77	0	0			
+10K		+31.55	+29.78	+19,886			
25K		+13.77	+12.00	+8,013			
50K		+7.78	+6.01	+4,013			
100K		+4.78	+3.01	+2,010			
500K		+2.37	+0.60	—			

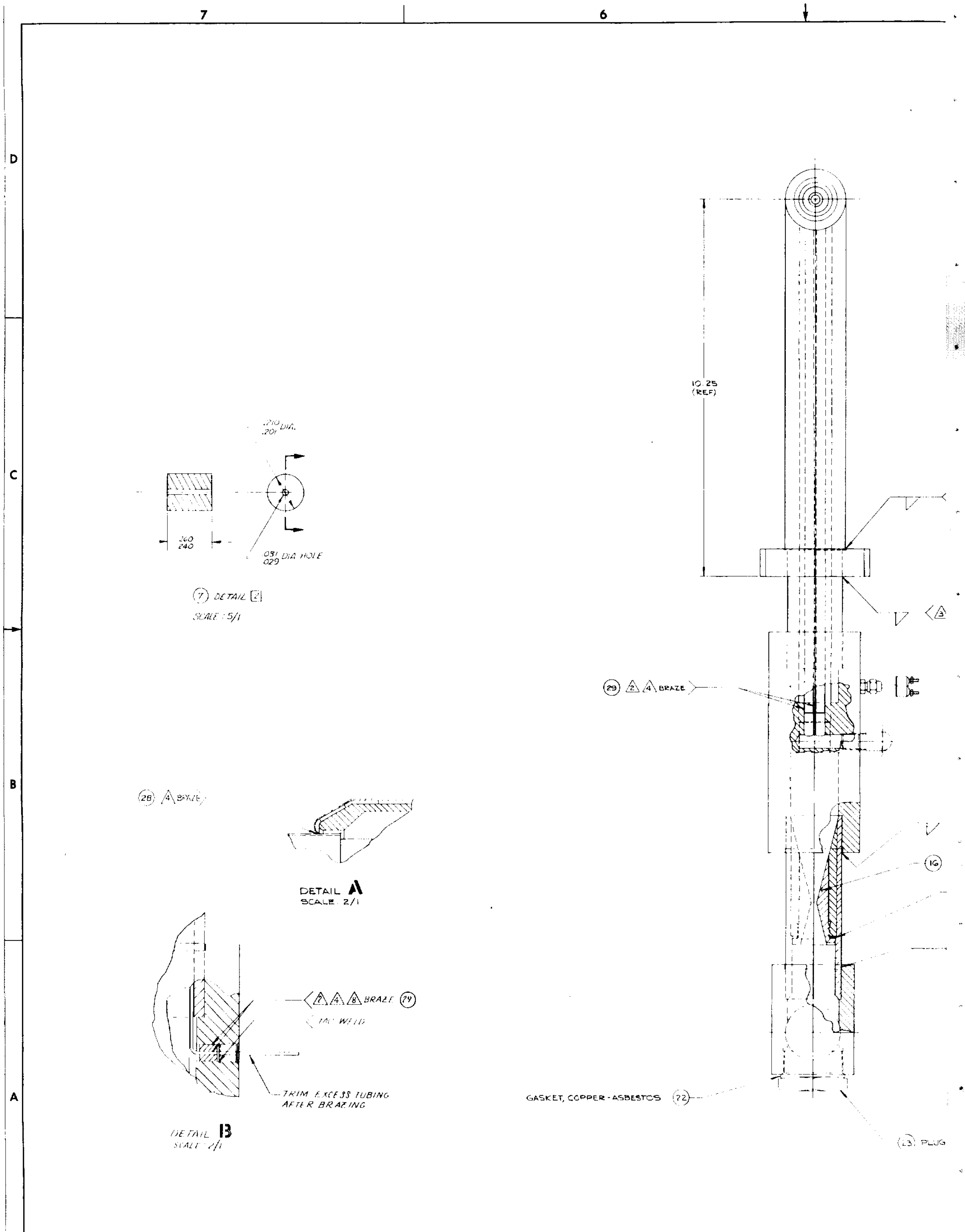

FOLDOUT FRAME

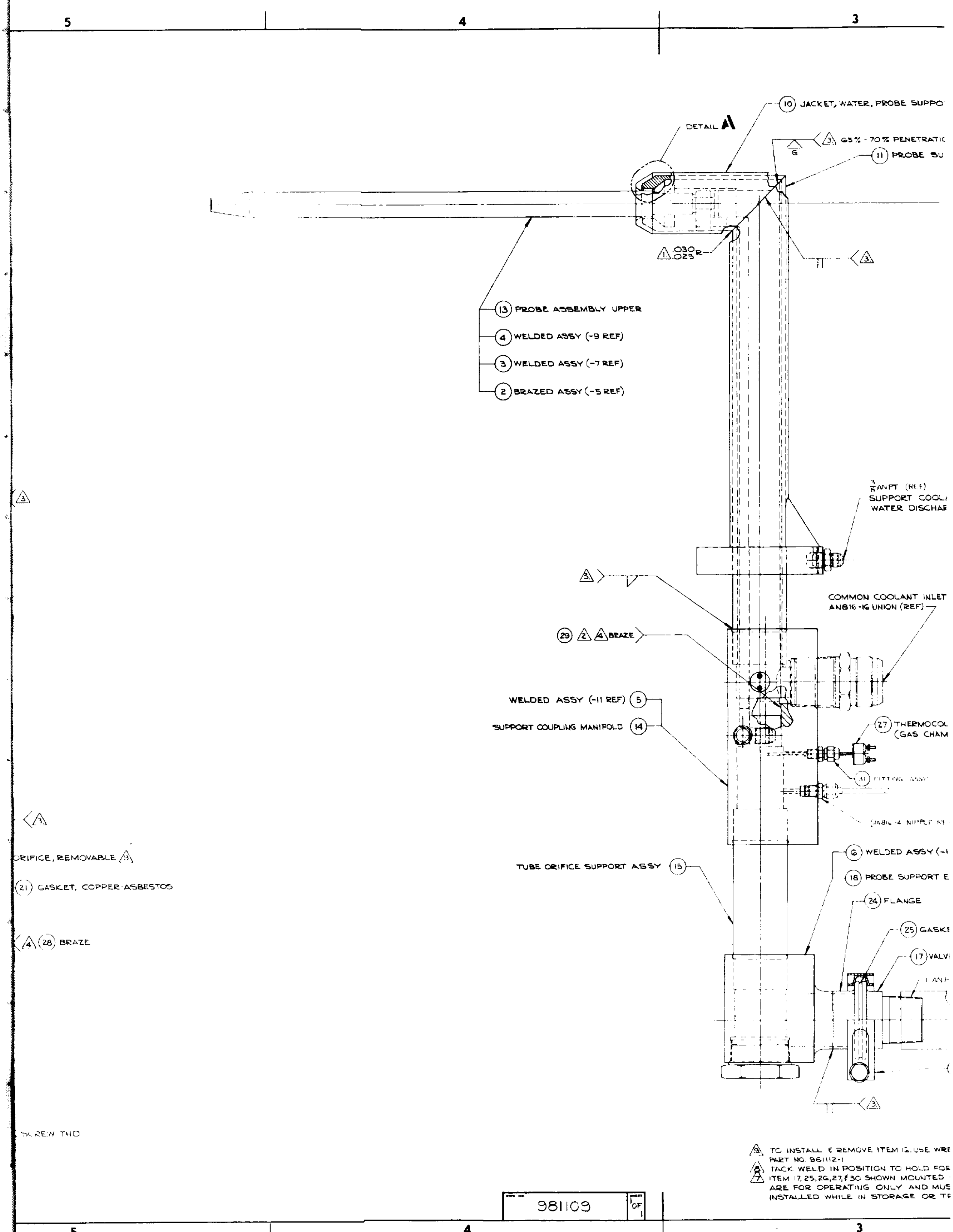

FOLDOUT FRAME 2

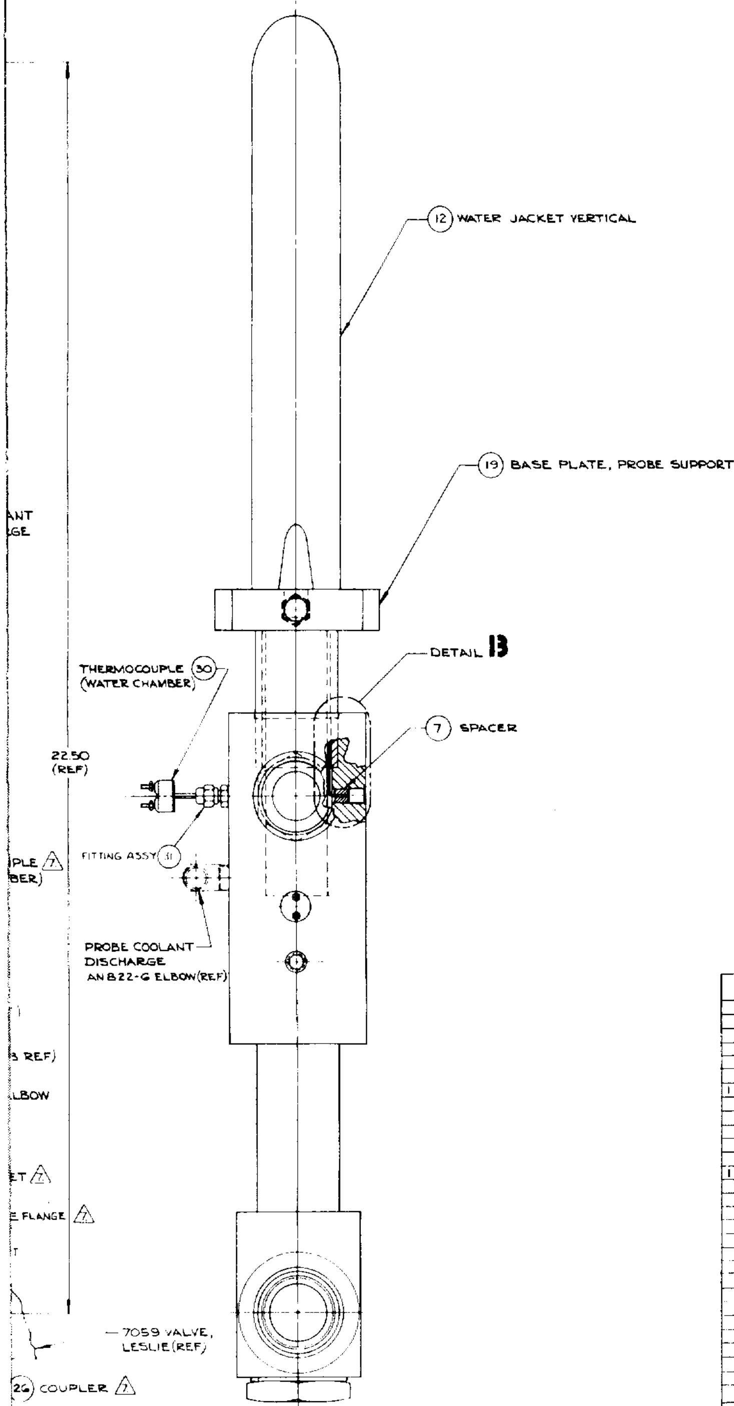

6. SOURCE: SEMCO INC
NO. HOLLYWOOD, CALIF.
5. SOURCE: MARMAN, AEROQUIP CORP
BURBANK, CALIF.
4. INERT ATMOSPHERE, VACUUM OR INDUCTION BRAZE PER AIRESEARCH SPEC WBS-27 USING BRAZE ALLOYS NOTED
3. INERT ATMOSPHERE OR VACUUM WELD PER AIRESEARCH SPEC WBS-18
2. ITEM 29, MUST BE APPLIED BEFORE WELDING
1. .030R MAX ON INSIDE MITER AFTER WELDING

NOTES: UNLESS OTHERWISE SPECIFIED

ENCH
BRAZING
ON THIS DWG
T NOT BE
RANSIT

QTY REQD -13	-11	-9	-7	-5	-3	-1	ITEM NO.	CODE IDENT NO.	PART OR IDENTIFYING NO.	NOMENCLATURE OR DESCRIPTION	SYM	ZONE
							32					
						2	31		94 4A 516 1	FITTING ASSY (MODIFIED)		3
						1	30		TC2400-K-6-U	THERMOCOUPLE (WATER CHAMBER)	6	2
				A/R			29		B.T. LITHO	BRAZE ALLOY	2	4,5
					A/R		28		-17	PALNIRO 1 WBS 27	4	5,7
						1	27		TC2400-K-11-E	THERMOCOUPLE (GAS CHAMBER)	6	3
						1	26		24502-150	COUPLER	5	3
						1	25		17188-150-N	GASKET	5	3
1							24		16933-150-6	FLANGE	5	3
						1	23		AN814-20	PLUG, SCREW THD		5
						1	22		MS35769-42	GASKET, COPPER - ASBESTOS		6
						1	21		MS35769-18	GASKET, COPPER-ASBESTOS		5
		1					19		981051-1	BASE PLATE, PROBE SUPPORT		2
1							18		981105-1	PROBE SUPPORT ELBOW		3
						1	17		981101-1	VALVE FLANGE ASSY		3
						1	16		981081-1	ORIFICE, REMOVABLE		3
	1						15		981113-1	TUBE ORIFICE, SUPPORT ASSY		3
	1						14		981083-3	SUPPORT COUPLING, MANIFOLD		4
		1					13		981102-1	PROBE ASSEMBLY, UPPER		4
		1					12		981075-1	WATER JACKET, VERTICAL ASSY		2
		1					11		981059-1	PROBE SUPPORT, TUBE ASSY		3
		1					10		981056-1	JACKET, WATER, PROBE SUPPORT		3
							9					2
							8					
							7		-15	SPACER .250 DIA x 1.0 LG CRES 304 MIL-S-5059		2,7
				1			6		-13	WELDED ASSY		3
			1				5		-11	WELDED ASSY		4
			1				4		-9	WELDED ASSY		4
				1			3		-7	WELDED ASSY		4
					1		2		-5	BRAZED ASSY		4
						1	1		-3	PROBE ASSY		

-13 -11 -9 -7 -5 -3 -1 ← ASSY

PARTS LIST

REVISIONS				
ZONE	LTR	DESCRIPTION	DATE	APPROVED

UNLESS OTHERWISE SPECIFIED:
DIMENSIONS ARE IN INCHES.
MACHINE FILLET RADII .015 — .030
SURFACE ROUGHNESS PER MIL-STD-10
BURR CONTROL PER 50853
DIMENSION LIMITS HELD AFTER PLATING
IDENT MARKING PER MC16
DIMENSIONING AND TOL PER MIL-STD-8

HEAT TREATMENT	PROCESS
HARDNESS AND SPEC	NAME AND SPEC

	NEXT ASSY	USED ON
REQD	NEXT ASSY	USED ON
	FINAL	H.R.E.

APPLICATION

CONTRACT NO.

DFT DAN ROBLES 11-2-67
CHK
DESIGN CHKR
MATL
STRESS
APPD
AIRESEARCH APPD
OTHER AGENCY APPD

AIRESEARCH MANUFACTURING COMPANY
A DIVISION OF THE GARRETT CORPORATION
LOS ANGELES, CALIFORNIA

TOTAL PRESSURE & TEMPERATURE SAMPLE PROBE, DOUBLE SONIC

SIZE	CODE IDENT NO.	DWG NO.
J	70210	981109

SCALE 1/1 NORM | SHEET 1 OF 1

981109

FOLDOUT FRAME 3